ISAS - INTERNATIONAL SCHOOL
FOR ADVANCED STUDIES

SISSA

COMBINED CONFOCAL MICROSCOPY AND PATCH-CLAMP STUDY OF THE EFFECTS OF $[Ca^{2+}]_i$ AND OTHER MODULATORS ON LIGAND-GATED CHANNEL DESENSITIZATION

Thesis submitted for the degree of

"doctor Philosophiae"

Candidate:

Leonard Khiroug

Supervisor:

Prof. Andrea Nistri

Academic year 1996/97

TRIESTE

SISSA - SCUOLA
INTERNAZIONALE
SUPERIORE
DI STUDI AVANZATI
TRIESTE
Strada Costiera 11

TRIESTE

Table of contents

Summary

Neuronal type nicotinic acetycholine receptors (nAChRs) of rat chromaffin cells and ionotropic P2 (P_{2X}) receptors of pheochromocytoma (PC12) cells were studied using simultaneous whole-cell patch-clamping and confocal microscopy intracellular calcium imaging. To this end, confocal laser scanning microscopy (CLSM), previously not available in the lab, was first set up using rat cultured hippocampal neurons as a test system to develop this method (Andjus *et al.,* 1996a; Andjus *et al.,* 1996b; Andjus *et al.,* 1996c). The CLSM was adapted for use in combination with patch-clamp recording. On chromaffin cells or PC12 cells focal pressure pulses of nicotine or ATP, respectively, were applied to test receptor sensitivity and/or to induce receptor desensitization. The time-course of desensitization and recovery from it was described for both nAChRs and P_{2X} receptors, and two distinct types of desensitization (fast and slow ones) were suggested for ATP-receptors while confirming fast and slow phases of nAChRs desensitization (Giniatullin *et al.,* 1996; Khiroug *et al.,* 1997c). The first desensitization type was experimentally revealed as rapidly fading current flowing during the application of high doses of extracellular ATP which was followed by a large, sustained rebound current upon pulse cessation. Changes in intracellular Ca^{2+} ($[Ca^{2+}]_i$) imaged with fluo-3 based confocal microscopy were assessed during different phases of desensitization and recovery from it (Khiroug *et al.,* 1997a; Khiroug *et al.,* 1997c). No correlation with $[Ca^{2+}]_i$ was found for desensitization onset of nAChRs or for fast desensitization of P_{2X} receptors. Conversely, both recovery from nAChRs desensitization and recovery from slow P_{2X} desensitization were found to be strongly $[Ca^{2+}]_i$-dependent with high temporal

correlation between the recovery time-course and that of $[Ca^{2+}]_i$ decay. Finally, strong depressant action of the neuropeptide substance P on ATP-induced responses (without affecting $[Ca^{2+}]_i$ or producing any ion current) was demonstrated and attributed to enhancement of both fast and slow types of P_{2X} receptor desensitization (Khiroug *et al.*, 1997b). Kinetic schemes, $[Ca^{2+}]_i$ regulation and possible physiological relevance of different types and phases of desensitization studied in the present thesis are discussed and compared for nAChRs and P_{2X} receptors.

Introduction

I. Desensitization as an intrinsic property of nAChRs and P_{2X} receptors

Ionic channels are gated selective filters in the cell membrane which allow ions, otherwise membrane-impermeant, to pass through (Nicholls *et al.*, 1992). Among the superfamily of ligand-gated channels nicotinic acetylcholine receptors (nAChRs) have been extensively investigated. These receptors are broadly divided in two classes: muscle and neuronal type nAChRs.

I-1. Muscle nAChR - the best studied ligand-gated receptor

Historically, the muscle type nAChRs were the first ones to be observed as single channels under patch-clamp conditions (Neher & Sakmann; 1976); their gene sequence was the first one to be determined (Noda *et al*, 1983); finally, these receptors were the first ones to be expressed in foreign cells by injection of cloned mRNA (Mishina *et al.*, 1984; see Hille, 1992). There are two main types of muscle nAChR: adult and embryonic ones (Jaramillo & Schuetze, 1988). At the neuromuscular junction of adult animals, postsynaptically expressed nAChRs are involved in fast synaptic transmission during which their activation by acetylcholine (ACh) produces depolarization and eventual contraction of the muscle cell. This action of the natural agonist ACh can be mimicked by nicotine or carbachol. Under voltage-clamp conditions, the effect is observed as membrane current (end-plate current) which is due to cationic flux (mainly Na^+ and, to a lesser extent, K^+ and Ca^{2+}). These nAChRs-

generated currents exhibit voltage dependence, rectify at positive membrane potentials and reverse around 0 mV. Together with neuronal type, muscle type nAChR currents are blocked by *d*-tubocurarine in μM concentrations.

After determining the molecular structure of nAChRs (Numa *et al.*, 1983), it was demonstrated by means of direct cryoelectron microscopy (Unwin *et al.*, 1988) that the muscle type nAChR is constituted by five subunits (two identical α subunits, β, γ and δ subunits; Fig. I-1; Nicholls *et al.*, 1992). This method, together with combining different subunits (Stafford *et al.*, 1994) for mRNA injection into *Xenopus* oocytes (Mishina *et al*, 1984) helped to elucidate the functional role of particular subunits. For instance, the ACh binding sites were shown to be located within the α subunits (Criado *et al.*, 1992), while the β one seems to be responsible for binding the nAChR modulating neuropeptide substance P (Stafford *et al.*, 1994). Both the γ and δ subunits were shown to be phosphorylated by PKA and/or PKC (Safran *et al.*, 1989) which is supposed to enhance receptor desensitization.

I-1a. Desensitization of muscle nAChRs

In the absence of free agonist, the most probable receptor state is the closed, unbound one. Upon binding of one or more than one (2 for nAChR) agonist molecules, the probability of receptor transition to the open state increases dramatically. The muscle type nAChRs would stay open for a millisecond or so at a time during a burst of activity (Sine, 1988; Changeux 1990), before changing its conformation to the one

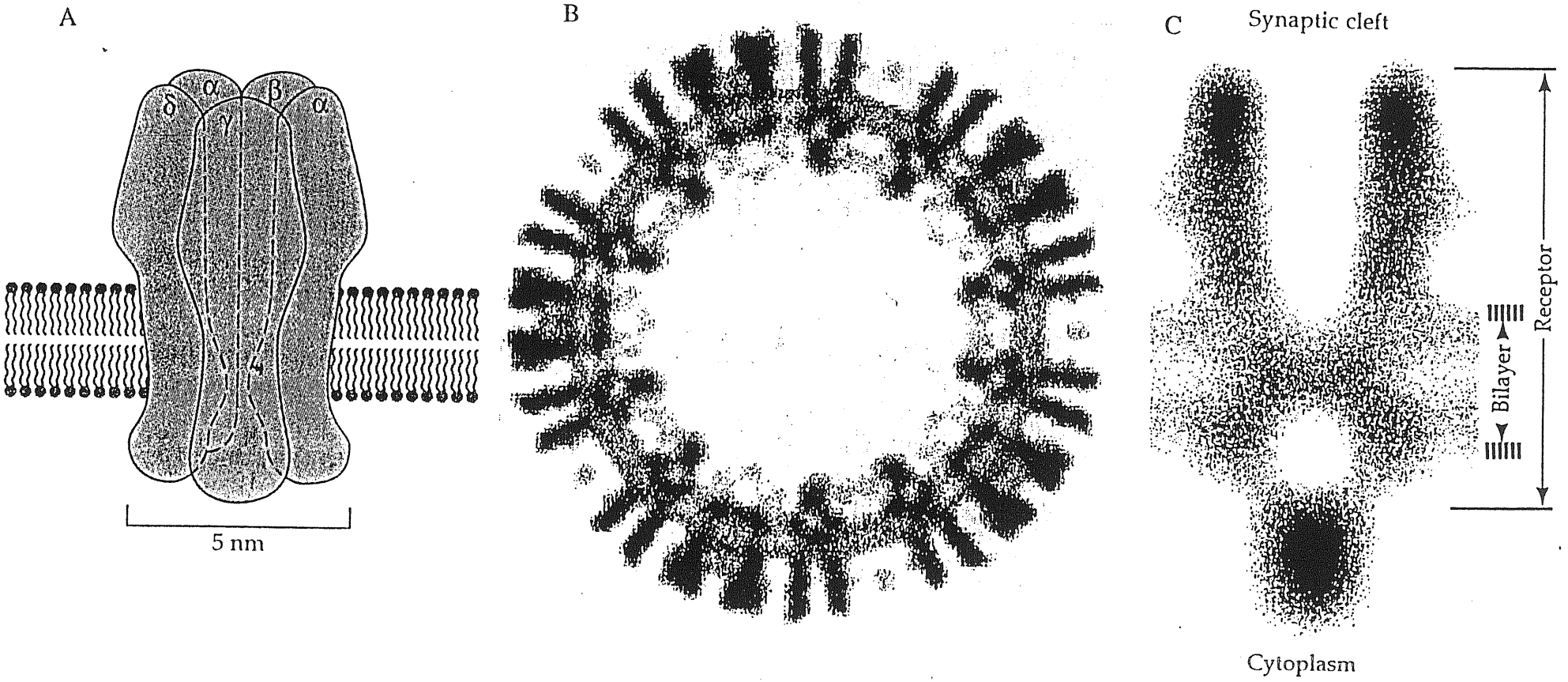

4a

Figure I-1. Structure and subunit composition of complete AChR. A, Five subunits constituting the receptor are spaced radially in increments of about 72 degrees around a central core. Dashed lines indicate the approximate dimensions of the internal passage in the open channel. B, Reconstructed image of transverse section through cylindrical vesicle from postsynaptic membrane of *Torpedo*, showing closely packed AChRs. C, Enlarged image of a single AChR, showing position and size relative to the membrane bilayer (From: Nicholls, 1992).

characterized by high affinity for agonists and a closed channel (Lindstrom, 1996). This agonist-bound but closed state of the receptor channel is called desensitized.

The term "desensitization" was first proposed by Katz and Thesleff (1957) to describe the decrease in the depolarizing response of the muscle at the neuromuscular junction during prolonged application of ACh. Recording intracellularly from the muscle fiber, they applied repetitive brief ionophoretic pulses of ACh to test receptor sensitivity. Conditioning doses of ACh (much lower effective concentrations than those applied ionophoretically) were delivered from a second pipette. The latter applications of ACh induced dose-dependent steady state depolarizations and produced decrease in the amplitude of test pulse responses as the receptors desensitized. The effect was dose-dependent and the receptor sensitivity recovered upon cessation of the conditioning pulse.

The desensitization phenomenon should be distinguished from a variety of processes associated with decrease in cell responsiveness. These include irreversible loss of sensitivity due to receptor deactivation (Noble *et al.,* 1978; Boyd, 1987) and internalization of receptors (Clementi & Sher, 1985). Thus, desensitization can be defined as a temporal loss of receptor sensitivity to agonists due to its functional and conformational changes. Ability to desensitize to sustained or repetitive action of the agonist is a common property of the majority of ligand-gated receptors (*cf.* Nicholls *et al.*, 1992). Desensitization is a phenomenon which develops with a certain time-course depending on the agonist concentration and other factors discussed later. The phases of the desensitization time-course include onset, steady-state and recovery from desensitization. Both onset of and recovery from nAChR desensitization were

shown to be complex processes which could be fitted by polyexponential functions (Feltz & Trautmann, 1982; Boyd, 1987), suggesting the existence of more than one desensitized state for many ligand-gated receptor channels.

I-1b. Kinetic scheme for receptor desensitization

Del Castillo & Katz (1957) and Katz & Thesleff (1957) suggested that desensitization proceeds from the open conformation. They proposed that desensitization could be best described by a cyclic reaction model where the receptor can exist in two interconvertable conformations or irreversibly pass to a deactivated form:

$$\begin{array}{ccc} 2A + R & \longleftrightarrow & A_2R^* \\ \uparrow\downarrow & & \uparrow\downarrow \\ 2A + D & \longleftrightarrow & A_2D \rightarrow R_{DA} \end{array} \qquad (1)$$

where A is the agonist molecule, R is the receptor molecule, A_2R^* is the open receptor with two agonist molecules bound, and D is the receptor in desensitized state. This desensitized state possesses a high affinity to ACh as confirmed with biochemical studies (Heidmann & Changeux, 1979). The scheme of Equation 1 assumes the existence of only one desensitized state and therefore predicts monoexponential timecourse for desensitization and recovery from it, which has later been shown to be oversimplified (Feltz & Trautmann, 1982). It also simplifies the process of receptor activation which can be better described according to Anderson & Stevens (1973) and Peper *et al.* (1982):

$$A + R \underset{k_{-1}}{\overset{k_1}{\longleftrightarrow}} A_1R + A \underset{k_{-2}}{\overset{k_2}{\longleftrightarrow}} A_2R \underset{k_{-3}}{\overset{k_3}{\longleftrightarrow}} A_2R^* \qquad (2)$$

where A_1R is the closed state of the receptor bound to only one ACh molecule (initially prevailing during the rising phase of ACh concentration), A_2R is a short-existing closed state with two ACh molecules from which the receptor transits to the more stable open state A_2R^*. All transition are characterized by their constants k_n and k_{-n}.

I-1c. Desensitization mechanism and modulation

Even if the molecular mechanism by which ligand-activated channels become desensitized is not known, desensitization is a intrinsic property of the receptor itself (Ochoa *et al.,* 1989). The timecourse of the slow phase of desensitization and that of the second phase of the biphasic processes of recovery from desensitization (tens of minutes; Boyd, 1987) suggested that the rate-determining step in the recovery is unlikely to be simply a protein conformational transition. It seems plausible that the receptor may have undergone a reversible biochemical modification that produces long-lasting desensitization. One candidate for such a modification can be protein phosphorylation, which has been suggested to be involved in the regulation of various ion channels in neurons (Levitan, 1994). In fact, post-synaptic membranes from the *Torpedo* electric organ have been shown to contain at least three different endogenous protein kinases: protein kinase A, C and tyrosine kinase (Huganir &

Greengard, 1983; Huganir *et al.*, 1984). On the other hand, activation of the protein phosphatase calcineurin has recently been shown to extend the recovery from nAChRs desensitization (Hardwick & Parsons, 1996).

These studies suggested a role for Ca^{2+} which might activate protein kinases. Thus, this ion may act indirectly via a Ca^{2+}-dependent phosphorylation step. In fact, not only the extracellular concentration of this ion has been shown to regulate desensitization of muscle type nAChRs (Mantley, 1966; Magazanik & Vyskocil, 1970), but also an increase in its intracellular concentration (Miledi, 1980) and in the transmembrane influx (Mulle *et al.,* 1992) facilitates receptor desensitization. The considerable effect of Ca^{2+} on nAChR makes an intriguing story of receptor regulation by the ion permeating it. This aspect, together with the role of other $[Ca^{2+}]_i$ increasing factors, will be addressed in the present study.

Other substances such as neuropeptides are also known to affect nAChRs desensitization (Clapham & Neher, 1984). One of the tasks of the present thesis was, therefore, to study the role of the neuropeptide substance P in receptor desensitization.

I-2. Protocols to study DS

Along with the classical approach by Katz and Thesleff (1957) described above, other protocols are used to study the phenomenon of receptor desensitization. For example, to study whether desensitization of glutamate receptors can proceed directly from the closed state, a slow pre-desensitizing concentration ramp has been applied (Dudel *et al.,* 1992). In such an experiment, the glutamate concentration is gradually increased

to 10 mM within 2 s (by moving the glass barrell laterally so that the concentration gradient slowly crosses the excised patch), and then suddenly lowered to zero. During the ramp, no channel opening is generally observed. Probability of glutamate receptor activation by a subsequent 10 ms square pulse of 10 mM glutamate increases proportionally to the interval between the ramp and the test pulse, presumably following the recovery from the glutamate ramp-induced desensitization which occurred without channel opening.

Another protocol to study the process of recovery from desensitization is provided by double-pulse experiments (Dudel *et al.,* 1992). In the case of glutamate receptors, the first pulse of the agonist causes receptor opening and their subsequent complete desensitization (this conclusion is reached on the basis of absence of current in the sustained presence of glutamate). The second pulse, that is given following a varying interval, tests how much desensitization was removed during the interpulse interval. The second desensitizing pulse can be substituted by a brief test pulse. During whole-cell recording, the time course of responses to endogeneously applied large doses of agonist shows fading of the current inspite of the continuos presence of the agonist. This fading can be used as a parameter which reflects the receptor desensitization (see for example Medina *et al.*, 1996).

I-3. Neuronal type nAChR

In mammals, an important type of neurotransmission in the peripheral nervous system is via cholinergic receptors (which includes muscarinic and nicotinic pathways). In central neurons this kind of transmission is much less frequent. Nevertheless, some

neurons or closely related cells such as chromaffin medullary cells have been found to possess nAChRs of neuronal type (Lindstrom, 1996). Neuronal nAChRs are divided in two subclasses according to their sensitivity to α-bungarotoxin. Thus, some neuronal type nAChRs do not bind the toxin at all, while the others have a binding site for α-bungarotoxin which, however, produces no block of normal synaptic transmission.

I-3a. Structure and function of neuronal nAChR

The α-bungarotoxin insensitive neuronal nAChR has been shown to be formed from combinations of α2, α3 or α4 subunits with β2, β4 and/or β5 subunits (Sargent, 1993; Role, 1992). In particular, recent cloning of neuronal nAChRs from bovine chromaffin cells has shown that they consist of is α3, α5 and β4 subunits, but not α2 or β2 ones (Campos-Caro *et al.,* 1997). The α7, α8 and/or α9 subunits (perhaps in combination with unknown ones) form the α-bungarotoxin sensitive neuronal nAChR (Clarke, 1992). Generally, much more is known about the properties of expressed cloned neuronal AChR subunit combinations than about the properties of different subtypes of neuronal AChRs expressed in intact cells.

The function of neuronal nAChRs seems in many cases to be less straightforward than that of muscle type nAChRs at the neuromuscular junction (Lindstrom, 1996). For example, these receptors, as compared to muscle type ones, are characterized by an even higher Ca^{2+} permeability (Vernino *et al.,* 1994). Thus, Ca^{2+} influx through both α3 and α7 AChRs is likely to play important functional roles (Lindstrom *et al.,*

1995), extending the activity of neuronal nAChRs from simply providing a mechanism for depolarizing the membrane to trigger an action potential (Rathouz & Berg, 1994).

I-3b. Desensitization of the neuronal nAChRs

For neuronal type nAChRs, the general schemes 1 and 2 are also applicable, except for particular kinetic constants (Lindstrom, 1996). The functional role of nAChR desensitization is unclear in central nervous system as much as at the neuromuscular junction. It has been found that a single amino acid change in the second transmembrane domain (which is thought to line the cation channel of $\alpha 7$ neuronal AChRs) produced a receptor which could be activated even when their acetylcholine binding site assumed a desensitized conformation (Revah *et al.,* 1991). It seems worth noting that smoke-related doses of nicotine have little effect on muscle type AChRs but cause extensive desensitization of neuronal $\alpha 4\beta 2$ AChRs which have high affinity to nicotine (Lindstrom, 1996).

The higher Ca^{2+} permeability of the neuronal nAChRs as compared to the muscle type ones (Vernino *et al.,* 1994), together with the known importance of this ion for nAChR desensitization (Miledi, 1980), makes this receptor a suitable model to study the effects of $[Ca^{2+}]_i$ on receptor sensitivity. Neuronal nAChRs are readily available on the rat chromaffin cells in culture (D'Andrea *et al.,* 1993).

I-4. P_{2X} receptors: structure, function and desensitization

It is recognized that ATP, in addition to its essential role to provide a metabolic energy source, may have important physiological and/or pathological functions as an extracellular humoral mediator. One of the three main effects of ATP on cell membrane excitability, together with opening potassium-selective channels and modulation of many other channels (such as voltage-dependent Ca^{2+} channels or AChRs; Bean & Friel, 1990), is activation of ATP sensitive receptors (see Burnstock, 1990). To distinguish them from P1 receptors (activated by adenosine), these receptors were termed P2 receptors, or purinoceptors. P2 receptors are blocked by suramin and are widely divided in two classes, P_{2X} and P_{2Y}, although more recent data suggest that the current classification and nomenclature are undergoing rapid change (Humphrey *et al.,* 1995). The first class, P_{2X} receptors, comprises ligand-gated ionotropic receptor channels, while the P_{2Y} receptors are G-protein coupled and their activation triggers a cascade of intracellular second messengers including Ca^{2+} (Surprenant *et* al., 1995).

ATP-activated conductances were first found in sensory neurons (Krishtal *et al.*, 1983) and in muscle cells (Hume & Honig, 1986); in a variety of cells, including PC12, these channels mediate cationic currents with rapid activation, reversal potential around 0 mV and generally rapid desensitization to high doses of ATP (Krishtal *et al.*, 1983; Bean, 1990). Besides the natural agonist ATP, the P_{2X} receptors subclasses are activated by their selective agonists such as α,β-methylene ATP (P_{2X1}), ATPγS (P_{2X2}, P_{2X4}) and 2-MeSATP (P_{2X3}). P_{2X} receptors are selectively blocked by pyridoxal-phosphate-6-azophenyl-2',4'-disulphonic acid (PPADS).

P_{2X} receptor cDNA has been only recently isolated from rat vas deferens (Valera *et al.*, 1994) and from PC12 cells (P_{2X2} subtype; Brake *et al.*, 1994) by direct expression cloning. Fig. I-2 (from Humphrey *et al*, 1995) shows that P_{2X} receptors (Fig. I-2B) are clearly distinguished from the nAChR superfamily of ligand-gated channels (Fig. I-2A), which have putative hydrophobic leader sequences and long extracellular N-termini. The membrane predicted topography of P_{2X} receptors is rather similar to that of the recently cloned amiloride-sensitive epithelial Na^+ channel subunits (Fig. I-2C).

Expressed in *Xenopus* oocytes and mammalian cells, these channels were found to be cation-selective with relatively high Ca^{2+} permeability, similar to that of smooth muscle cells (Valera *et al.*, 1994). Responses recorded from P_{2X} receptors, heterologously expressed in oocytes and mammalian cells, show remarkable similarity to those of native cells in terms of kinetics, high calcium permeability and agonist/antagonist profile (Evans *et al.*, 1995). The expression studies suggest that functional receptor-channels are formed by homopolymerization of single subunits of the receptor (Humphrey *et al*, 1995). The P_{2X} receptor is of a particular importance physiologically as a mediator of fast transmission in both peripheral and central neurons (Edwards *et al.*, 1992; Evans *et al.*, 1992).

The ability of P_{2X} receptors to desensitize varies between the cell types in which they are expressed (Valera *et al.*, 1994; Evans *et al.*, 1995). Desensitization of these channels and its regulation by Ca^{2+} and other substances (such as, for example, neuropeptides known to affect receptor desensitization; Clapham & Neher, 1984), are much less studied than those of nAChRs. Details of the kinetics of their activation and

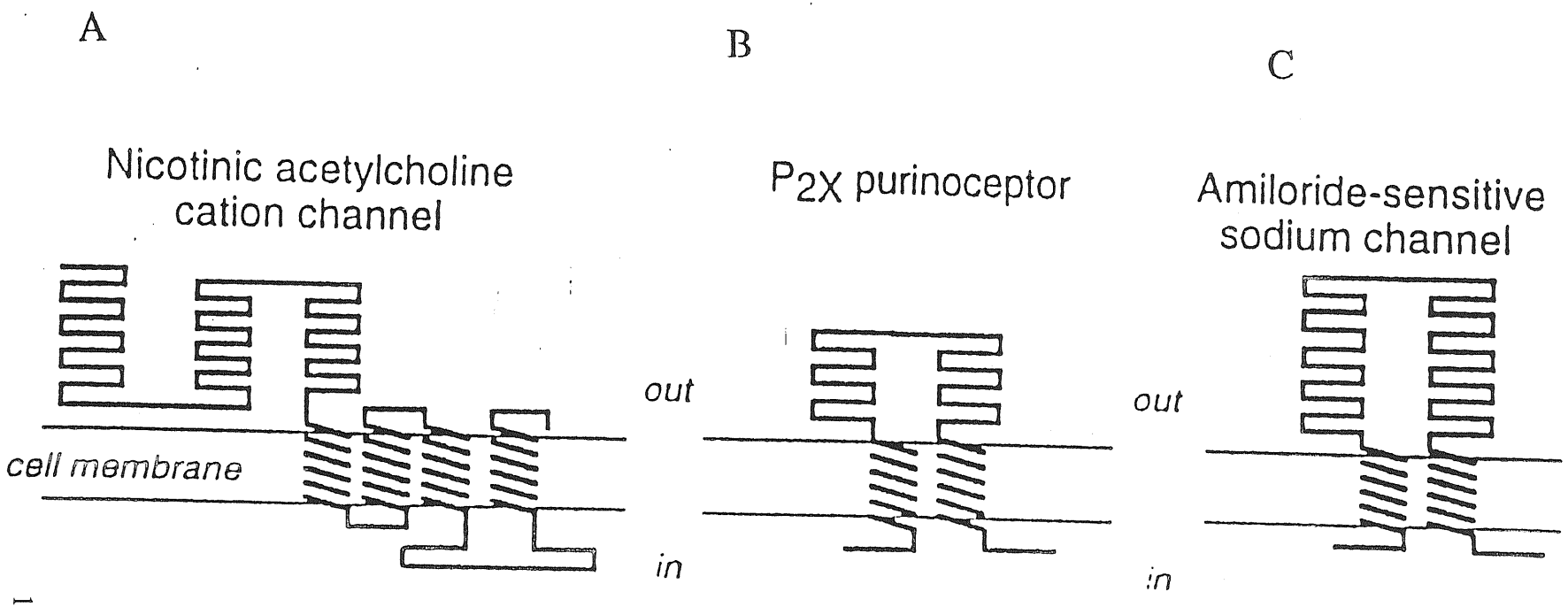
A
Nicotinic acetylcholine cation channel
cell membrane
out
in
B
P2X purinoceptor
out
in
C
Amiloride-sensitive sodium channel

Figure I-2. Schematic diagrams depicting the primary amino acid sequences for three different structural types of channel-forming proteins. Broken lines represent putative transmembrane regions. Note that the P_{2X} receptor (B) topography is more similar to that of amiloride-sensitive sodium channel (C) than that of classical ligand-gated cation channels like nicotinic receptor (A) (From: Humphrey *et al.*, 1995).

desensitization are not known. Considering the high Ca^{2+} permeability of these channels (Rogers & Dani, 1995), they seem to be a useful paradigm to study the role of this cation in regulation of the receptor desensitization.

II. Studying changes in neuronal $[Ca^{2+}]_i$

Transmembrane gradients for the main ions are not only the basis for membrane potential maintenance, but provide (together with electric field) the driving force underlying membrane currents. In the case of Ca^{2+}, its normal extracellular concentration (millimolar range) is 4 orders of magnitude higher than the resting intracellular one (about 100 nM).

II-1. Sources and sinks for $[Ca^{2+}]_i$ in neuronal cells

Opening of Ca^{2+}-permeable ligand-gated channels such as nAChR or P_{2X} receptors would lead not only to calcium influx through them, but also to depolarization of the cell membrane and thus to opening of voltage-activated calcium channels (VACCs). Regardless of the mechanism by which $[Ca^{2+}]_i$ is increased, this elevation can produce important physiological actions such as catecholamine release from rat chromaffin cells (reviewed by Marley, 1988); interestingly, sufficient $[Ca^{2+}]_i$ elevation can be achieved either by nAChR activation in voltage-clamped cells (that is, without activation of VACCs by membrane depolarization; Mollard *et al.*, 1995) or via non-cholinergic pathways by substances such as bradykinin (D'Andrea *et al.*, 1993), a neurophil-derived factor (Shibata *et al.*, 1996) or pituitary adenylate cyclase-activating

polypeptide (PACAP; Przywara *et al.,* 1996). The latter agents mainly act through G-protein coupled receptors triggering cascades of intracellular events involving second messengers which cause release of Ca^{2+} from intracellular stores (Berridge, 1993).

When coexisting, Ca^{2+} influx and intracellular Ca^{2+} release might have complex interactions. These can range from calcium-induced calcium release (CICR) through ryanodine receptors (Fabiato, 1985), and bell-shaped dependence on $[Ca^{2+}]_i$ of inositol-trisphosphate receptors (Bezprozvanny *et al.,* 1991) to induction of Ca^{2+} entry by depletion of intracellular calcium stores (Hoth & Penner, 1992). Similarly, in PC12 cells activation of P_{2X} receptors by extracellular ATP causes membrane depolarization and subsequent secretion of catecholamines (Inoue *et al.,* 1989). In these cells, ATP is shown to produce both Ca^{2+} influx through P_{2X} channels (Raha *et al.,* 1993) and Ca^{2+} release form intracellular stores (Zacchetti *et al.,* 1991).

When $[Ca^{2+}]_i$ increases, the intracellular level of this ion fades relatively quickly (seconds to tens of seconds) to its resting value. This recovery is either due to removal or binding (buffering) of free calcium ions. In bovine chromaffin cells, about 98-99% of the Ca^{2+} entering the cell after a brief depolarization is thought to be taken up by a fast endogenous buffer on a millisecond time scale, while retrieval of Ca^{2+} by pumps and slow buffers occurs on second-long timescale (Neher & Augustine, 1992). Low affinity of this fast buffer makes it possible for even small concentrations of fluorescent dyes to significantly influence the amplitude and especially the time-course of $[Ca^{2+}]_i$ signals (Neher & Augustine, 1992; Helmchen *et al.,* 1996).

II-2. Tools to monitor and manipulate $[Ca^{2+}]_i$

Until the end of 1980s, indirect methods were mostly used to measure $[Ca^{2+}]_i$. One of them is electrophysiological recording of $[Ca^{2+}]_i$-dependent membrane currents, for instance, in whole-cell patch clamp mode. A limitations of such an approach would be that these currents would only monitor $[Ca^{2+}]_i$ immediately beneath the membrane rather than the overall $[Ca^{2+}]_i$ (Lipp & Niggli, 1996). A more reliable measurement of this perimembrane $[Ca^{2+}]_i$ would be provided, for example, by recording electrogenic Na/Ca-exchange which has a liner relation to $[Ca^{2+}]$ and therefore could be successfully combined with a direct method of imaging $[Ca^{2+}]_i$ (Lipp *et al.*, 1990). Application of ion-sensitive electrodes not only allows to measure Ca^{2+} flux through plasma membrane but also to monitor both intra- and extracellular Ca^{2+} concentrations (Thomas, 1978; Orchard *et al*, 1991). However, the real revolution in $[Ca^{2+}]_i$ measurements took place in the late 1980s when a new generation of Ca^{2+}-sensitive fluorescent indicators was elaborated by the group of R.Y.Tsien (Grynkiewicz *et al.,* 1985).

II-2a. Use of fluorescent $[Ca^{2+}]_i$ probes

Fluorescent indicators possess a molecular system of conjugated double bonds which allows the delocated electrons to be raised to a higher molecular orbital (in other words, higher energy level) upon absorption of a photon. The indicator molecule then remains in this excited state for a period of time (usually nanoseconds) and then emits energy as a single photon while the electron drops to the resting energy level. The wavelength of the emitted light is generally longer (and the energy lower) than that of

the excitation light; the difference between the two is called Stoke's shift. For ion-sensitive fluorescent indicators, these spectral properties can be strongly influenced by binding of specific ions. Indicators (or dyes) that exhibit a shift in their excitation or emission spectra upon binding of ions, are called excitation ratiometric or emission ratiometric dyes, respectively. The best known example of emission ratiometric dye is Fura-2 (Grynkiewicz *et al.,* 1985). Fig. I-3A shows fluorescence excitation spectrum of Fura-2 at different free Ca^{2+} concentrations (note that when free Ca^{2+} is increased, emission increases when excited at 340 nm while it remains unchanged when excited at 360 nm).

Conversely, dyes exhibiting changes either in emission or excitation intensity when ligand-binded, are called single-emission or single-excitation, respectively. Such dyes are not suitable for ratiometric measurements, unless combined with other fluorescent molecules (see Methods). Fluo-3 is the most widely used single-emission $[Ca^{2+}]_i$ indicator (Minta *et al.,* 1989). I-3B shows the Ca^{2+}-dependent fluorescence emission spectrum of fluo-3. Fluorescence is undetectable in Ca^{2+}-free solution, while upon the increase in the concentration of this ion the fluorescence increases displaying maximum around 530 nm. Fluo-3 can be used for $[Ca^{2+}]_i$ studies with confocal laser-scanning microscope (CLSM) which allows high resolution optical sectioning of living cells due to physical rejection of out-of-focus fluorescence by a tiny aperture placed in the confocal point of the system (see Methods for details). The ways of loading living cells with fluorescent Ca^{2+} indicators (dialysis via patch-pipette and/or incubation with cell permeant form of the dye) will also be discussed in Methods.

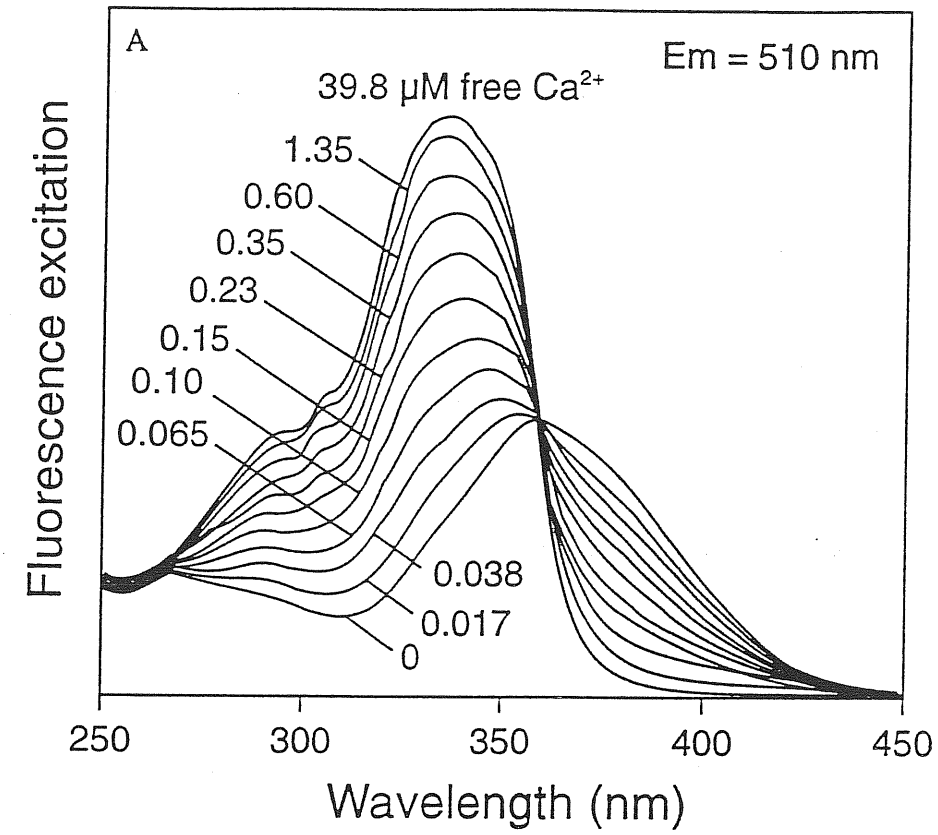
A
Em = 510 nm
39.8 µM free Ca2+
1.35
0.60
0.35
0.23
0.15
0.10
0.065
0.038
0.017
0
Fluorescence excitation
250
300
350
400
450
Wavelength (nm)

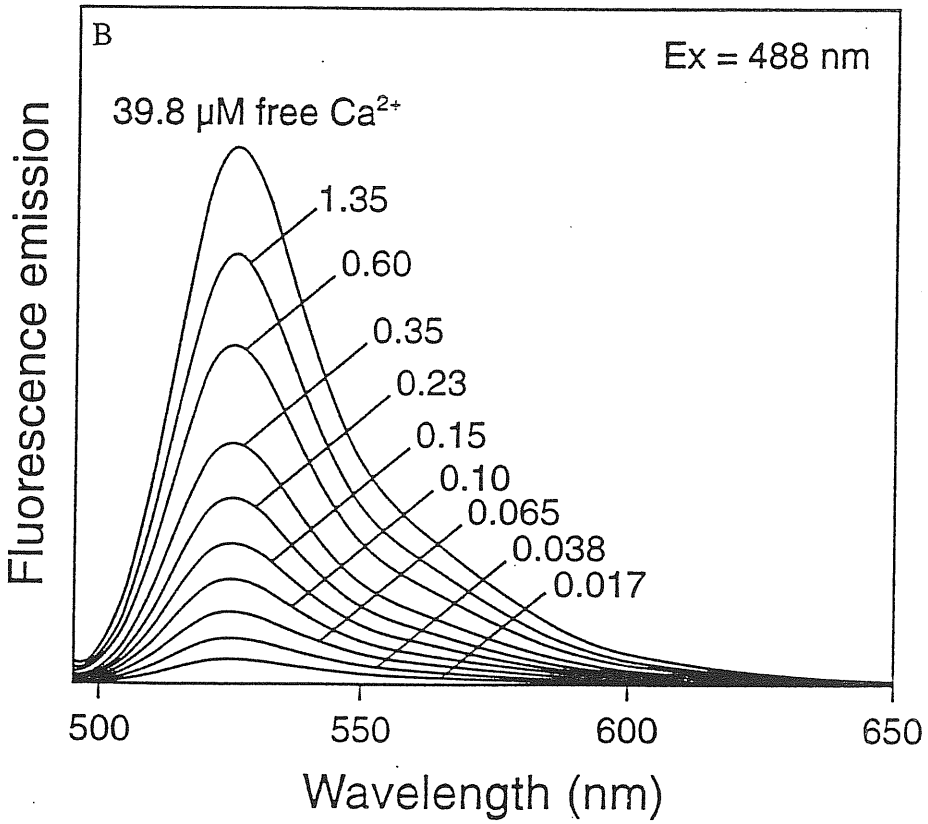
B
Ex = 488 nm
39.8 µM free Ca2+
1.35
0.60
0.35
0.23
0.15
0.10
0.065
0.038
0.017
Fluorescence emission
500
550
600
650
Wavelength (nm)

Figure I-3. Spectral characteristics of fluorescent Ca^{2+} indicators Fura-2 (A) and fluo-3 (B). A, Excitation-emission spectrum of Fura-2 is obtained by changing excitation wavelength between 250 and 450 nm and recording fluorescence at 510 nm at gradually increasing levels of free Ca^{2+}. Note the increase in fluorescence excited at 340 nm while the one excited at 360 nm is unchanged. B, Emission spectrum of fluo-3 excited at 488 nm shows maximal fluorescence around 530 nm which increases with rising free Ca^{2+} level (From: Haugland, 1996).

II-2b. Use of chelators and caged second messengers

There are several methods to control and rapidly manipulate the intracellular concentration of free Ca^{2+} or related second messengers. The first and most widely used method is based on loading cells with Ca^{2+} chelators of known buffering capacity, which allows to calculate and maintain free calcium at a desired level. Like Ca^{2+} indicators, chelators can be applied either via patch-pipette or by incubation with their cell permeant form; buffering capacity and dynamics would range from relatively weak and slow for EDTA and EGTA to strong and fast for BAPTA (Tsien, 1981).

A second class of methods related to controlling $[Ca^{2+}]_i$ is based on so called caged compounds, including "caged Ca^{2+}", caged chelators and caged inositol-trisphosphate (Gurney & Lester, 1987; Kaplan & Somlyo, 1989). The characteristic feature of these compounds is a photo-cleavable group (for example, *o*-nitrobenzyl) that masks their biological activity. Photoactivation of these groups by illumination with bright UV light leads to a rapid photo-degradation of these substances, finally releasing the biologically active compound. This process usually takes milliseconds or even shorter times (Kaplan & Somlyo, 1989). A combination of modern imaging techniques such as confocal microscopy and the application of caged second messengers has been recently used in different systems, such as cardiac myocytes (Lipp & Niggli, 1996b) or neurons (Luscher *et al.,* 1996) and has provided new information about elementary and fundamental events in Ca^{2+}-signaling (Lipp & Niggli, 1996). Use of caged compounds would, however, require the use of either a UV lamp with a fast shatter or a pulse UV laser which were not available in the lab during the present project.

III. Aims of the present thesis

The main goal of this research project was to investigate desensitization of neuronal nAChRs and P_{2X} receptors. For this purpose, rat chromaffin cells and the closely related PC12 cells, expressing these receptors, were cultured. A particular interesting aspect was the modulatory role of intracellular Ca^{2+} in this phenomenon since Ca^{2+} permeates both receptor channels. In fact, inspite of the established importance of this ion for receptor desensitization, few studies have been done to compare, in direct experiments, the timecourse of $[Ca^{2+}]_i$ with that of receptor desensitization and recovery. Therefore, the above aim was addressed by using the combination of the patch-clamp technique and the laser-scanning confocal microscopy (CLSM). The patch-clamp recording would allow to study with high temporal resolution the fast phase of desensitization onset and to follow the recovery of receptor sensitivity, while simultaneous $[Ca^{2+}]_i$ imaging with confocal microscopy would make it possible to detect with high spatial resolution changes in $[Ca^{2+}]_i$ and correlate them with the receptor desensitization.

To reach this aim, the following steps were taken:

1. to set up for the first time the CLSM system which had just been made available to the lab. This objective included optimizing the methods for confocal image acquisition and analysis as well as 3-dimensional object reconstruction with double fluorescence image acquisition and analysis;
2. to set-up the CLSM-based method for dynamic $[Ca^{2+}]_i$ imaging using as ready-available model the rat cultured hippocampal cells. This system allowed me to

investigate the effects of amyotrophic lateral sclerosis IgGs on $[Ca^{2+}]_i$ homeostasis, although this work is not reported in the present thesis;

3. to adapt the CLSM $[Ca^{2+}]_i$ imaging system to work in combination with patch-clamp recording;

4. to implement the combined recording of $[Ca^{2+}]_i$ and membrane current for the study of desensitization of nAChRs and P_{2X} receptors.

Methods

IV. Cell preparation

In order to set-up the confocal microscopy technique which had not been used in the lab before, we first used cultured cells which were routinely available at that time, namely rat hippocampal neurones.

IV-1. Rat hippocampal CA1-CA3 pyramidal neurone culture

According to the method by Malgaroli and Tsien (1992), hippocampi were dissected from 2-4 day old postnatal animals. Isolation and slicing was performed in 100 μM kynurenate and 25 μM 2-amino-5-phosphonovalerate (Tocris Neuramin) to block ionotropic glutamate receptors. Tissue slices were digested with trypsin in the presence of DNase and, after stopping the reaction with trypsin inhibitor on ice, triturated in dissection medium containing DNase. After two successive centrifugations at 500 rpm the resuspended cell pellet was distributed to 12 mm Nunc Petri dishes previously coated with 20 mg/ml polyornythine and 2 % Matrigel (Collaborative Research), each one containing 2 ml of foetal calf serum supplemented, modified minimal essential medium (Gibco). Experiments were performed on large (20 μm somatic diameter) pyramidal-like neurones (5-15 days in culture).

These cells were used at the initial stage of the project to find out the appropriate conditions for confocal imaging of $[Ca^{2+}]_i$ following pre-loading with the cell

permeant form of the fluorescent dye fluo-3 (see details below). These cells were not however used for combined patch-clamping and confocal $[Ca^{2+}]_i$ imaging for the following reasons: first, hippocampal cultures comprise a heterogeneous cell population. Second, these cells possess extensive processes which may introduce "space-clamp" problems under voltage-clamp conditions and uneven dye loading. Third, continuous superfusion with TTX should be used to block interneuronal communication via synaptic contacts. Hence, hippocampal cell cultures were employed to study changes in $[Ca^{2+}]_i$ in response to NMDA (Andjus *et al.,* 1996a), and effects of ALS IgGs on P/Q-type calcium channels (Andjus *et al.,* 1996b) and on calcium homeostasis in general (Andjus *et al.*, 1996c). The preliminary data and experience obtained with these cultures were thus applied to the project with chromaffin and PC12 cells.

IV-2. Rat chromaffin cell culture

Rat chromaffin medullary cells were cultured according to the method of Brandt *et al.* (1976). Ether-anaesthetised female rats (200-250 g body weight) were killed by decapitation and their adrenal glands were removed, dissected free of the cortex, and rinsed in a medium (pH 7.2) containing (mM): NaCl 137, KCl 3, Na_2HPO_4 0.7, HEPES 25, glucose 10, and 350 units/ml of penicillin and streptomycin. Cells were dissociated by treating adrenal tissue fragments at 37°C with collagenase A and DNase I (0.5 units/ml and 10 μg/ml, respectively) and drawing them gently up and down a Pasteur pipette every 15-20 min. The cell containing suspension was centrifuged at 500 *g* for 4 min, and rinsed twice with the HEPES-buffered medium. Finally, cells were suspended in Dulbecco's modified Eagle's medium supplemented

with 10 % foetal calf serum, plated on poly-Lysine (1.25 mg/ml)-coated Petri dishes, and cultured for 1-3 days under an atmosphere containing 5 % CO_2.

IV-3. Pheochromocytoma (PC12) cell-line

Rat PC12 cells (Greene & Tischler, 1976) were kindly provided by the C.N.R. Institute of Neurobiology, Rome. Cells were grown in a 5% CO_2 atmosphere at 37° C in RPMI medium (Gibco; Milan) supplemented with 10 % heat inactivated horse serum (Gibco; Milan) and 5 % foetal calf serum (Seromed; Berlin) with addition of penicillin/streptomycin (200 units/ml). Culture medium was changed twice a week. On the day of the experiment, cells were detached from the bottom of the dish and dissociated by passing them through a 0.9 mm o.d. needle, and subsequently transferred to 24 mm Petri dishes covered with poly-Lysine (1.25 mg/ml). After 40-60 min the culture medium was replaced with control solution containing (in mM): NaCl 132, KCl 5, $MgCl_2$ 2, $CaCl_2$ 2, glucose 10, HEPES 10 (pH was adjusted to 7.4 with NaOH).

V. Confocal laser-scanning microscopy

V-1. Theory and background of confocal microscopy

Confocal microscopy has gone through various stages of development and popularity (Inoue, 1995). In conventional light microscopy, the numerical apertures (NA) of the objective and condenser are known to be important for image resolution. The objective NA is a product of the sine of the half-angle of the cone of light acceptable

by the objective lens and the refracive index of the medium between the specimen and the objective lens. The condenser NA similarly depends on the half-angle of light emerging from the condenser lens and the refractive index of the medium between the condenser and the medium. According to Abbe (1884), the minimal resolvable object length is equal to the wavelength of illuminating light (in vacuum) divided by the sum of the objective NA and the condenser NA (NA_{obj} + NA_{cond}). The image of an infinitely small, luminous object point consists of a circular diffraction image with a central bright disk and progressively weaker concentric dark and bright rings. The light intensity along the radius of these diffraction rings is called point spread function of the lens. Point spread function of the complete optical path is an important characteristic of a microscope. The images of two luminous points are said to be resolved if the distance between the points is larger or equal to the radius of the central bright disk. The impact of the quality and NA of the condenser on the resolution of point objects was addressed by Hopkins and Bahram (1950).

Similar considerations could be applied to the axial resolution (measured along the optical axis of the microscope). Luminescent objects that are out of focus produce unwanted light. This out-of-focus light is collected by the objective and expands the apparent depth of field (which is in theory equal to the axial resolution for brightfield microscopy).

These theoretical considerations set conditions for an approach that would allow to effectively eliminate out-of-focus light and decrease the illuminated field (field of view).

In 1957, a young postdoctoral fellow at Harward Univerity Marvin Minsky applied for a patent for a stage-scanning confocal optical microcope (see Minsky, 1988). In that system, the conventional microscope condenser is replaced by a lens identical to the objective one. Two pinholes are used to restrict both illumination and image field. The specimen is scanned through a point of light by moving the former over short distances in a raster pattern. Signal from a photoelectric cell forms point-by-point image of the specimen on a long-persistence oscilloscope. As Minsky points out, the unwanted non-focal light is rejected by the pinhole of the system to an extent never realized before.

In 1960, Maiman announced the developement of the first operating laser. Shortly thereafter, two types of laser application were sought in microscopy. One took advantage of the high degree of monochromaticity and the attendant long coherence length (temporal coherence), which makes lasers an ideal tool to produce holograms. The other practical application of lasers in microscopy is their use as an intense, monochromatic light sourse. While monochromaticity and intensity of the beam fit the requirements of confocal microscopy, the coherence length must be reduced to eliminate interference from out-of-focuse defects and to increase resolution. One of the best ways of meeting this requirement is to use condenser aperture, which allows to reduce the temporal coherence of illumination at the object plane to less than the response time of the image detector. Nevertheless, lateral coherence is maintained.

Progress in this direction culminated in the developement of the *confocal laser-scanning microscope* (CLSM; Aslund *et al.,* 1983) and the publication of its biological application by Carlsson et al. (1985) and Amos *et al.* (1987). CLSM was a

microscope that could generate clear, thin optical section images (totally free from out-of-focus fluorescence) from whole cells and at NAs as high as 1.4. A series of optical sections could be converted into and displayed as a stereo-pair or projection to elucidate the 3-dimensional structure of the cell (Inoue, 1995).

V-2. The Multiprobe 2001 system

One of the commercially available CLSM, Multiprobe 2001 from Molecular Dynamics, provides many of the above mentioned advantages. Multiprobe 2001 is a point-scanning microscope, which ensures the highest possible "confocality" as compared to slot-scanning or real-time confocal systems. Perfect alignment is crucial for successful confocal imaging, which is achieved by minimizing the number of optical elements and using a very stable platform. Direct connection of the Ar/Kr laser to the optical system without using an optical fiber preserves single-mode and polarisation of the beam. The confocal effect is achieved as illustrated in Fig. M-1. The laser beam is focused to a focal point by the lenses of the incorporated, inverted Nikon TMD microscope. Very little laser light falls on other points in the focal plane. Laser light with a decreased density reaches points below (point A) and above the focal plane. Both fluorescent and reflected light from the sample pass back through the microscope. The light reflected from the specimen or other parts of the optical path is rejected by the primary beamsplitter which allows through the longer-wavelength fluorescent light. The microscope and the optics of the scanner compartment focus the light from the focal point to a second point, called the confocal point. The pinhole aperture (see Fig. M-1), located at the confocal point, allows light from the focal point (solid lines) to pass through to the detector. Light emitted outside

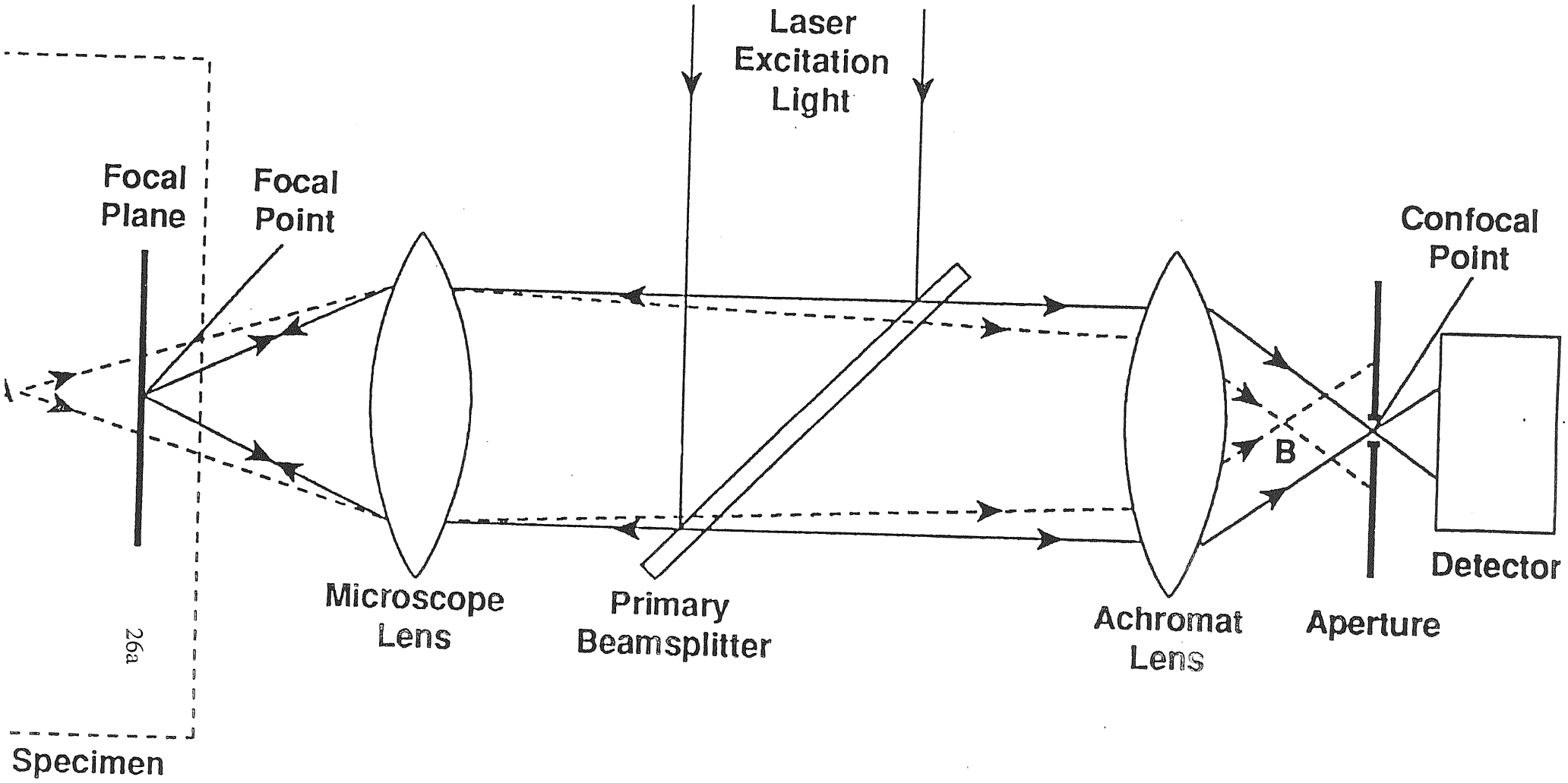
Laser
Excitation
Light
Focal
Plane
Focal
Point
Confocal
Point
B
Microscope
Lens
Primary
Beamsplitter
Achromat
Lens
Aperture
Detector
Specimen

Figure M-1. Focal point and confocal point in confocal system. Note that very little laser light reaches points below (for example, point A) or above the focal plane, and that the light emerging from these points is rejected by the apperture placed in the confocal point. (From: The CLSM System, Molecular Dynamics).

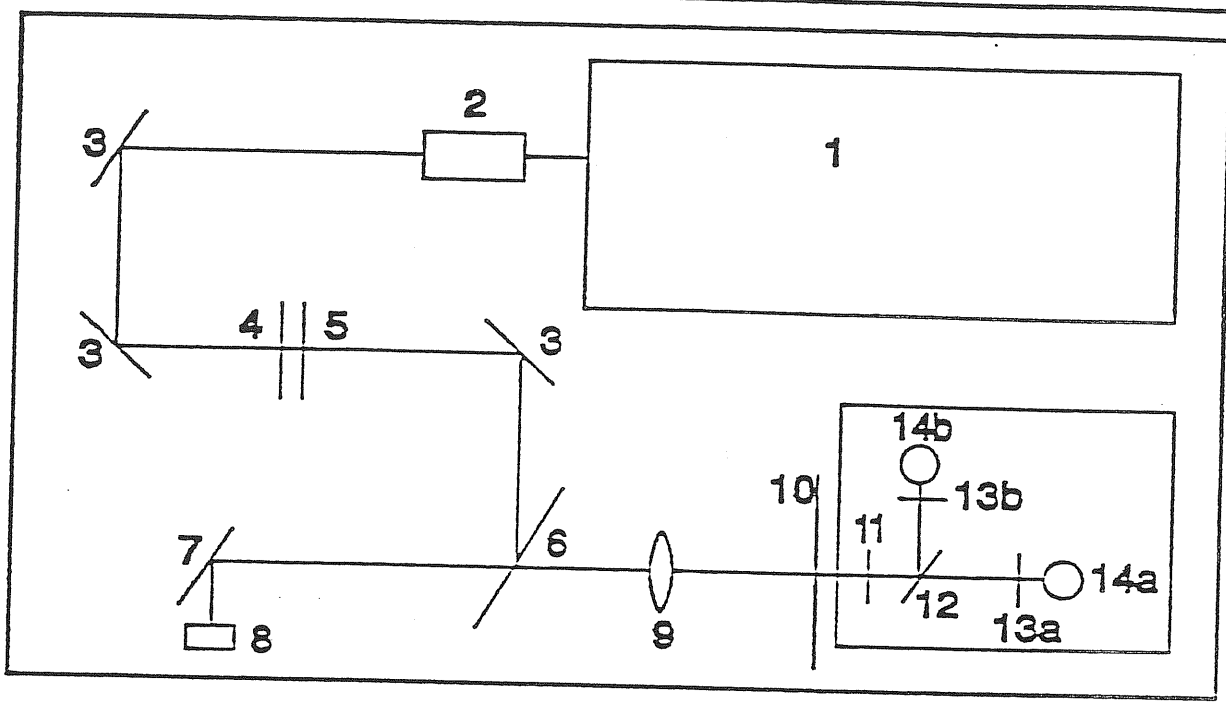

1. Laser
2. Beam expander
3. Mirrors
4. Laser wavelength filter wheel
5. Laser attenuation filter wheel
6. Primary dichroic beamsplitter wheel
7. Slow-scanning mirror
8. Fast-scanning mirror
9. Achromat lens
10. Confocal aperture wheel
11. Barrier filter
12. Secondary dichroic beamsplitter

13a. Detector 1 filter

13b. Detector 2 filter

14a. Photomultiplier detector 1

14b. Photomultiplier detector 2

Figure M-2. Light path and optical components in the optical compartment of Multiprobe 2001 CLSM. The light travels from the laser (1) to the fast scanning mirror (8), passes through the microscope to the specimen and back to the scanning mirrors (8,7), and is then directed to the detectors (14). (From: The CLSM System, Molecular Dynamics).

the focal point is not in focus at the confocal point (light from A is focused to B, see dashed lines) and is therefore rejected by the aperture.

The complete optical path of the Multiprobe 2001 system is shown in Fig. M-2. The laser (1) emits a collimated (parallel) beam of light. The beam expander (2) then increases the diameter of the beam while keeping the rays of light parallel. The expanded beam fills the back aperture of the objective. Directed by two mirrors (3), the laser beam is then filtered and attenuated. Filtering by the laser wavelength filter wheel (4) allows to select one or a combination of several wavelengths used for different fluorescent dye excitation protocols. By attenuation of the beam intensity through the laser attenuation filter wheel (5) it is possible to adjust the effective laser power in order to avoid cell damage or dye bleaching. The first function of the primary dichroic beamsplitter is to direct the expanded beam of light toward the scanning mirrors (7, 8). The mirrors direct the light through the microscope to its focal point. The emitted fluorescent light with a wavelength longer (due to the Stoks shift) than that of the laser light travels back through the microscope and follows, in reverse, exactly the same path the laser beam followed. The fluorescent light passes through the primary beamsplitter (6) while the laser beam with a shorter wavelength is cut off. The achromat lens (9) focuses the fluorescent light to the confocal point, and light in focus at the confocal point passes through the pinhole aperture (10) and the barrier filter (11) to the photomultiplier detectors (14a,b) (photomultiplier tube, PMT). The photomultiplier detectors convert light to an analog (continuously varying) signal, which is converted to a digital signal in the electronics control unit and passed on to the computer. When fluorescence is studied at two wavelengths, the secondary

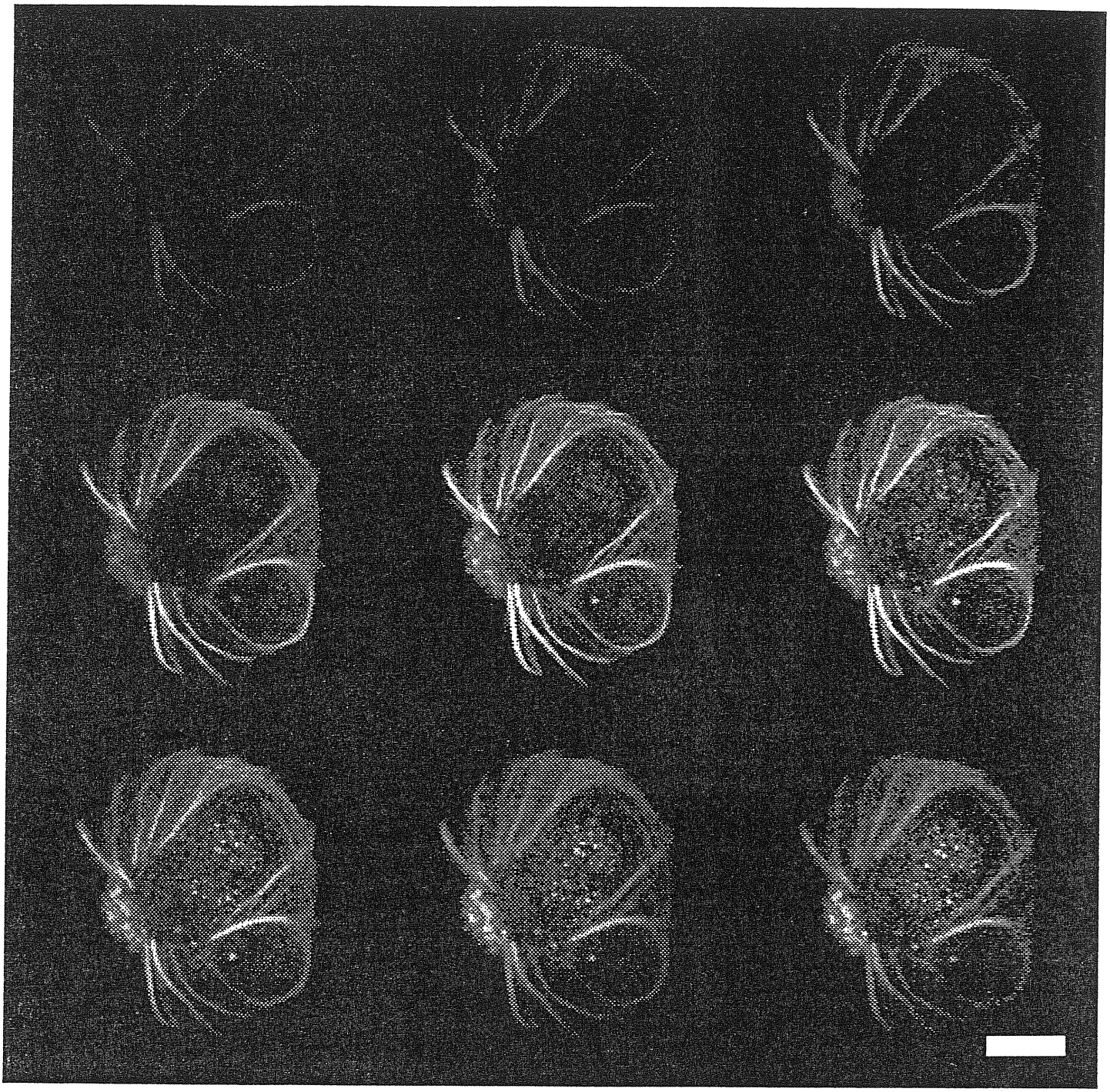

Figure M-3A. Section series of COS cells stained with anti-τ monoclonal antibodies using biotinylated secondary antibodies coupled to fluorescein and scanned with 1 μm vertical step. (In collaboration with Dr. Luisa Fasulo, Molecular Biology Lab, SISSA). The calibration bar = 10 μm.

beamsplitter (12) is used to separate light detected by PMT1 and PMT2. Band separation is enhanced by two detector filters (13a,b).

During scanning, the CLSM acquires an optical section in a sweeping pattern by moving these two perpendicular mirrors (7,8 in Fig. M-2), systematically recording from individual points called *voxels* (single volume elements in the digitized volume). The movement of the fast-scanning mirror (8) only results in scan along a single line and provides high temporal resolution (10 ms per line) which can be used to obtain information about fast changes in voxel fluorescent signals along that line. Two-dimensional section is scanned by stepwise shifting between the single lines using the slow-scanning mirror (7). The ImageSpace software displays an image made up of the scanned voxels. The CLSM can scan a series of horizontal sections by moving the focal plane through the sample. Three pre-set pinholes of 50, 100 and 200 μm are available, providing thus a possibility to choose optimal confocal resolution *versus* signal/noise ratio.

For a fixed fluorescent specimen, the section series mode can be used to reconstruct the 3-dimensional structure while having all voxels scanned in focus, and view the 3-D image from different angles or cut different planes. An example of section-series and projection view is shown in Fig. M-3. COS cells were stained with the 7.51 anti-τ monoclonal antibodies using biotinylated secondary antibodies coupled to fluorescein to study the 3-D structure of the filaments, in collaboration with Dr. Luisa Fasulo, Molecular Biology Lab, SISSA. Cells were scanned as section-series (Fig. M-3A) with a 1 μm vertical step. Upon image processing, series were passed to the

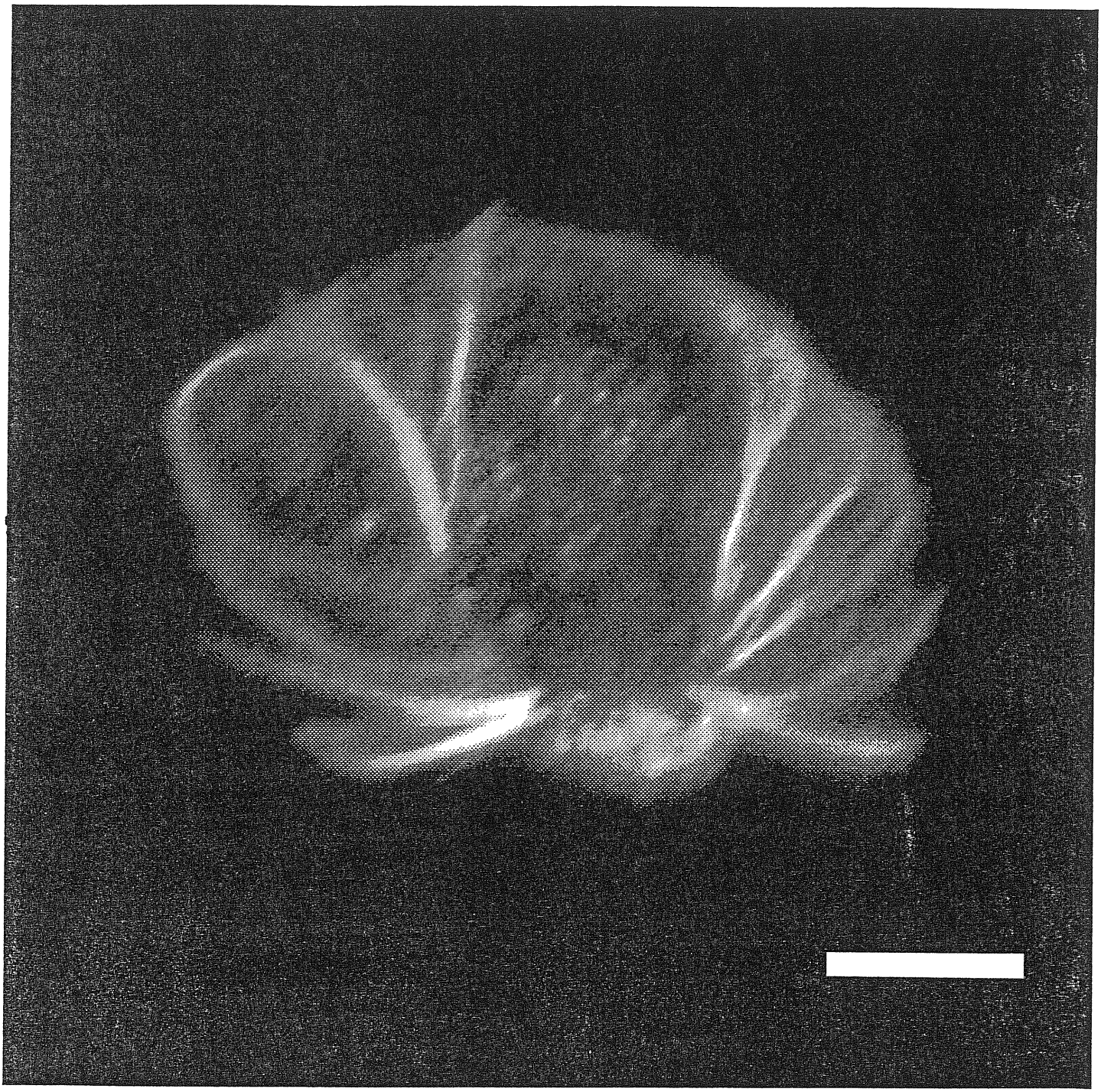

Figure M-3B. The series of Fig. M-3A, presented as a projection ("look-through" mode) at an angle different from that of scanning. The calibration bar = 10 μm.

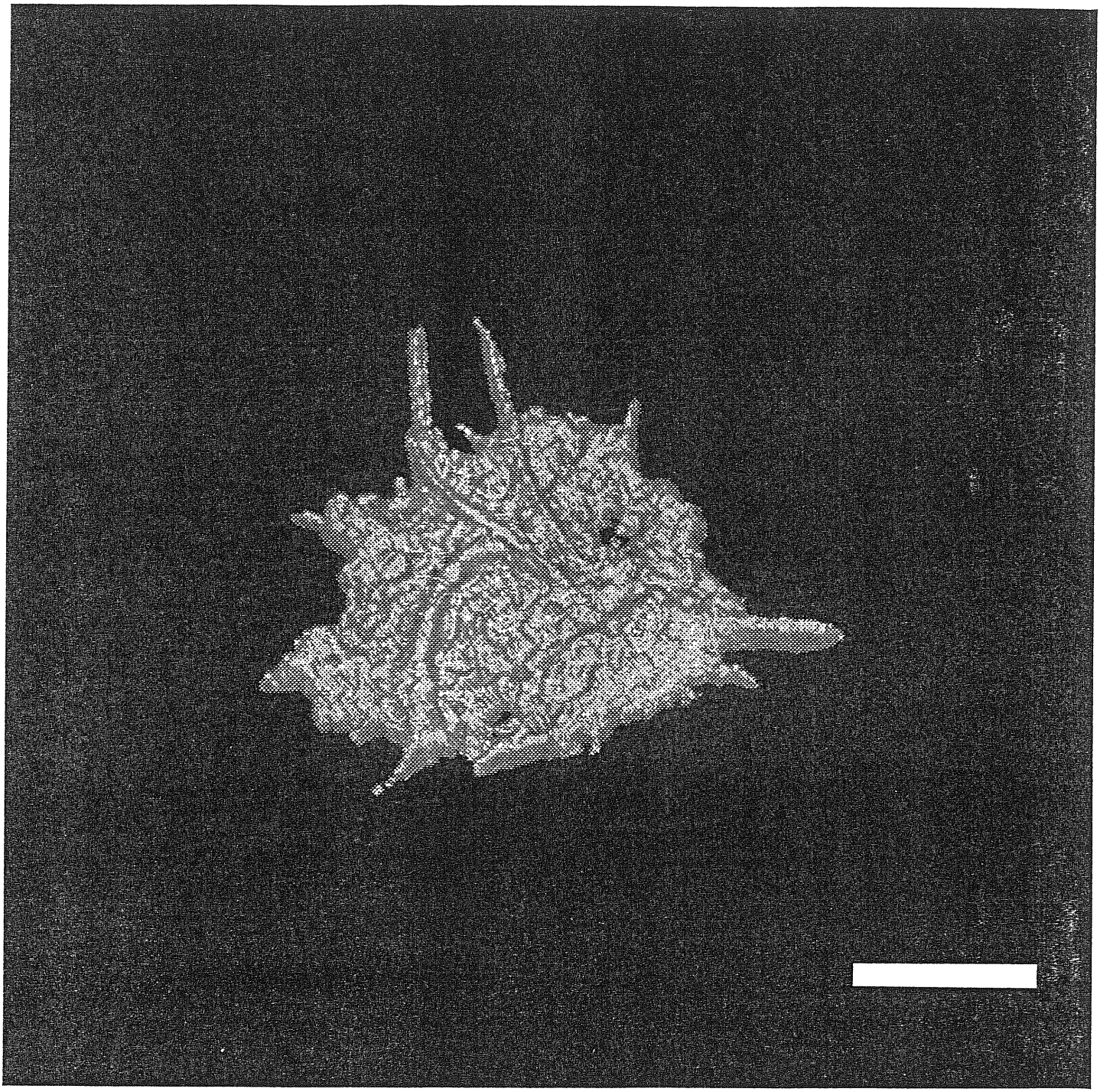

Figure M-4. The structure of a COS cell different from the one in Fig. M-3 presensted in surface reconstruction mode. The calibration bar = 10 μm.

VolumeWorkbench software (part of ImageSpace, Molecular Dynamics) for the 3-D reconstruction. The projection can be generated at an angle different from that of scanning, as shown in Fig. M-3B in look-through mode. The structure of another COS cell (different from the one in Fig. M-3) is presensted in surface reconstruction mode (Fig. M-4).

For multispectral excitation of dyes or dye mixtures, several combinations of the three laser wavelengths could be chosen including 488, 488/568, 488/647 nm or all three of them. For example, a preparation stained with two dyes based on fluorescein (green fluorescence) and rhodamine (red fluorescence) can be scanned with a laser beam consisting of two wavelengths (488 and 568 nm) where the first light frequency is used to photo-excite the molecules of fluorescein whereas the second one for the rhodamine molecules. In the optical way from the preparation to the PMTs, the 488 nm band will be reflected back by the primary beamsplitter and the first optical filter (510 long-pass) immediately next to the confocal pinhole while the 568 nm band together with the fluorescent light will pass through. Both green fluorescence and 568 nm band will then be reflected by the secondary beamsplitter to the PMT1, where the informative green fluorescence will be separated from the excitation light by a band-pass filter (530±30 nm). The red fluorescence which passed through the secondary beamsplitter will be then collected by the PMT2, with additional filtering over 590 nm threshold. Thus, fluorescence from the specimen can provide two signals recorded simultaneously which contain information about 2- or 3-dimensional distribution and co-localisation of the two dyes. In Fig. M-5, AtT 20 cells are shown incubated with monoclonal antibodies against ACTH (CY3, red fluorescence) and then with affinity purified antibodies against Rab3d (FITC, green fluorescence), in collaboration with

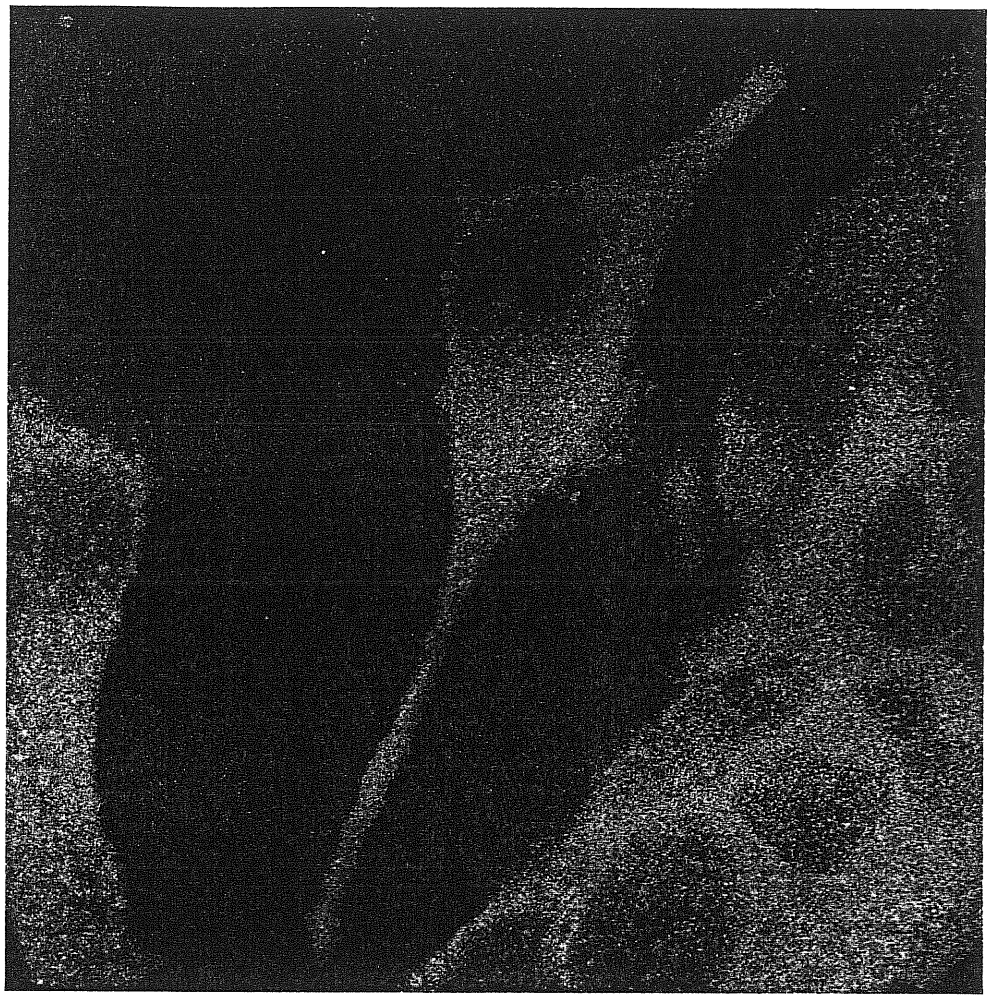

Figure M-5. An AtT 20 cell incubated with monoclonal antibodies against ACTH coupled to CY3 (red) and with affinity purified antibodies against Rab3d (FITC; green). Fluorescence recorded at both channels is presented in pseudo-colors. Note that the regions of poor co-localization are either green while the area of co-localization is yellow (bottom right). In collaboration with Dr. Giovanna Baldini, Morphology Department, University of Trieste. The image size = 100 X 100 μm.

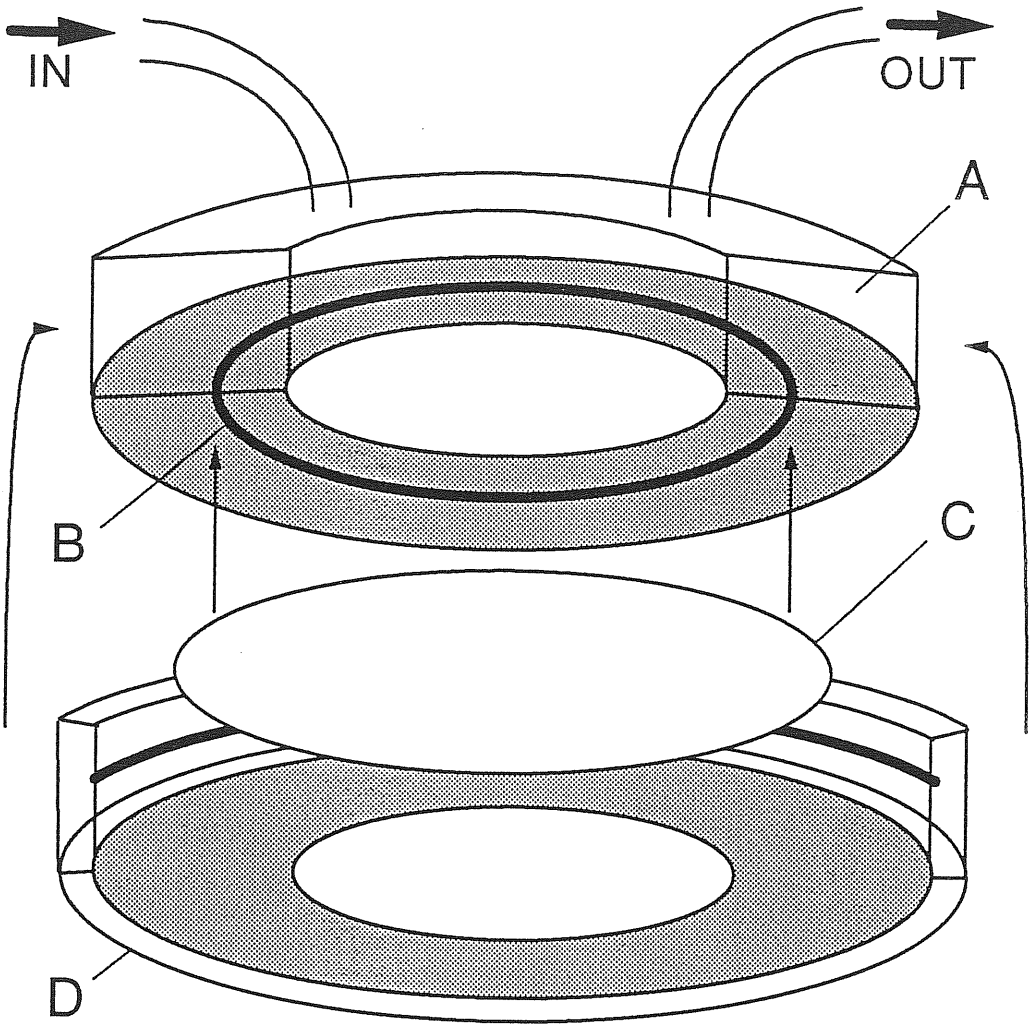
IN
OUT
A
B
C
D

Figure M-6. Superfusable bath for studies of cells growing on glass coveslips. A, plastic frame of 1 ml inner volume; B, O-ring fixed to the bottom of the frame; C, cell-containing round glass coverslip placed on the O-ring; D, metal cap pressing the coverslip against the O-ring; IN and OUT indicate perfusion and suction tubes, respectively.

Dr. Giovanna Baldini, Morphology Department, University of Trieste. Double-fluorescence image presented in pseudo-colors shows lack of co-localization as red or green segments while the area of co-localization is yellow (bottom right).

This method can also be applied to imaging molecules which contain two fluorescent components with distinct spectral characteristics. One of such molecules, CalciumGreen-TexasRed dextran available from Molecular Probes, provides a tool for ratiometric confocal measurements which will be discussed later.

V-3. Specificity of living-cells imaging

Living cells must be loaded with a $[Ca^{2+}]_i$ indicator in a way that does not affect their viability or disrupt their functions. The widely used $[Ca^{2+}]_i$ indicator fluo-3 (excitable with visual light) was first introduced (Minta *et al.,* 1989) in two forms. The cell-impermeant form (for instance, pentapotassium salt) can be either loaded via a patch pipette or microinjected. Conversely, the cell-permeant form of the dye (acetoxymethyl ester, AM), is bath-applied, diffuses into cells and is hydrolized intracellularly to release fluo-3 (Kao *et al.,* 1989). In early experiments on rat hippocampal pyramidal cells, cells were incubated for 45-60 min at 37°C in 2 μM fluo-3/AM (Molecular Probes) in the presence of 0.5 % bovine serum albumin and 0.05 % Pluronic-F127 in the perfusion solution containing (in mM) NaCl, 132; KCl, 3.5; $MgCl_2$, 1; $CaCl_2$, 2; glucose, 10; Hepes, 10; pH 7.4. Sufficient loading with fluo-3/AM for both chromaffin and PC12 cells required higher fluo-3/AM concentration (5 μM) and appeared to be independent of the presence of bovine serum albumin and Pluronic-F127 which were therefore omitted. The combination of the two loading methods can also be used in special cases as indicated in the Results section.

Unlike scanning fixed specimens, studies of living cells with confocal microscopy require additional facilities. The first one is continuous bath superfusion to maintain living cells in culture. Such a superfusion system should be compatible with the inverted microscope stage of the Multiprobe 2001. The bottom of the bath should be transparent for visible light and its optical density should be corrected for. When using a dry 40X objective with a correction ring, a standard Petri dish can be used as a bath, with gravity perfusion input and grounded suction tube. However, confocal image resolution is often compromised by the use of a 40X objective which has numerical aperture of 0.56. In fact, it only allows 0.16 μm as minimal pixel (single digitized surface element) size (resolving power 0.27 μm) while the brightness of the image is reduced due to the low NA. A much higher resolution (0.06 μm minimal pixel size; resolving power 0.17 μm) can be achieved using the oil-immersion 100X objective with the very high numerical aperture of 1.4, which provides brighter images and therefore requires lower laser power and lower intracellular dye concentration; this reduces dye bleaching and excessive $[Ca^{2+}]_i$ buffering by the dye. Vertical resolution of this lens is also better than that of 60X one (0.54 *vs* 0.97 μm).

A considerable limitation of the oil-immersed 100X objective is its short working distance (less than 1 mm) which does not allow the use of this microscope with a standard Petri dish with a bottom thickness of 1.2 mm. To meet this requirement, a special bath was designed with the advice of Dr. Paola D'Andrea (University of Trieste, Department of Biochemistry) and constructed for the setup (Fig. M-6). The bath consists of: 1) a round plastic frame (A) of 1 ml inner volume with an O-ring (B)

fixed to the bottom; 2) the cell-containing round glass coverslip (C) placed on the O-ring and pressed against it by a metal cap (D) to ensure tight contact. Being only 0.17 mm thick, the coverslip bottom of the bath allows use of the short-working distance 100X objective and requires minimal optical density correction. The bath is also readily accessible to perfusion (gravity flow input and suction pipette are indicated by IN and OUT in Fig. M-6) or for introduction of electrodes and micropipettes.

Another important requirement for some cells is temperature control. This was achieved by passing the perfusion input tube through a water-heated 50 ml syringe. Effective control of the temperature at about 37°C was necessary, for example, for optimiziong the optical recording of exocytosis in response to ATP application on PC12 cells. For this purpose, the fluorescent membrane marker FM1-43 (Molecular Probes; Betz & Bewick, 1992) was added extracellularly at the concentratioon of 5 μM. Confocal section of the stained cell membrane appeared as a ring (Fig. M-7). Sections were scanned in a series at a rate of 3 s/section with a zero vertical step. The membrane area was selectively analysed and its fluorescence is presented as function of time in Fig. M-8. In response to a 2 s pulse of 5 mM ATP from a micropipette, the FM1-43 fluorescence increased stepwise with a timecourse comparable with the time resolution of the system in the section series mode (3 s per section) presumably due to exocytotic increase in the cell membrane area. This increase was usually about 5-10 % of baseline fluorescence and was clearly distinguishable from background noise.

V-4. Rapid scan mode of confocal $[Ca^{2+}]_i$ imaging

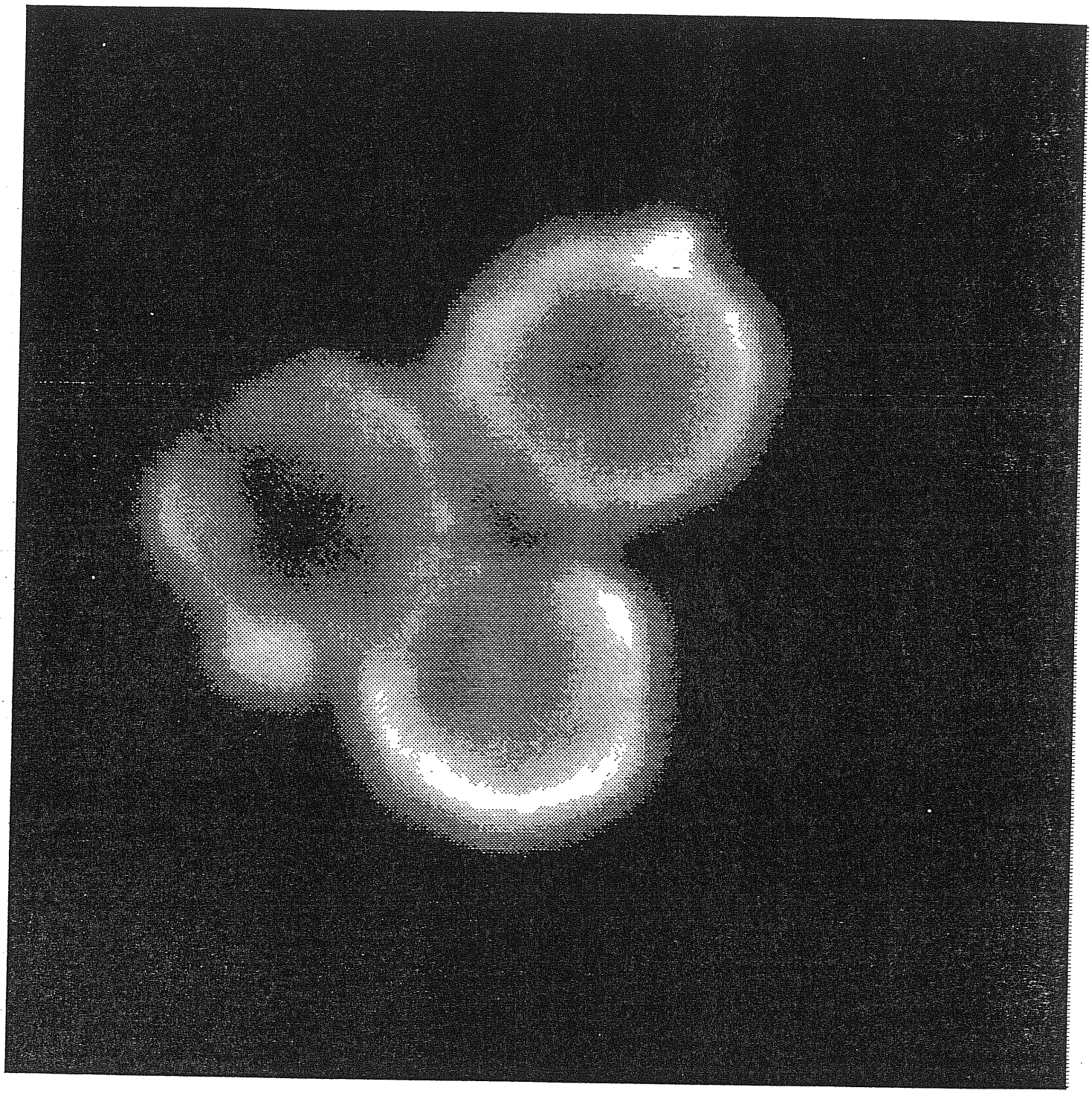

Figure M-7. Confocal image of PC12 cells membrane stained with the non-permeant membrane indicator FM1-43. The fluorescent dye was added to the superfusion solution at the concentration of 5 μM. Section thickness is 0.5 μm, pixel size is 0.16 μm.

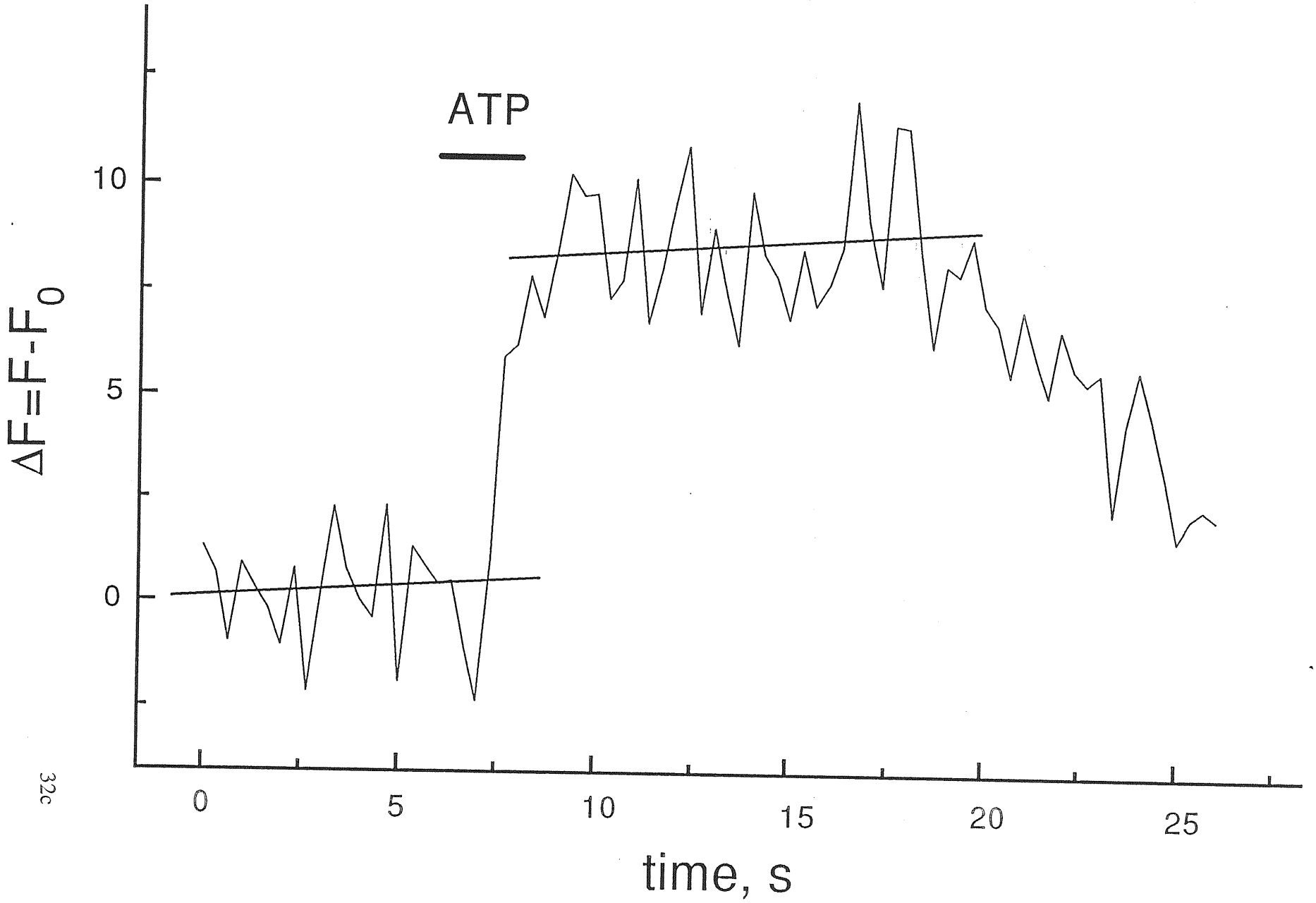
ATP
10
5
0
ΔF=F-F0
0
5
10
15
20
25
time, s

Figure M-8. Time plot of fluorescence of FM1-43. Baseline fluorescence (F_0) is subtracted from the overall fluorescence (F) to obtaine the fluorescence change over baseline (ΔF). A 2 s pressure application of ATP is indicated by a horizontal bar. Note a rapid increase in FM1-43 fluorescence (and in the cell membrane area, presumably, due to catecholamine release) which persists for about 10 s and then gradually fades back to the baseline.

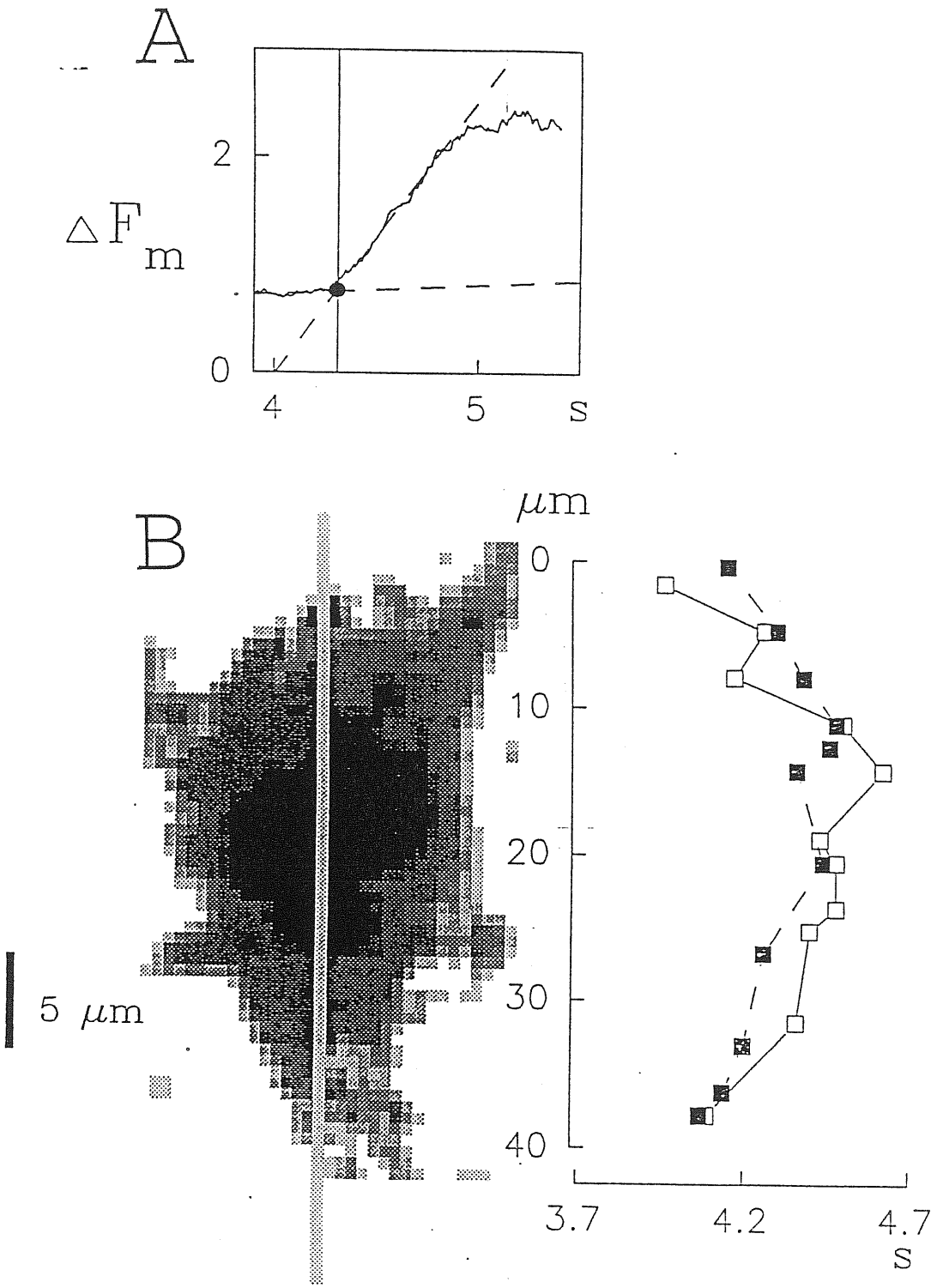
A
2
ΔF
m
0
4
5
s
B
μm
0
10
20
30
40
5 μm
3.7
4.2
4.7
s

Figure M-9. $[Ca^{2+}]_i$ waves evoked in rat hippocampal pyramidal neurone by pressure application of 0.1 M KCl or 0.1 mM glutamate loaded with fluo-3. A, The latency of a response to glutamate is calculated from the beginning of the scan to the foot of the response. B, 32x64 pixel image of the cell (pixel size 0.63 μm) provides the environment through which the vertical line scan (1x128 pixel, pixel size 0.32 μm; temporal fluorescence changes are analysed every 0.32x1.6 μm along the scan line). Graph in B, plot of response latency versus the position on the line of scanning. Note that the response to glutamate (filled symbols) or KCl (open symbols) first appeares simultaneously near the perimembrane area of the basal and apical dendrites and then spread to the rest of cytoplasm and the nucleus.

In the rapid 32-line scanning mode, the overall cell "section" is scanned at 320 ms rate (10 ms per line), while the spatial resolution is minimal (32 x 64 pixels). Thus, the scan-series mode is valid not only for those applications in which a higher spatial resolution is required and the temporal aspect can be compromised, but also for dynamic imaging simultaneously at two wavelengths, which is not available in rapid-scan mode.

When the number of scanned lines is reduced to 1, the maximal rate of 100 Hz can be reached with the Multiprobe 2001 system. This mode can be most successfully applied when information about fast changes in one-dimensional space are sought. For example, many groups have reported $[Ca^{2+}]_i$ waves (both linear and circular, or of more complex shape) and oscillations (see Lechlester & Clapham, 1992; Berridge, 1993). Unidirectional waves can be studied by repetitive scanning of a single line within the cell at a rate high enough to follow the waves. Even in the case of "non-oscillating" cells (in terms of $[Ca^{2+}]_i$) like neurones, single-line rapid scan can help to reveal transient $[Ca^{2+}]_i$ gradients during or immediately after the activation of ligand-gated channels such as nAChRs, P_{2X} or ionotropic glutamate receptors. Analysis of the "wave" spread along the cell axis helps to reveal the triggering factor for $[Ca^{2+}]_i$ increase, whether it is transmembrane Ca^{2+} influx or its release from internal stores. Fig. M-9 B shows an example of such analysis of $[Ca^{2+}]_i$ wave evoked in a fluo-3 loaded rat hippocampal pyramidal neurone by pressure application of 0.1 M KCl or 0.1 mM glutamate. The graph of Figure M-9B (plotting response latency versus cellular topography along the line of scanning) shows that the response to glutamate (filled symbols) or KCl (open symbols) first appeared simultaneously near the perimembrane area of the basal and apical dendrites and then spread to the other areas

of the cell. The latency was calculated from the foot of the response as indicated in Fig. M-9A. It is evident that the $[Ca^{2+}]_i$ increase initiated in the perimembrane area and then gradually involved the rest of cytoplasm and the nucleus.

V-5. Ratiometric confocal $[Ca^{2+}]_i$ measurements

The Multiprobe 2001 CLSM is equipped with the visual light Ar/Kr laser and cannot therefore be used with the ratiometric dye Fura-2 which operates in the UV range. CLSMs which use UV laser (Bliton & Lechleiter, 1995) are still relatively uncommon and very expensive. Initially, attempts were thus made to employ the present system to express the results in terms of calcium concentrations, namely: 1) co-loading cells with two separate dyes with different $[Ca^{2+}]_i$ sensitivity and distinct spectral characteristics, and 2) developing a molecule containing such pair of fluorescent dyes.

The first of the two approaches was proposed by Lipp and Niggli (1993) who loaded cells with a 1:2 mixture of fluo-3 and Fura Red (cell permeant AM form). Fura Red is a calcium indicator excited at 488 nm (the same wavelength as fluo-3) and emitting light around 660 nm which can be clearly separated from the fluo-3 emission (Fig. M-10; Haugland, 1996). Besides, fluorescence of Fura Red decreases upon Ca^{2+} binding. Assuming co-localization of the dyes (which is not, however, the case for all cell types), pixel-by-pixel division of their fluorescent images will provide correction for the artifact of heterogeneous dye loading which cannot be eliminated using a non-ratiometric dye alone. In fact, in the latter case the fluorescence intensity of a sample voxel is mainly determined by two factors: $[Ca^{2+}]_i$ and the dye concentration. Calibration of such a signal in terms of $[Ca^{2+}]_i$ becomes impossible if the dye

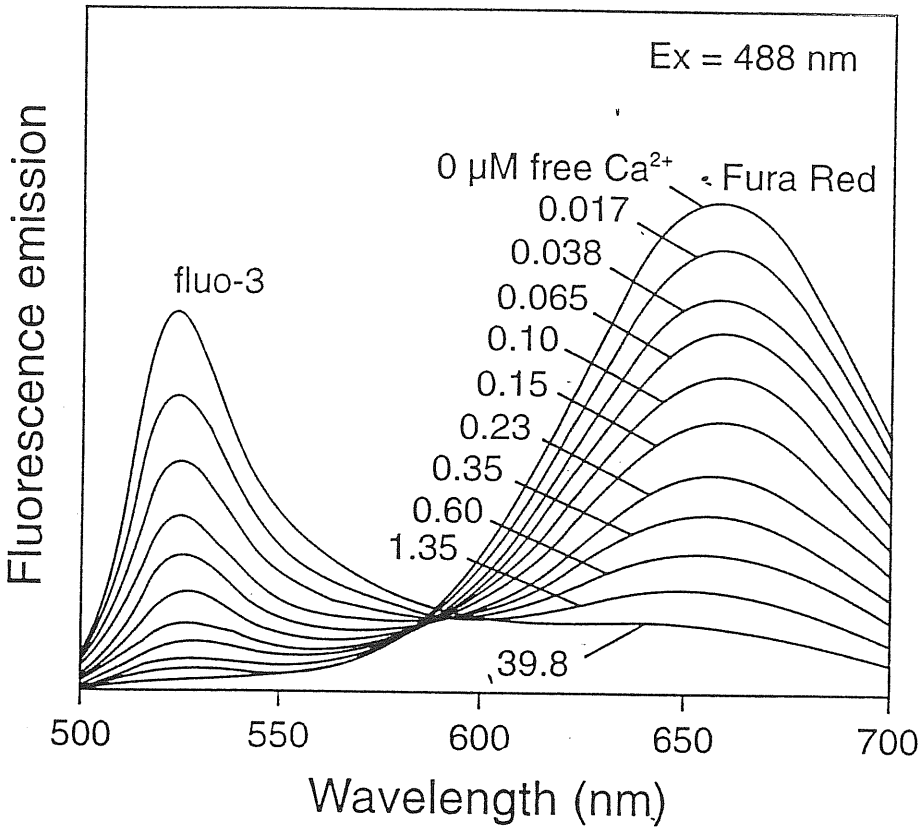
Ex = 488 nm
0 μM free Ca2+
Fura Red
0.017
0.038
0.065
0.10
0.15
0.23
0.35
0.60
1.35
39.8
fluo-3
Fluorescence emission
500
550
600
650
700
Wavelength (nm)

Figure M-10. Fluorescence spectra of the mixture of fluo-3 and Fura Red indicators, simultaneously excited at 488 nm, in solutions containing 0 to 39.8 μM free Ca^{2+}. From: Haugland, 1996.

concentration is not constant within the scanned area, i.e. if the ditribution of the dye is not homogeneous. This dye distribution artifact can be avoided by a pixel-by-pixel division of images arising from two equally distributed dyes. The resulting ratio is proportional to $[Ca^{2+}]_i$ but not to the dye concentration, and can be further calibrated to provide measurement of $[Ca^{2+}]_i$. On the other hand, insufficient degree of co-localization of the two indicators can prevent use of this method, as in fact found for rat chromaffin cells (Khiroug, 1994; in collaboration with Dr. Paola D'Andrea).

The second approach was made possible by the recent development by Molecular Probes of the dextran molecule (70,000 m.w.) which contains two different fluorophores: Calcium Green and Texas Red. The first one is a widely-used $[Ca^{2+}]_i$ indicator very similar to fluo-3. It can be excited at 488 nm and emits green fuorescence. The second one is calcium insensitive and emits red light when excited at 568 nm. After optical separation of the signals, they can be used to calculate a ratio depending on $[Ca^{2+}]_i$ but insensitive to the dye concentration. The ratio can be further calibrated in terms of $[Ca^{2+}]_i$. An advantage of this method is a high degree of co-localization of the two fluorophores which constitute the same dextran molecule. A disadvantage of this method is the necessity to load the cells through a patch pipette rather than incubation with its cell permeant form which is not yet available. Initial experiments using this method revealed a relatively weak fluorescence of Calcium Green fluorophore and the resulting requirement for high concentrations of the dextran which might introduce abnormal Ca^{2+} buffering thus prolonging and attenuating the $[Ca^{2+}]_i$ responses (Helmchen *et al.*, 1996). The use of this method was thus not pursued further.

V-6. Use of non-ratiometric $[Ca^{2+}]_i$ indicator fluo-3

Calibration procedures can be used to obtain quantitative measurements of $[Ca^{2+}]_i$ with fluo-3. One of them is based on the use of ionophores such as ionomycin (Kao *et al.,* 1989). Control responses of rat hippocampal pyramidal cells to pressure applications of KCl and/or glutamate (as described in the Drug Application section) were first obtained, then the Ca^{2+} ionophore ionomycin (5 μM) was superfused to saturate the fluorescence signal due to maximal transmembrane Ca^{2+} influx. Mn^{2+} (5 mM) was subsequently added, in the continuous presence of ionomycin, to displace bound Ca^{2+} from the dye and thus to obtain a stable fluorescence signal of lower intensity. Then the cell was lysed by adding 1 % Triton-X 100 to obtain the background fluorescence level. With such an approach it was possible to estimate that intracellular Ca^{2+} went from 41 ± 5 nM (n=5) at rest to 296 ± 96 nM at the peak of the KCl or glutamate-induced response (seven responses from five cells were pooled as they did not differ), which was considerably lower than the ionomycin-induced value (1.3 ± 0.2 μM, n=5).

Attention should be paid to avoid two possible artefacts which may arise from mechanical distortion of the scanned area and from dye bleaching. In both cases, the results of calibration would be incorrect. The first requirement was met in the present study by minimizing the pressure of drug application to 10-20 p.s.i., which produced no measurable cell movements while providing a rapid onset of drug responses (about 20 ms; see below). The dye bleaching artifact was eliminated by limiting the laser power to 30 mW and further attenuating it to 30% by a neutral density filter. The

signal/noise ratio of the $[Ca^{2+}]_i$ signals was sufficient while no dye bleaching was observed under these conditions.

VI. Whole-cell patch clamp technique

To study ligand-gated conductances the whole-cell patch clamp technique was used (Hamill *et al.,* 1981). This method applies the principles of voltage-clamp consisting in recording currents directly proportional to the conductance of interest while membrane potential is kept at preset value. In contrast to the two-electrode voltage-clamp method (Hodgkin *et al.,* 1952) where one electrode serves as a voltage sensor and the other one functions as a current source, for patch-clamping the single-electrode amplifier is used (List L/M-PC amplifier, List, Darmstadt). The amplifier uses the electrode in the continuous mode (unlike the switching sampling of single-electrode amplifiers) for voltage recording and passage of current (Sontheimer, 1995). Consequently, the recording arrangement contains an unknown and potentially varying series resistance in the form of the electrode and its access to the cell. To obtain satisfactory results, it is essential that this series resistance be small relative to the resistance of the cell. Ways to satisfy this requirement include the use of low resistance electrodes, small cells with high impedance, and electronic compensation for the series resistance error. In the present experiments, these approaches were used both for chromaffin cells and their derivative PC12 cells. These cells are relatively small (10-20 μm diameter) and round which facilitates their space clamping (in fact, some cells like, for instance, neurones in slices have a very complex spatial structure making the voltage clamp of the distal processes very difficult; Armstrong & Gilly, 1992; Sontheimer, 1995). Patch pipettes were pulled from the 1.5 mm o.d. glass and

had resistance of 1.5-3 MΩ (that is, an order of magnitude lower than that for intracellular electrodes). The pipettes were filled (in mM) with CsCl 120; EGTA 5 (unless omitted for $[Ca^{2+}]_i$ imaging); HEPES 20; $MgCl_2$ 1; Mg_2ATP_3 3. EGTA was added to compensate for the lack of endogenous $[Ca^{2+}]_i$ buffers dialysed during the whole-cell configuration (Walz, 1995). Cells were usually voltage-clamped at -70 mV (unless otherwise indicated) in the whole-cell configuration with GΩ seals. On a sample of cells (n=7) used for the present experiments uncompensated series resistance was 37±2 MΩ while cell capacitance was 7±0.5 pF. The series resistance value was compensated by up to 80 %. Electrophysiological responses were filtered at 1 kHz and stored on disk using pCLAMP software (5.5 version; Axon Instruments, Foster City, California).

VI-1. Combination of patch clamp and confocal imaging

Combination of the whole-cell patch clamp method with the confocal microscopy provides an opportunity to compare temporal changes in $[Ca^{2+}]_i$ with those in membrane currents. With the conventional patch-clamp technique, calcium buffers such as EGTA are usually added to the pipette solution to substitute for the endogenous $[Ca^{2+}]_i$ buffers which are washed out after whole-cell dialysis, thus improving the seal quality and providing longer-lasting recordings (Walz, 1995; Plant *et al.,* 1995). Addition of these buffers, however, completely blocks $[Ca^{2+}]_i$ rise. In fact, in the present experiments after addition of 10 mM BAPTA to the fluo-3 containing patch pipette no $[Ca^{2+}]_i$ rise was detected in response to depolarization or

pressure application of agonists (not shown). In the absence of intracellular calcium chelators, however, fluo-3 or other $[Ca^{2+}]_i$ indicators can play the role of calcium buffers; fluo-3 possesses the same calcium-binding activity of BAPTA since this dye actually contains the chelating site of the latter (Minta *et al.*, 1989). Only low concentrations of indicator dyes, which disturb Ca^{2+} buffering only slightly, can thus be used to study physiological changes in $[Ca^{2+}]_i$. High concentrations that swamp the endogenous buffer capacity may allow measurement of Ca^{2+} influx through voltage- or transmitter-gated channels and an estimate of the fraction of the membrane current carried by Ca^{2+} (Plant *et al.*, 1995). Use of relatively high indicator concentrations has recently been shown to decrease and prolong $[Ca^{2+}]_i$ rises following action potentials (Helmchen *et al.*, 1996). For rat cromaffin cells and PC12 cells, initial experiments were run to determine the optimal intrapipette concentration of fluo-3. At a concentration below 20 μM, the fluorescent signal in response to membrane depolarization produced by a voltage step from -70 to -20 mV was indistinguishable from background noise. On the other hand, rising intrapipette dye concentration to 50-200 μM lead to response prolongation and gradual decrease in its amplitude (data not shown). After these initial tests, 25 μM fluo-3 was used throughout. This allowed to reliably detect repetitive changes in $[Ca^{2+}]_i$.

Combination of the cell-permeant (AM ester) and cell-impermeant (salt) forms of fluo-3 was used in some experiments to compare responses in patch-clamped and intact cells simultaneously activated by pressure-applied ATP (5 mM). In this case, cells were incubated with 5 μM fluo-3/AM for 45 minutes at 37 °C. Two neighbouring cells were imaged, after which one of them was patched in the whole-

cell configuration with 25 μM fluo-3 added to the pipette solution. Pulses of ATP were applied to both cells simultaneously from the same micropipette positioned equidistantly from the two cells. In the example of Fig. M-11, during a 2 s pulse of ATP (horizontal bars) in the intact cell there was an initial, rapid rise (labelled as A_1 in Fig. M-11B) in $[Ca^{2+}]_i$ followed by a decline and a much larger and slower increase (labelled as A_2 in Fig. M-11B). On the other hand, the response of the adjacent, patched cell had monophasically slow onset and offset (Fig. M-11A). Similar findings were obtained from 10 patched and 9 intact fluo-3 loaded cells (not shown). The initial peak (A_1) was attributed to activation of voltage-gated calcium channels by ATP-elicited membrane depolarization which was absent in the voltage-clamped cell. Thus, the combined loading method allowed to monitor the role of voltage-gated Ca^{2+} channels in the timecourse of ATP evoked $[Ca^{2+}]_i$ rise in intact cells.

VII. Drug application

VII-1. Application by bath superfusion

In a bath superfused by gravity, the straightforward way of drug application is via the bathing solution. This method is suitable for studies of slow action of drugs such as desensitization of nAChRs by bath-applied ACh by (Katz and Thesleff, 1957), for it offers a simple way to control the drug concentration upon solution equilibration. However, equilibration can take several seconds depending on the bath construction and superfusion rate. On the other hand, activation of ligand-gated receptors is a much faster process developing on a μsec timescale, suggesting the need to use more rapid

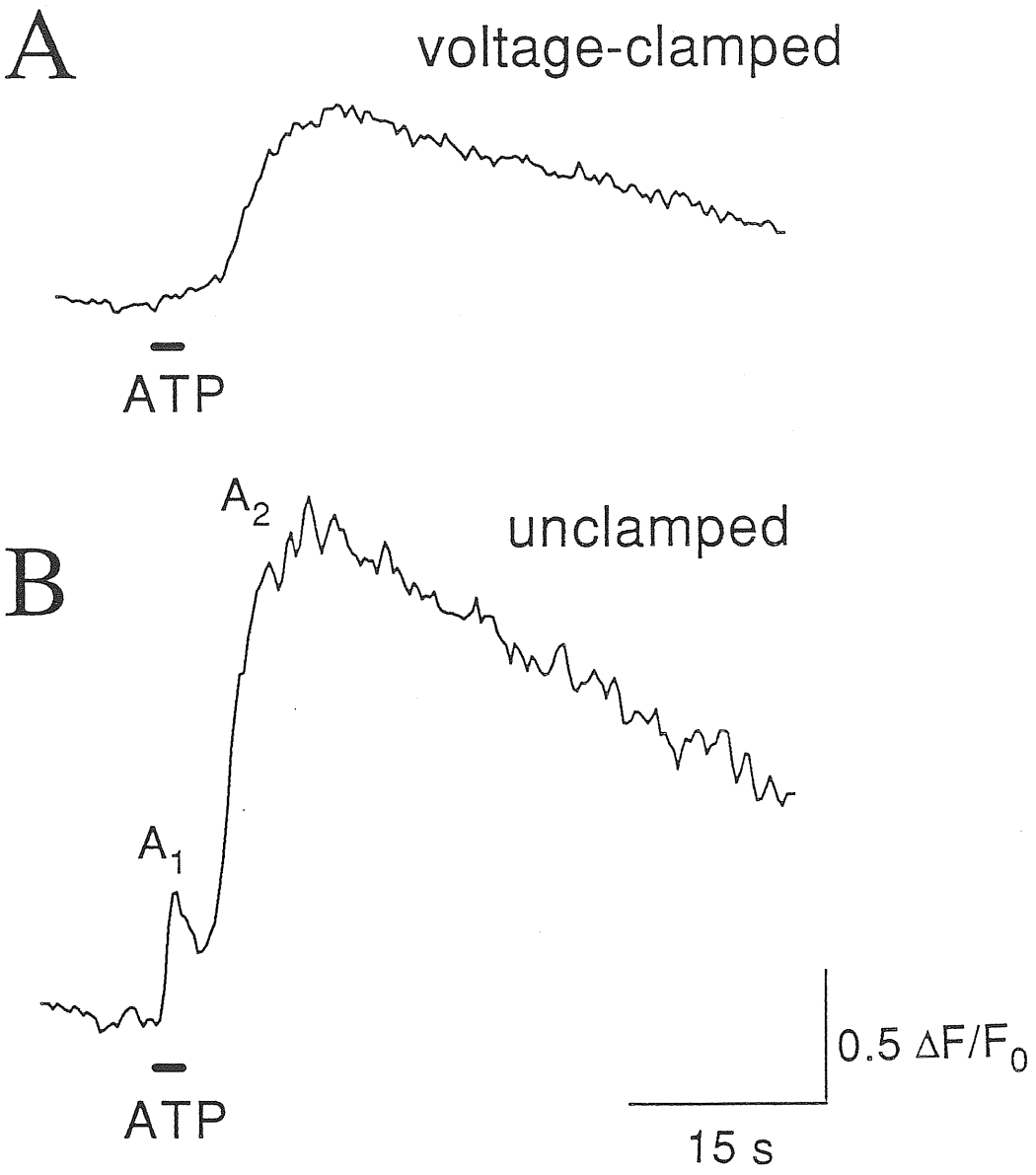
A
voltage-clamped
ATP
B
A2
unclamped
A1
ATP
0.5 ΔF/F0
15 s

Figure M-11. Comparison of $[Ca^{2+}]_i$ transients in patched or intact PC12 cells. A and B are responses recorded simultaneously from a pair of cells in which only one (B) was patched (voltage clamped at -70 mV). Note faster and biphasic nature of $[Ca^{2+}]_i$ response of unclamped cell (B; the first is indicated by A_1 and the second one by A_2). ATP (5 mM) was applied for 2 s from a pressure pipette equidistant from both cells.

application techniques in these studies. Another drawback is that bath application affects the whole population of cells, making impossible repeated application of drugs which induce desensitization or tachyphylaxis of their action.

VII-2. Pressure pulse from micropipette

In comparison with bath application by gravity perfusion, a significant improvement in terms of rapid drug onset is offered by pressure application from a micropipette using for example the Picospritzer II instrument (General Valve Co., Fairfields, New Jersey). In initial experiments on rat hippocampal pyramidal cells, stimulation was performed by brief (100-500 ms) pressure application (30 p.s.i.) of 0.1-0.2 M KCl (in SES without NaCl), 0.1 mM glutamate or 20 μM NMDA (both in SES) from a distance of 50-100 μm. For chromaffin cells and PC12 cells, drugs such as ATP, its analogues ADP and α,β-methylene ATP, and (-)-nicotine (hydrogen tartrate salt; all drugs purchased from Sigma Chemical Co., Milan) were diluted in control solution and delivered by pressure application (10-20 p.s.i.) from similar pipettes (located about 20 μm away from the recorded cell) using the Picospritzer II.

A disadvantage of this method of application is the degree of drug dilution in the bath which makes it impossible to know the precise drug concentration at the cell surface. Tests were run, however, to estimate both the dilution factor and the speed of drug delivery (and removal) according to the method by Zhang *et al.* (1994). The application time course was measured as a change in liquid junction potential of a recording pipette (filled with 150 mM KCl) placed in the external solution following pressure application (5 ms-10 s) of KCl (75 mM) from a nearby pipette (10-30 μm

away). With such a method peak concentrations were estimated to be reached within 15-20 ms, represented a 3.7-4 fold dilution of the pressure pipette dose (extrapolated from plots of potential amplitude against various concentrations of KCl). The junction potential remained at plateau during application, and disappeared with a decay time constant of 46.5 ± 1.4 ms (n=6) due to the fast superfusion rate (Fig. M-12Aa). Both rapid onset and rapid drug removal by superfusion were essential to study the process of fast desensitization of ATP receptors which presumably underlies the fast current fading during ATP application as shown in Fig. M-12 Ab.

VII-3. Drug application using Y-tube

Some experiments were also carried out with a different method for rapid application and removal of drugs: this consisted of the so-called "Y-tube" technique (Akaike *et al.*, 1991) which is a modification of the microflow system developed by Krishtal and Pidoplichko (1980). With the Y-tube (upper right cartoon in Fig. M-12 B), a known concentration of agonist is quickly delivered by gravity (thick arrow) and equally quickly removed by suction (thin arrow) through the same tube. Switching between drug delivery and back-suction is achieved by changing the flow rate in the tube (middle-thickness arrow). In Fig. 12 Ba the temporal profile of application is shown as recorded from a KCl-filled pipette during the liquid potential changes (Zhang *et al.*, 1994). Not only the time course of KCl liquid potential change obtained with the Y-tube (Fig. M-12 Ba) is similar to that with pressure pipette application (Fig. M-12 Aa), but also the fast fading and rebound of ATP induced currents can be observed with this method (Fig. M-12 Bb). However, the use of Y-tube was often associated

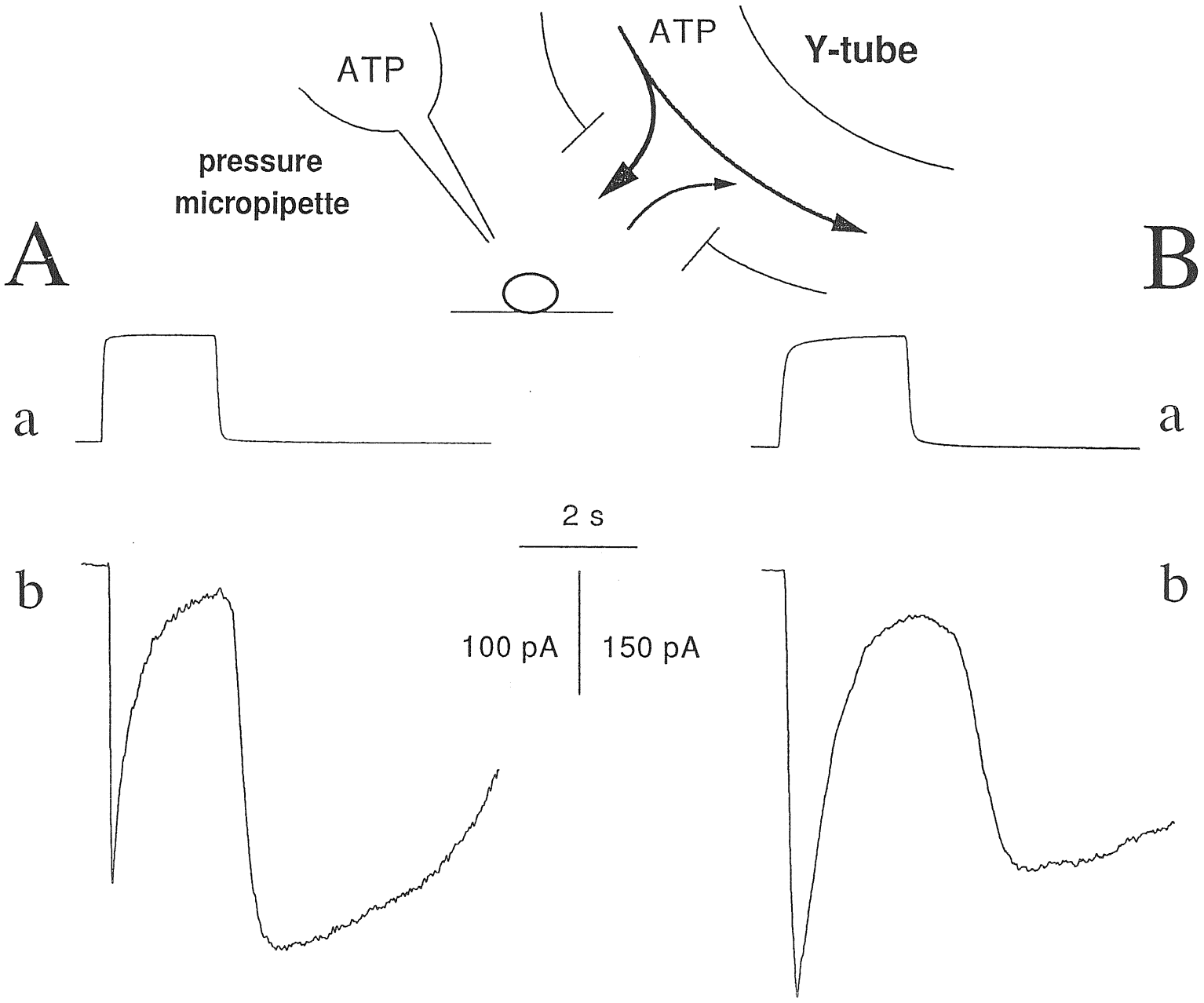
ATP
ATP
Y-tube
pressure
micropipette
A
B
a
a
2 s
b
b
100 pA
150 pA

Figure M-12. ATP (5 mM) induced current fade and rebound following pressure pulse or Y-tube application. A, comparison of the time course of the liquid junction change induced by pressure application of KCl (KCl calibration signal, a) with that of 5 mM ATP-induced membrane current elicited with the same method of application (b). B (different cell from A) shows comparable results obtained with Y-tube application. The cartoon on top schematically shows represents application principle with micropipette and Y-tube. In the latter case, the solution is applied to the cell by gravity (thick arrow) when the flow rate through the Y-tube (middle-thickness arrow) is lowered; prior to and at the end of application solution is sucked back into the Y-tube (thin arrow).

with cell movements and recording instabilities, therefore drug delivery by pressure pipette during fast bath superfusion was routinely used for the present experiments.

VIII. Data analysis and presentation

Membrane currents and $[Ca^{2+}]_i$ transients were measured in terms of amplitude (or amplitudes, when more than one peak was observed), exponential onset and decay (fitted with the program Clampfit for currents or Microcal Origin for $[Ca^{2+}]_i$ responses). Data are presented as mean±standard error. Statistical significance was assessed with paired *t*-test (for normally distributed data) or one-way ANOVA test (for non-parametric data). Graphs were constructed with Origin software (Microcal Software Inc, version 2.94 and version 4.0). Images were processed with ImageSpace software (Molecular Dynamics).

Results

IX. Regulation of nAChRs desensitization by $[Ca^{2+}]_i$.

While desensitization of muscle nAChRs is extensively described and the role of $[Ca^{2+}]_i$ changes in it is well established, in the case of neuronal nAChRs it seemed essential to compare the time course of the two processes directly monitoring both receptor sensitivity and agonist-induced $[Ca^{2+}]_i$ increase. This approach was realized on rat cultured chromaffin cells using combined whole-cell patch clamping and confocal laser scanning microscopy.

IX-1. Nicotine-induced currents and $[Ca^{2+}]_i$ rises

On chromaffin cells nicotine evoked inward currents and associated rises in $[Ca^{2+}]_i$ as shown in the example of Fig. R-1 A, B (left panels) for a 20 ms pulse application of this agonist (see thick arrows). Simultaneous records indicated that the current response (-610 pA) peaked in 82 ms while the $[Ca^{2+}]_i$ increased in parallel with the inward current and reached a peak of 0.96 $\Delta F/F_0$ at 3 s. Recovery of both responses could be fitted by a single exponential with time constants of 2.3 s for current and 9.3 s for $[Ca^{2+}]_i$. The decay timeconstant of the $[Ca^{2+}]_i$ transient was 9±1 s (n=13 cells). In order to aid comparison of the timecourse of both signals these records are also shown in the inset (see arrows) on a faster time scale (note that in this inset the vertical calibration was scaled down 2.8 fold for $[Ca^{2+}]_i$ and 2.4 fold for current). It is apparent that both signals developed simultaneously although the $[Ca^{2+}]_i$ grew at a slower rate

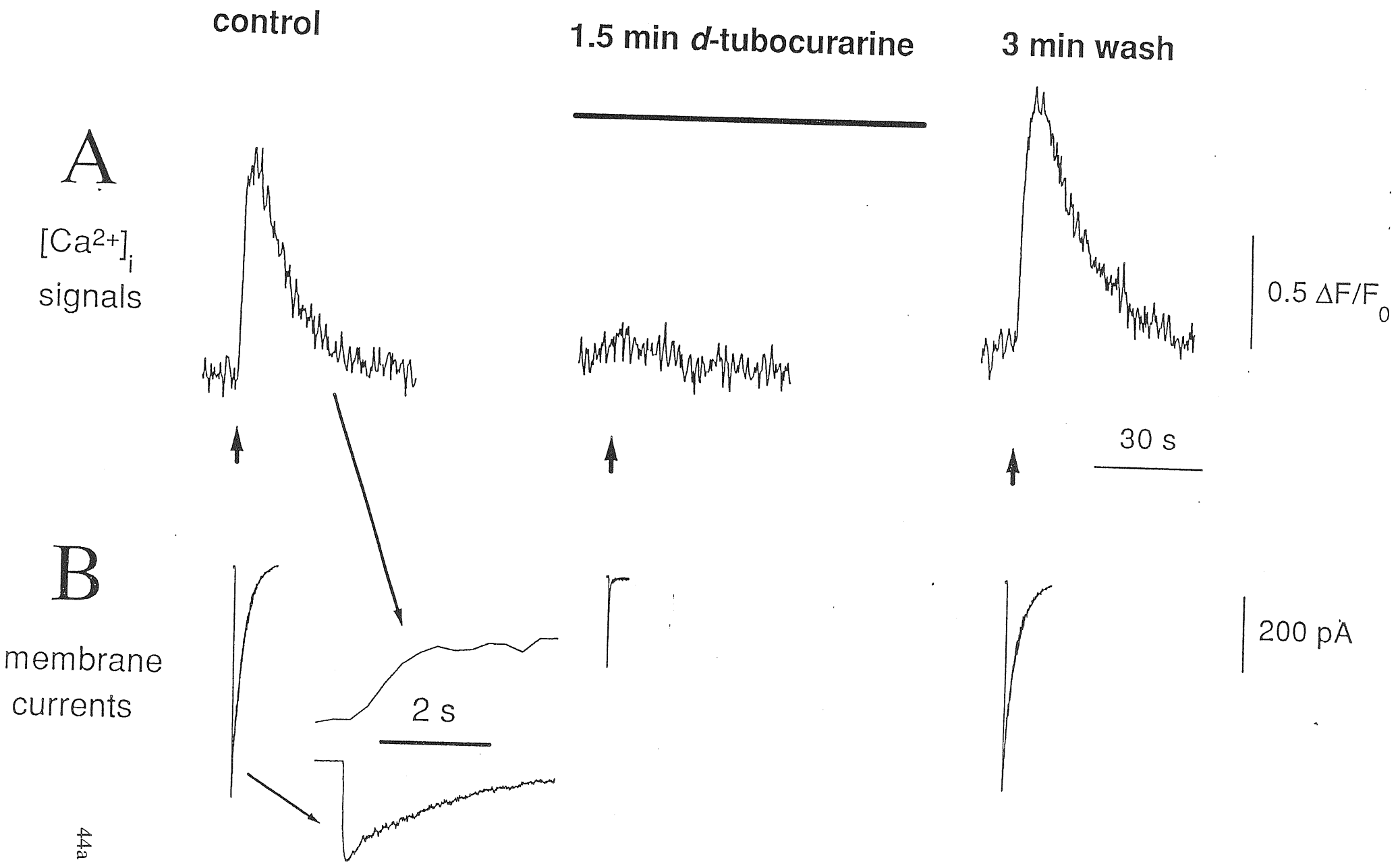
control
1.5 min d-tubocurarine
3 min wash
A
[Ca2+]i
signals
0.5 ΔF/F0
30 s
B
membrane
currents
2 s
200 pA

Figure R-1. Simultaneous recording form the same cell of $[Ca^{2+}]_i$ rises and membrane currents elicited by 20 ms pressure application of 1 mM nicotine (Picospritzer). A, $[Ca^{2+}]_i$ following application of nicotine (thick arrows) in control solution (left), 1.5 min after bath-applying *d*-tubocurarine (10 μM; horizontal bar; center) and after 3 min washout (right). B, inward currents elicited by nicotine in control (left), *d*-tubocurarine solution (center) and after washout (right). The traces of left panels are also shown (see arrows) on a faster time base to disclose their temporal relation. Note reversible depression of $[Ca^{2+}]_i$ and current responses by *d*-tubocurarine.

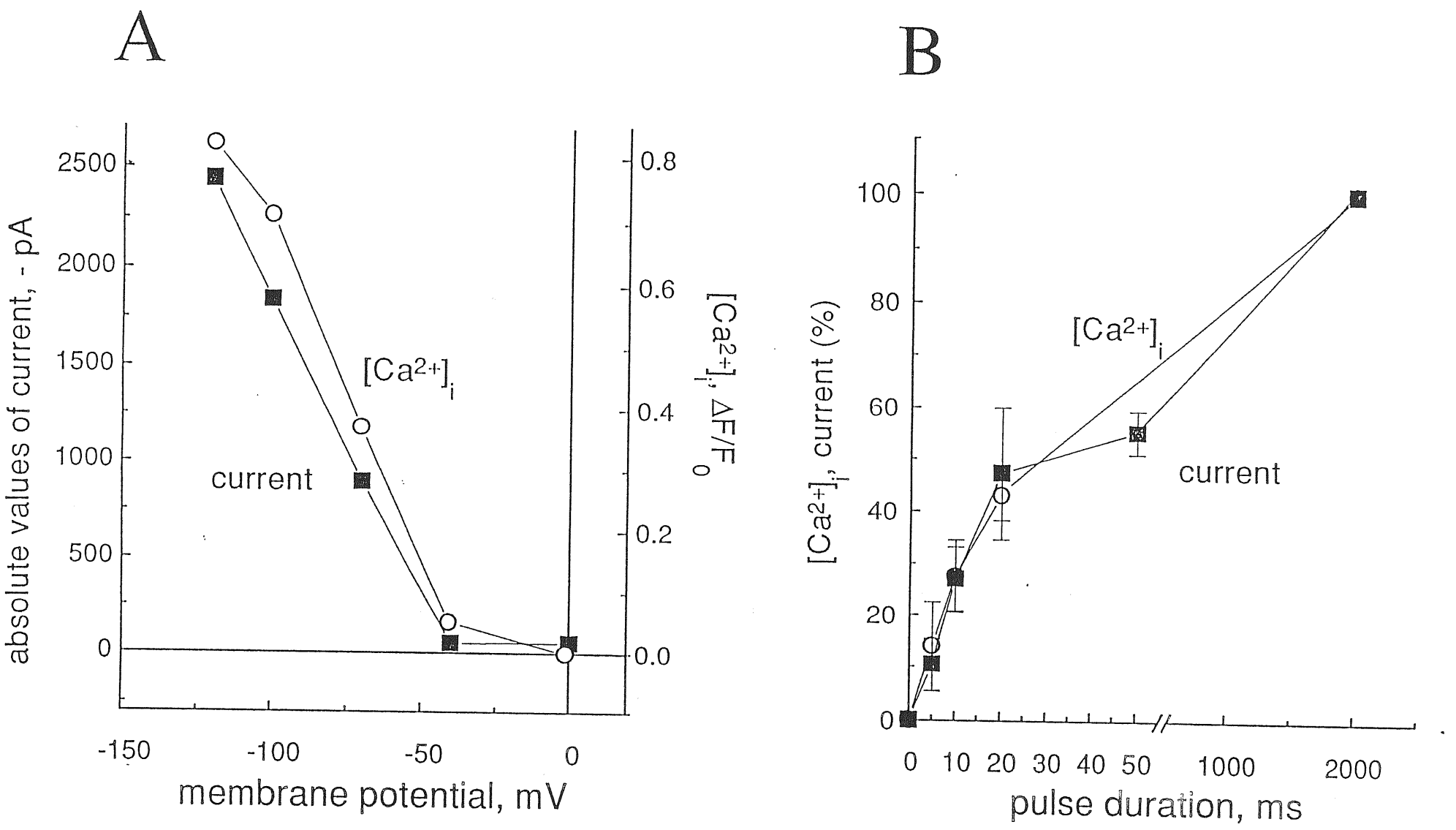
A
absolute values of current, - pA
2500
2000
1500
1000
500
0
0.8
0.6
0.4
0.2
0.0
$[Ca^{2+}]_i$, $\Delta F/F_0$
$[Ca^{2+}]_i$
current
-150
-100
-50
0
membrane potential, mV
B
$[Ca^{2+}]_i$, current (%)
100
80
60
40
20
0
$[Ca^{2+}]_i$
current
0 10 20 30 40 50 1000 2000
pulse duration, ms

Figure R-2. $[Ca^{2+}]_i$ and current responses induced by nicotine are similarly related to membrane potential and magnitude of nicotine application. A, relation between holding membrane potential (abscissa) and peak amplitude of 20 ms nicotine-evoked current (left ordinate) or size of associated $[Ca^{2+}]_i$ rise (right ordinate). Note similar dependence of both parameters on membrane potential. Data are from the same cell depicted in Figure 1. B, plot of duration of nicotine pressure application (indicative of the amount of applied nicotine; abscissa) versus $[Ca^{2+}]_i$ (open circles) and current (filled squares) responses (expressed as % of the maximum response). Datapoints are from 4-13 cells.

and peaked at the time when the amount of charge which moved across activated receptors reached its maximum as expected for neuronal nAChRs (Rathouz & Berg, 1994; Vernino *et al.*, 1994). Fig. R-1 A,B (center panels) also shows that bath-application of the nicotinic antagonist *d*-tubocurarine (10 μM) strongly and reversibly depressed both responses. On average *d*-tubocurarine depressed the charge transfer through activated receptors and the amplitude of $[Ca^{2+}]_i$ rises by 94±1 and 99±0.4 %, respectively (n=3), indicating that elevation of $[Ca^{2+}]_i$ required nAChR activation. α-Bungarotoxin (1 μM) was ineffective on responses induced by 20 ms nicotine.

The view that nAChR activity was necessary for observing $[Ca^{2+}]_i$ rises was also supported by the finding that, when the holding potential was changed between -120 and 0 mV in a stepwise fashion, the voltage-dependence of inward current and $[Ca^{2+}]_i$ rise was very similar with comparable degree of outward rectification (Fig. R-2 A, same cell of Fig. R-1). Peak inward currents and $[Ca^{2+}]_i$ rises had a similar hyperbolic relation to nicotine pulse duration as shown in Fig. R-2 B (pooled data from 4-13 cells). Since 20 ms pulses elicited sufficiently large and stable responses, subsequent experiments normally employed this length of pressure application for further tests of nicotinic receptor sensitivity: on average the inward current evoked under these conditions was -884±90 pA (n=12 cells).

IX-2. Source of nicotine-induced $[Ca^{2+}]_i$ rises

While the data with *d*-tubocurarine indicated that nicotinic receptor activation was needed to observe a $[Ca^{2+}]_i$ rise, the similar voltage sensitivity of the nicotine-induced

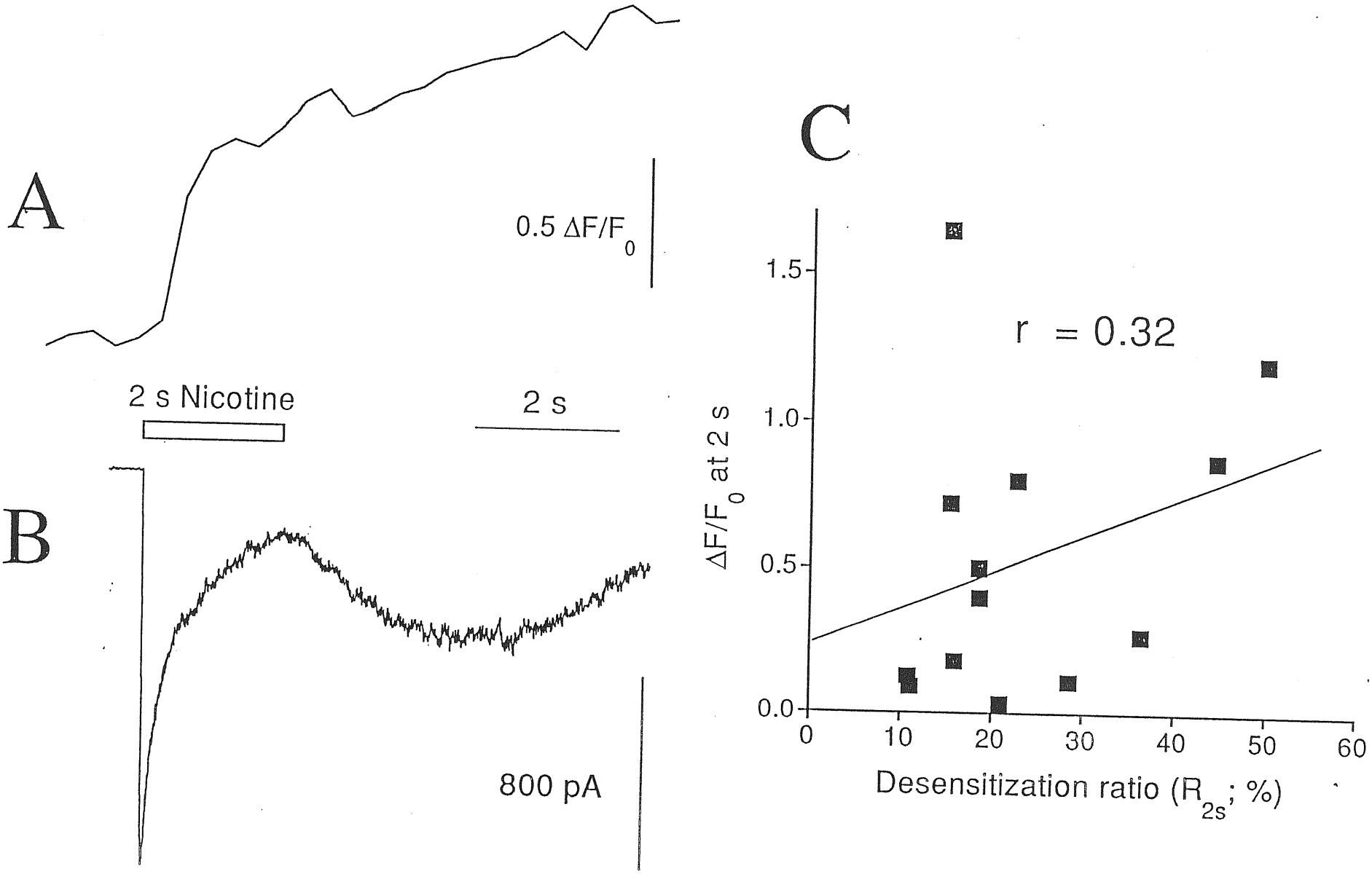
A
0.5 ΔF/F0
2 s Nicotine
2 s
B
800 pA
C
r = 0.32
ΔF/F0 at 2 s
1.5
1.0
0.5
0.0
0
10
20
30
40
50
60
Desensitization ratio (R2s; %)

Figure R-3. Combined record of $[Ca^{2+}]_i$ and membrane current following 2 s application of nicotine. A, $[Ca^{2+}]_i$ change, B, membrane current during pressure application of nicotine (open bar). Note current fade and rebound associated with biphasic rise in $[Ca^{2+}]_i$. C, linear regression plot of desensitization ratio (R_{2s}; ratio between residual current and peak amplitude; %) versus increase in $[Ca^{2+}]_i$ over baseline at 2 s. Each symbol refers to a single cell.

current and $[Ca^{2+}]_i$ elevation (see Fig. R-2A) suggested the possibility that the main source of Ca^{2+} might have been from the extracellular compartment through open nicotinic receptors. This view was supported by experiments carried out in an external solution from which Ca^{2+} was omitted while adding 5 mM BAPTA and 3 mM Mg^{2+}. In this condition (n=4) baseline $[Ca^{2+}]_i$ levels decreased by 29±6 % and were unchanged (1±0.7 %) following application of nicotine. The amplitude of nicotine currents in the same solution was not significantly different (80±13 %) from control one. These data thus indicate that the main source of Ca^{2+} for the rise in $[Ca^{2+}]_i$ was from the extracellular compartment although this ion was not the main charge carrier through the open nicotinic receptors (Vernino *et al.*, 1994).

IX-3. Desensitization of nAChRs

The nicotinic receptors of chromaffin cells can desensitize in the presence of large agonist doses (reviewed by Marley, 1988). In order to standardize the protocol to induce receptor desensitization and to investigate its possible relation with $[Ca^{2+}]_i$, in the present project the effect of a long (2 s) application of nicotine was examined. Fig. R-3 A, B shows an example of the inward current (peak current amplitude=-1640 pA) and $[Ca^{2+}]_i$ rise (1.16 $\Delta F/F_0$) evoked by a 2 s application of nicotine. In the presence of nicotine the inward current (Fig. R-3 B) rapidly faded with a biexponential timecourse (τ_1 and τ_2 values were 144 and 1997 ms, respectively; on average these values were 145±23 ms and 1418 ±190 ms for a sample of 13 cells). At the end of the 2 application the residual current was -260 pA, corresponding to 16 % of the peak one. Measuring the ratio (expressed as %) between residual and peak currents (R_{2s})

provided an estimate of the extent of nAChR desensitization. For 13 cells R_{2s} was found to be 23±4 %. After stopping the application of nicotine the current response transiently bounced back ("rebound"; see MacOnochie & Knight 1992) to 42 % of the peak value. On a random sample of 5 cells baseline current was always re-attained with a monoexponential timecourse of 4.6±1.4 s after the rebound peak.

Like in the case of brief applications of nicotine (see Fig. R-1), increase in $[Ca^{2+}]_i$ induced by 2 s nicotine developed at the same time as the inward current and reached a peak when the current had fully dissipated (Fig. R-3 A), *i.e.* when the charge transfer through the nAChRs was complete. Return of $[Ca^{2+}]_i$ to baseline was observed 30 s later (not shown). α-Bungarotoxin (1 μM) had no effect on responses elicited by 2 s nicotine.

Fig. R-3 C shows for 13 cells a plot of the R_{2s} values versus the % increase in $[Ca^{2+}]_i$ at the end of the 2 s pulse of nicotine. There was no apparent correlation between these two terms, outlining a minimal role of $[Ca^{2+}]_i$ in the development of desensitization. Further support was sought with a different experimental approach, which consisted in recording current responses (without Ca^{2+} imaging) with either no exogenous buffering of $[Ca^{2+}]_i$ or strong buffering by intracellularly-applied BAPTA (10 mM; see methods). The R_{2s} values were 15±4 % (n=6) and 10±3 % (n=7) with no exogenous buffers or 10 mM BAPTA, respectively: these values are not significantly different from those observed with cells loaded with 25 μM fluo-3. These results suggest that a rise in $[Ca^{2+}]_i$ was not the main factor to produce nAChR desensitization over this time scale.

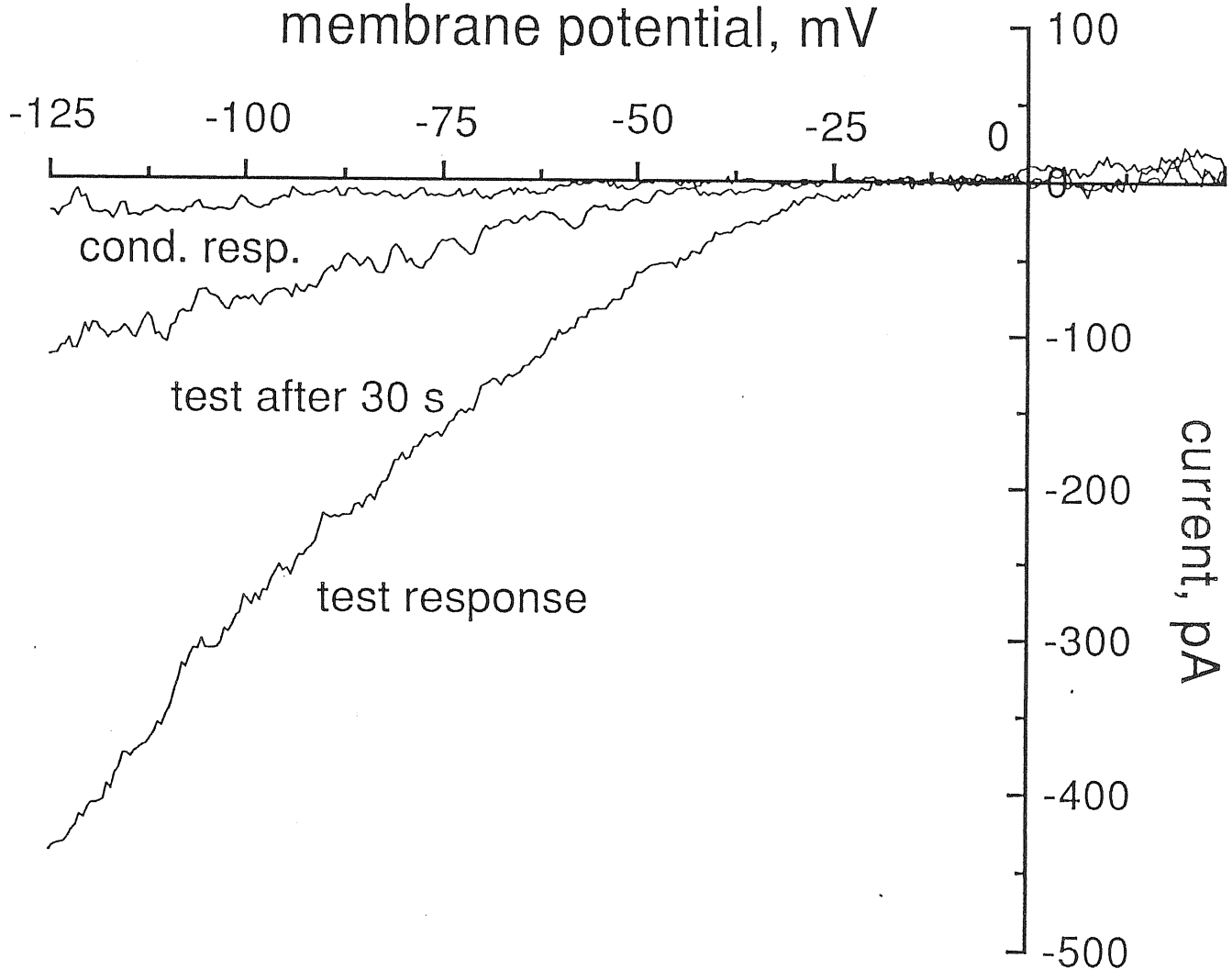
membrane potential, mV
-125
-100
-75
-50
-25
0
100
-100
-200
-300
-400
-500
current, pA
cond. resp.
test after 30 s
test response

Figure R-4. Current voltage relation during application of nicotine. Curves were generated by voltage ramps (400 mV/s) applied at the peak of a response induced by 20 ms nicotine (test response), during the plateau of the response to 2 s nicotine (cond. resp.) and at the peak of 20 ms nicotine response 30 s later (test after 30 s). Despite the large decrease in slope conductance of the plots during 2 s nicotine application and after it there was no change in reversal potential.

IX-4. Voltage dependence of nAChRs

The large fading of the nicotine current during 2 s application might have been caused by a shift in the current reversal potential rather than receptor desensitization. In order to explore this issue, voltage ramps (400 mV/s) were applied to the cell once the current decline reached quasi steady-state conditions (just before the end of nicotine delivery). The response was thus compared with those at the peak of the currents elicited by 20 ms test nicotine pulses while applying the same ramp protocol. Fig. R-4 shows an example of such an experiment in which the current null potential (-20 mV) was not altered during current fade (-26 mV) or during the first 20 ms test response 30 s after the conditioning application (-24 mV). Similar results were obtained in five cells in which null potentials obtained with control and conditioning pulses were -15±3 and -18±4 mV, respectively ($P>0.05$). Scaling of the current record during the conditioning pulse to the one obtained during the control test pulse indicated overlapping of the two traces, conferming that there was no distortion in the voltage dependence of the responses during various tests (data not shown).

IX-5. Recovery of nAChRs from desensitization

The question of how soon AChRs could recover from desensitization was addressed with experiments in which brief test applications of nicotine (20 ms) were applied every 30 s before and after a 2 s conditioning pulse of the same agonist. Test pulses at 30 s intervals elicited stable and reproducible responses. Non-decremental currents

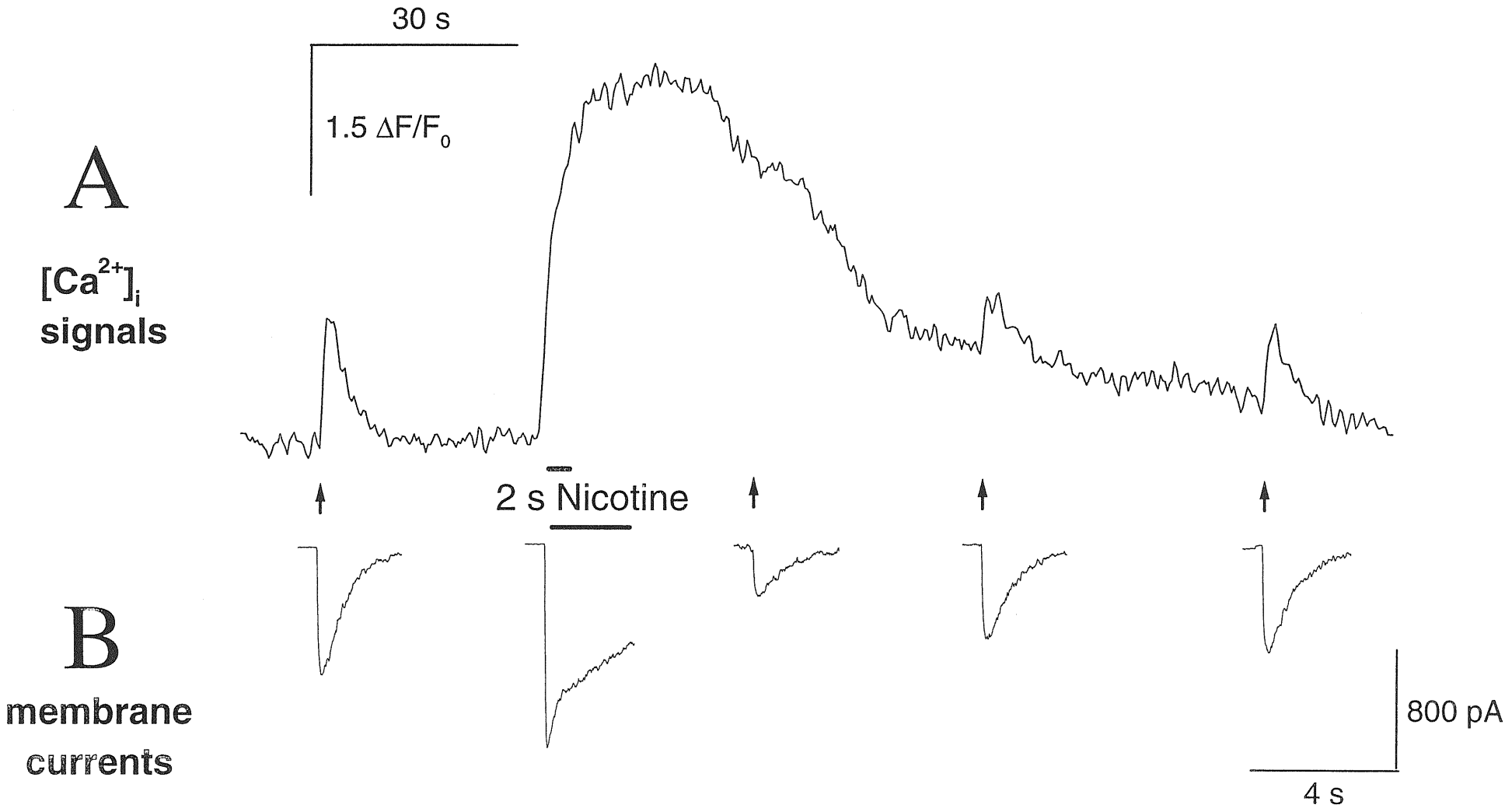
30 s
1.5 ΔF/F0
A
[Ca2+]i
signals
2 s Nicotine
B
membrane
currents
800 pA
4 s

Figure R-5. Simultaneous recording of $[Ca^{2+}]_i$ transients and inward currents evoked by nicotine. A, changes in $[Ca^{2+}]_i$ following 20 ms (arrows) or 2 s (horizontal bar) applications of nicotine, B, corresponding inward currents elicited by the same applications (note that timescale for current is much faster than for $[Ca^{2+}]_i$ changes).

were also observed if the interpulse interval of paired pulses was 5 s: in this case the second pulse evoked a current of the same amplitude as the first one (7±3 % change; n=5 cells) and a rise in $[Ca^{2+}]_i$ not exceeding the peak of the first one (3±15 % difference). The slow return to baseline of the current induced by a 2 s conditioning dose of nicotine (see Fig. R-3) suggested that a 30 s interval for test pulses was more adequate to avoid contamination of test currents by residual current.

Fig. R-5 A, B shows an example of the protocol used to test AChR desensitization and recovery: after 20 ms test applications (arrows) of nicotine (last one shown at the start of the traces) a 2 s administration of the same agonist (horizontal bars) induced a rapidly-waning inward current (-1150 pA peak amplitude) which was associated with an increase in $[Ca^{2+}]_i$ (note different time calibration) peaking 10 s after the end of the nicotine application. Recovery of baseline current was complete within 10 s but the effectiveness of subsequent test pulses in eliciting current responses was reduced with recovery attained approximately 90 s from the 2 s nicotine application (Fig. R-5B): for instance 30 s after the conditioning pulse of nicotine the test pulse evoked an inward current which was 41 % of control one. As depicted in Fig. R-5 A the peak $[Ca^{2+}]_i$ rise following 2 s nicotine application was larger than the ones elicited by 20 ms application (this difference is also quantified in Fig. R-2 B; open circles). Even more striking was the duration of the $[Ca^{2+}]_i$ elevation after 2 s nicotine compared with the one after 20 ms application as the area of the latter was on average only 25±5 % (n=13) of the former. Such a large difference was made up by the sustained nature of the $[Ca^{2+}]_i$ increase after 2 s nicotine. This is indicated in Fig. R-5 A by the slow

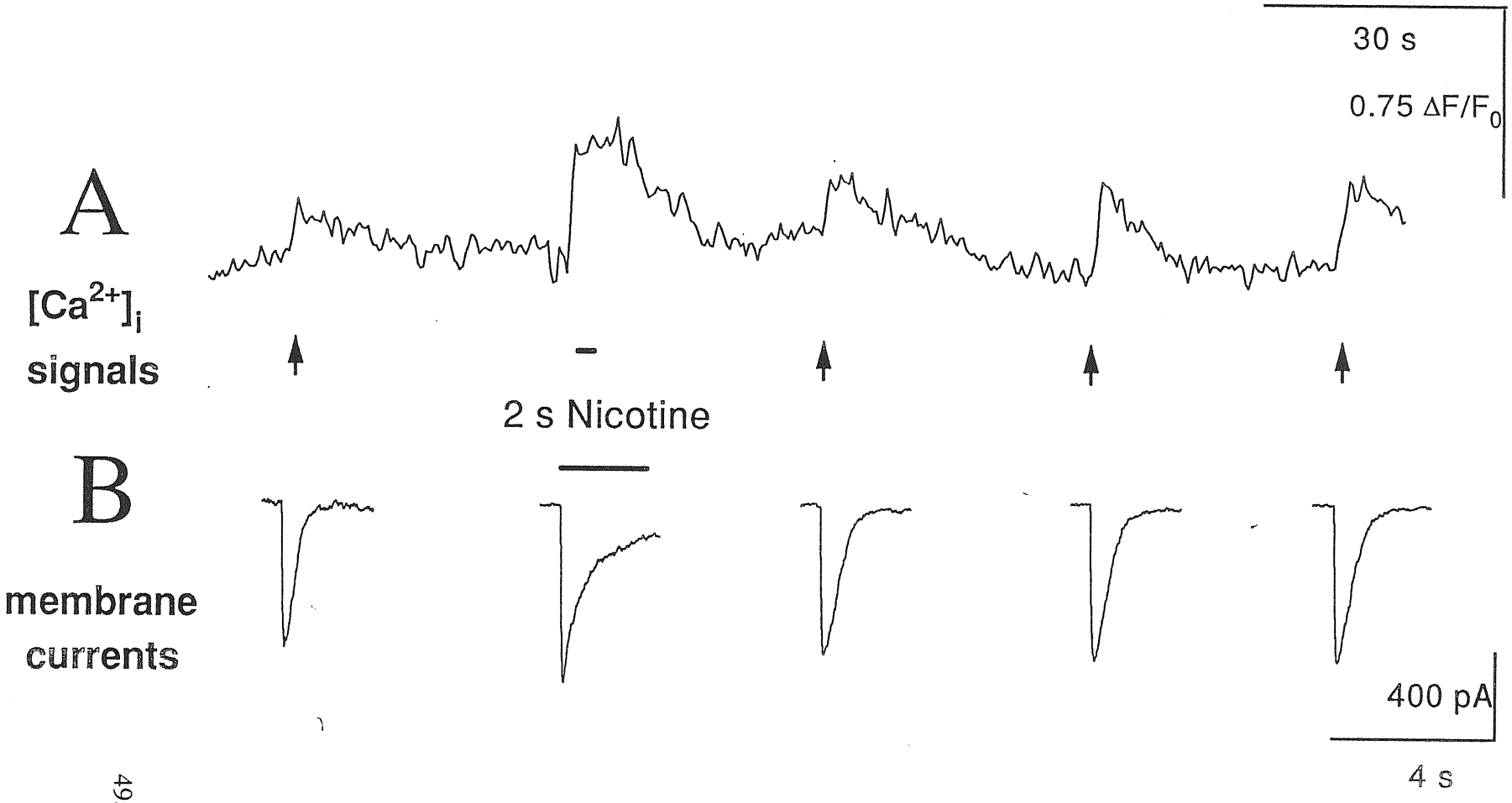
30 s
0.75 ΔF/F0
A
[Ca2+]i
signals
2 s Nicotine
B
membrane
currents
400 pA
4 s

Figure R-6. $[Ca^{2+}]_i$ transients and inward currents evoked by nicotine. A, B - same as Fig. R-5. Note smaller difference between changes in $[Ca^{2+}]_i$ evoked by 20 ms and 2 s applications of nicotine and less pronounced desensitization as assessed from test response amplitude.

process (89 s timeconstant) of recovery of $[Ca^{2+}]_i$ to baseline level. During this period $[Ca^{2+}]_i$ transients to subsequent nicotine applications were attenuated (Fig. R-5 A).

Fig. R-6 demonstrates an example of a cell in which the 2 s pulse of nicotine evoked only a small $[Ca^{2+}]_i$ rise. Recovery of nAChRs from desensitization was complete already 30 s after the conditioning pulse. In general, the return of $[Ca^{2+}]_i$ to control level following 2 s nicotine administration had a rather variable timecourse amongst different cells. This data scattering was exploited to explore any correlation between sustained rise in $[Ca^{2+}]_i$ and depression of the nicotine-induced current 30 s after the conditioning pulse. Fig. R-7 A shows test current amplitude 30 s after the conditioning pulse of nicotine (% of control; ordinate) plotted against decay of $[Ca^{2+}]_i$ from its peak (% of peak; abscissa). Each square represents a value from a different cell (n=15). The plot suggests that a persistent rise in $[Ca^{2+}]_i$ was associated with reduced sensitivity of nAChRs (r=0.85). Nevertheless, for the same time point no correlation (r=0.28) was found between depression of test currents and elevation of $[Ca^{2+}]_i$ measured as % rise over baseline (not shown). Fig. R-7 B shows a plot of $[Ca^{2+}]_i$ (open circles; as % of peak values) and amplitude of test nicotine current (filled squares; as % of controls) at three time points (30, 60 and 90 s) after a conditioning application of nicotine. While relative $[Ca^{2+}]_i$ values decreased over time there was a corresponding recovery of test currents: loss of correlation between these parameters occurred at 90 s. These observations suggest that a sustained level of $[Ca^{2+}]_i$ appeared to be predictive of persistent depression of inward currents evoked by test pulses of nicotine.

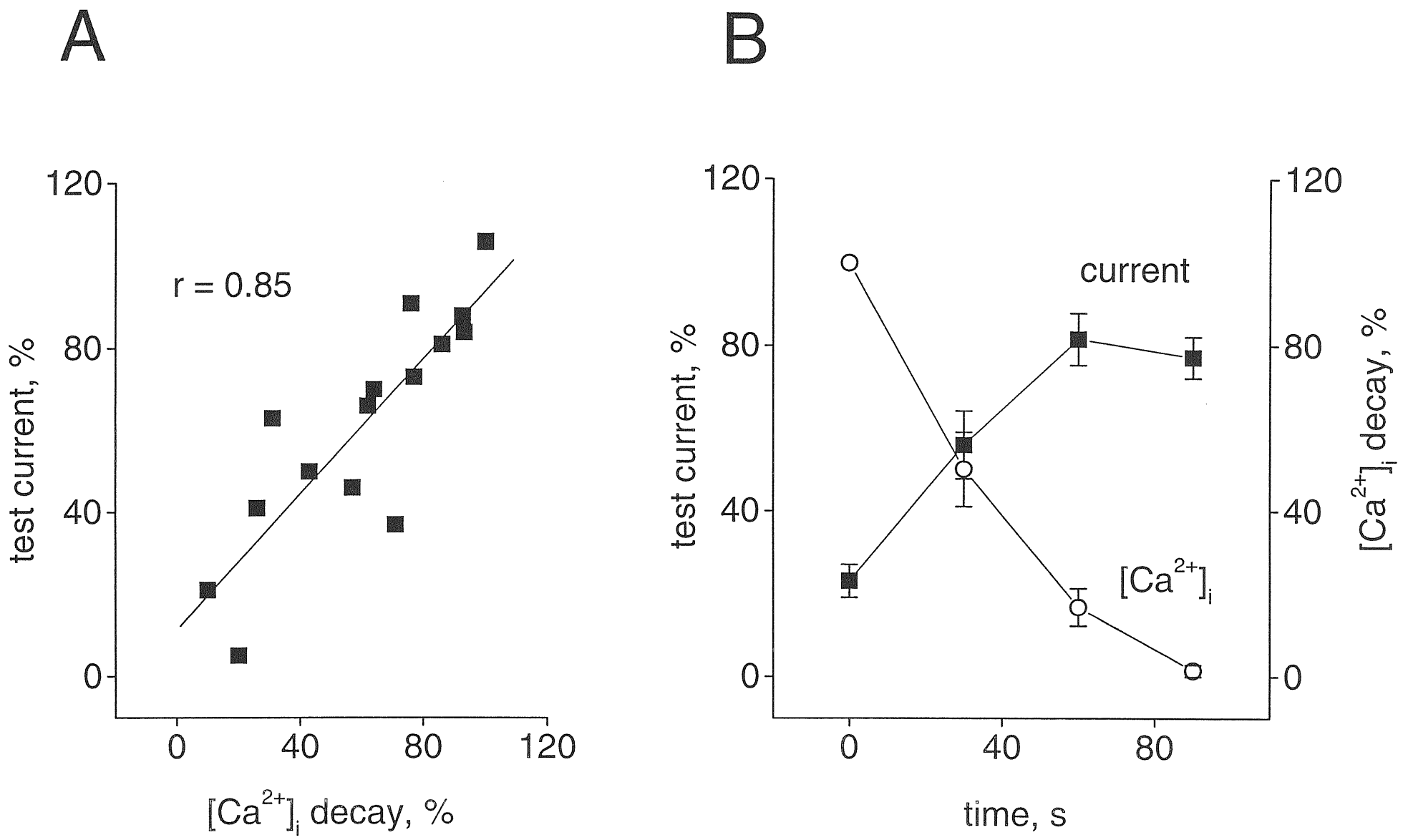
A
B
120
80
40
0
test current, %
r = 0.85
0
40
80
120
[Ca2+]i decay, %
current
[Ca2+]i
time, s
[Ca2+]i decay, %

50a

Figure R-7. Relation between $[Ca^{2+}]_i$ changes and recovery from desensitization. A, plot of test current amplitude at 30 s from conditioning pulse (expressed as % of control test pulses; ordinate) *versus* decay of $[Ca^{2+}]_i$ transient (as % of peak response; abscissa) at the same timepoint. r=correlation coefficient, n=15. B, amplitude of test currents after conditioning pulse (filled squares; left ordinate) and decay of $[Ca^{2+}]_i$ (open circles; right ordinate) are plotted as function of time from conditioning application of nicotine. Note reciprocal time profile of changes.

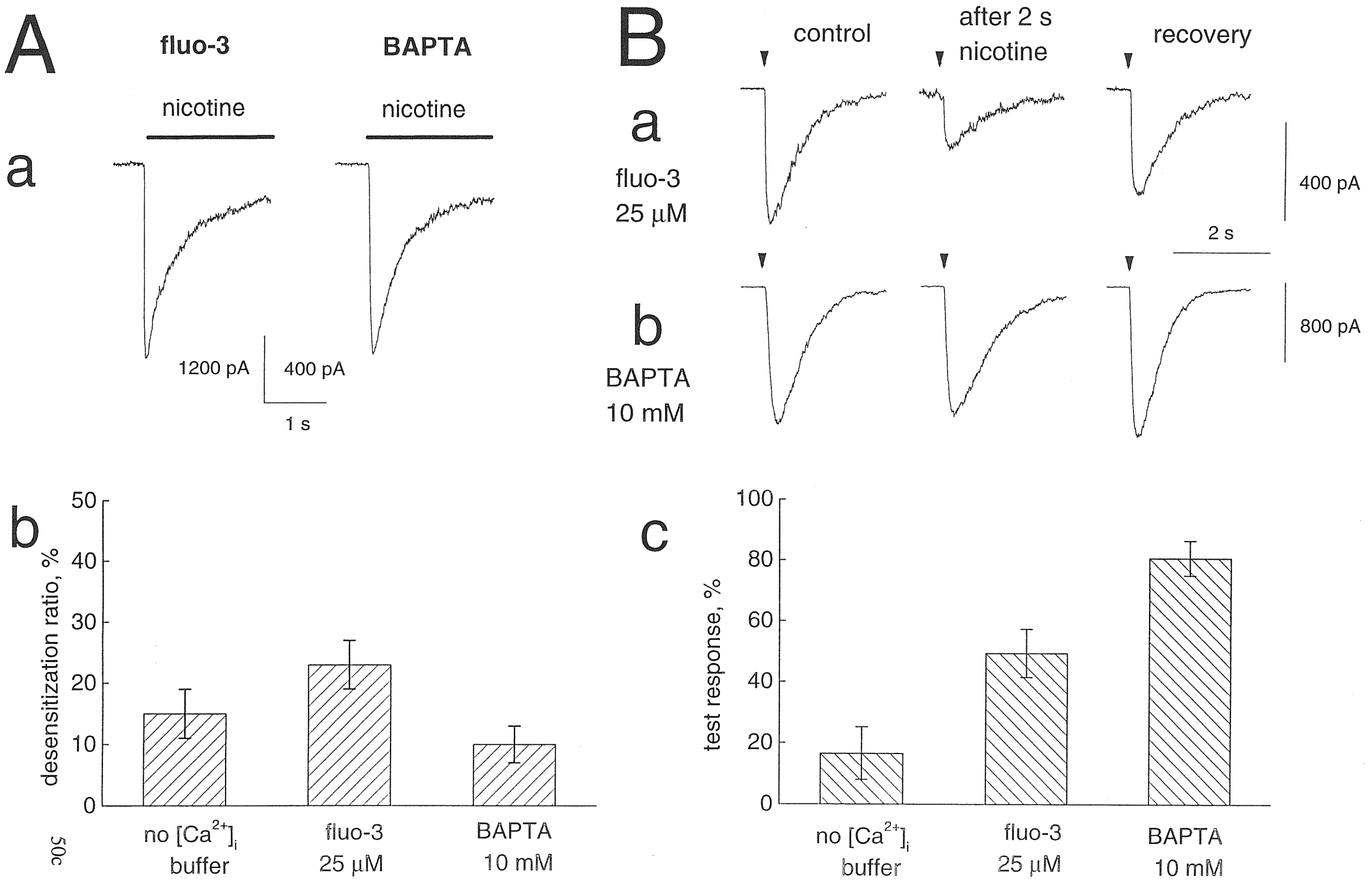
A
fluo-3
BAPTA
nicotine
nicotine
a
1200 pA
400 pA
1 s
B
control
after 2 s
nicotine
recovery
a
fluo-3
25 μM
400 pA
2 s
b
BAPTA
10 mM
800 pA
b
desensitization ratio, %
50
40
30
20
10
0
no [Ca2+]i
buffer
fluo-3
25 μM
BAPTA
10 mM
c
test response, %
100
80
60
40
20
0
no [Ca2+]i
buffer
fluo-3
25 μM
BAPTA
10 mM

Figure R-7I. Influence of $[Ca^{2+}]_i$ buffers on membrane currents induced by 1 mM nicotine. A: a, comparison of current fading evoked by 2 s nicotine pulse (horizontal bar) recorded in a cell with fluo-3 (left) *versus* a cell recorded with a BAPTA containing pipette (right). Note similar fading process to a comparable level of R_{2s} induced by nicotine application; b), histograms of desensitization ratio (R_{2s}) from cells recorded without addition of intracellular buffers, or with indicated buffers (25 μM fluo-3 or 10 mM BAPTA). Note similar results despite different pipette solutions. B: a, responses to 20 ms nicotine pulse before (control), 30 s after a 2 s nicotine pulse (middle), and 2 min recovery (right) recorded from a cell patch clamped with a fluo-3 containing pipette; b, comparable data obtained from another cell patch clamped with a BAPTA containing pipette; c, histograms depicting degree of recovery from desensitization (expressed as % of response to 20 ms nicotine 30 s after 2 s nicotine pulse) of cells recorded with no buffers, fluo-3 or BAPTA containing pipettes. Note that recovery from desensitization is maximal in the presence of BAPTA and smaller in the presence of fluo-3 or in the absence of exogenous chelators. The average value for no buffers was significantly different from the one for BAPTA ($P<0.05$).

IX-6. Effects of $[Ca^{2+}]_i$ chelators on nAChR desensitization.

An alternative method consisting in introducing different or no exogenous Ca^{2+} chelators through the patch pipette, was also used to investigate the role of this ion both in development of nAChRs desensitization and recovery from it. Figure 7I A demonstrates the lack of dependence of onset and steady-state desensitization on $[Ca^{2+}]_i$ buffering. As depicted in Aa, in cells patched with fluo-3 or BAPTA-containing pipettes, a 2 s application of nicotine induced inward currents which rapidly faded with a similar biexponential time-course to a comparable R_{2s} level in spite of the difference in absolute peak amplitude values. Figure 7I Ab summarises the data for R_{2s} obtained from cells patched with pipettes containing no buffers (left), fluo-3 (middle) or BAPTA (right). Note that there was no signifficant difference between the mean values. These observations indicated that $[Ca^{2+}]_i$ was relatively unimportant for development of nAChR desensitization. This issue was further addressed in the experiments where extracellular Ca^{2+} was removed and 0.5 mM BAPTA was added to the bathing solution. As shown in Figure 7II, none of the parameters characterising desensitization development (namely, peak current amplitude (A), desensitization ratio (B), fast (C) and slow (D) components of decay time-course) were found to depend on $[Ca^{2+}]_o$.

The degree of test current depression 30 s after the conditioning dose was also assessed in separate electrophysiological experiments when cells were patched with pipettes containing 10 mM BAPTA or no buffers. The results were compared with those obtained during the imaging experiments reported above when fluo-3 was added intracellularly. Fig. R-7I Ba shows an example of responses to 20 ms test pulse of

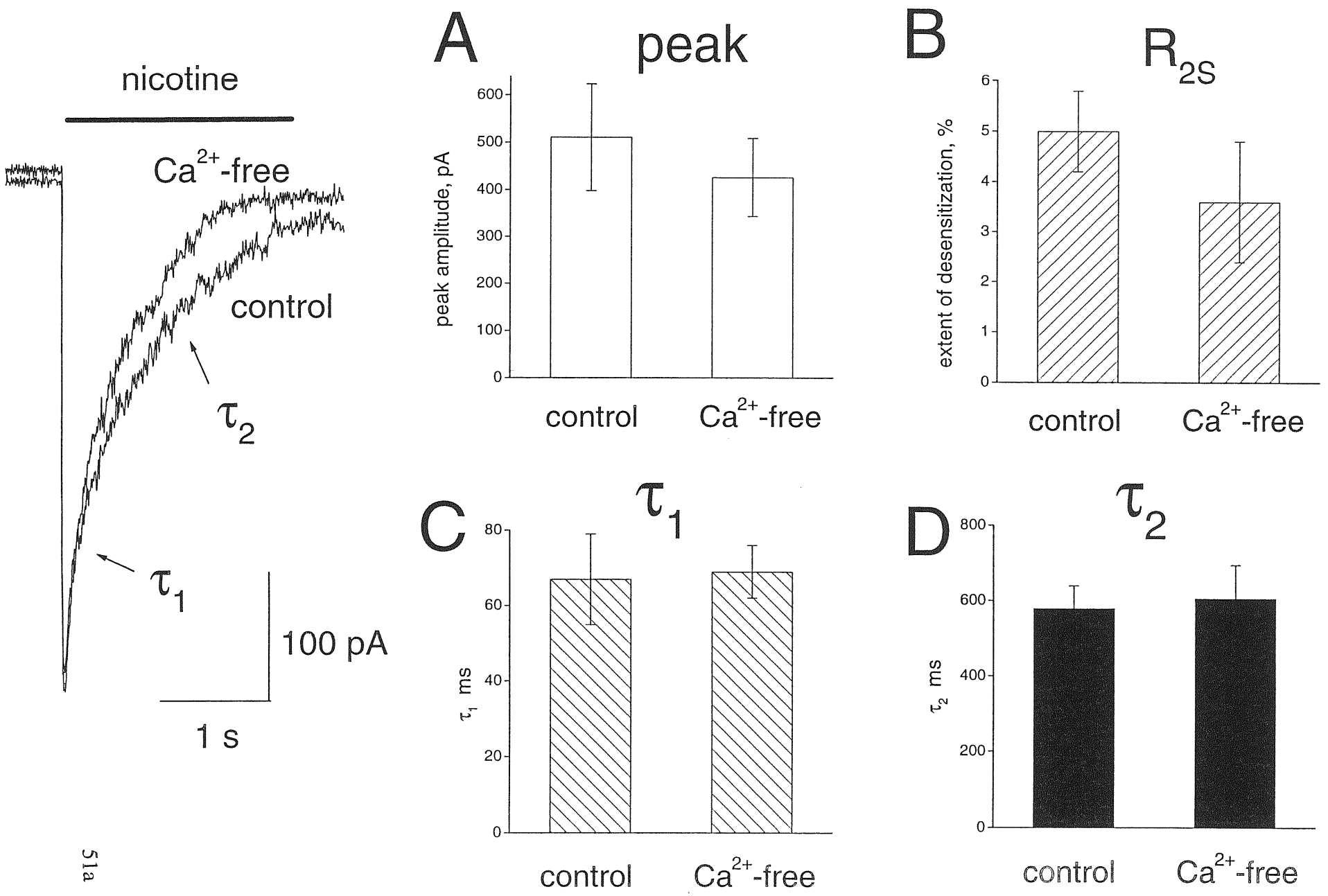
nicotine
Ca2+-free
control
τ2
τ1
100 pA
1 s
A
peak
peak amplitude, pA
600
500
400
300
200
100
0
control
Ca2+-free
B
R2S
extent of desensitization, %
6
5
4
3
2
1
0
control
Ca2+-free
C
τ1
τ1 ms
80
60
40
20
0
control
Ca2+-free
D
τ2
τ2 ms
800
600
400
200
0
control
Ca2+-free

Figure R-7II. Effects of Ca^{2+}-free solution on desensitization of nAChRs. The representative superimposed tracings illustrate similarity of currents recorded in response to 2 s application of nicotine in control or Ca^{2+}-free medium. A, comparison between peak amplitude of current evoked by 2 s pulse of nicotine in control conditions with that recorded from the same cells in Ca^{2+}-free solution. B, comparison between extent of desensitization (R_{2S}; residual inward current (% of peak) at the end of 2 s conditioning pulse of nicotine) with and without external Ca^{2+}. C-D, comparison between fast and slow components of current decay (τ_1 and τ_2; C and D, respectively) in control and Ca^{2+}-free conditions. Data are pooled from 3 cells.

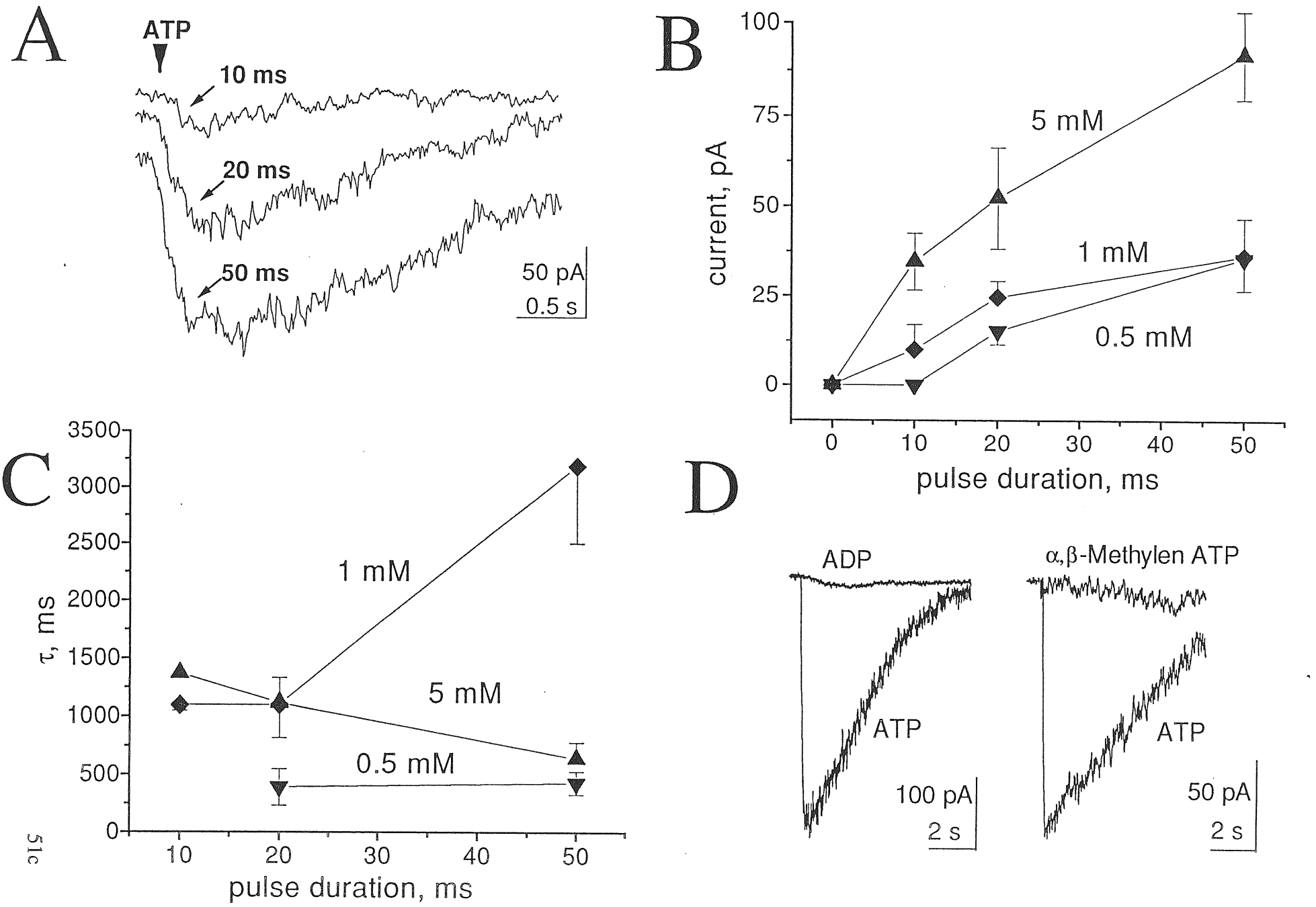
A
ATP
10 ms
20 ms
50 ms
50 pA
0.5 s
B
current, pA
100
75
50
25
0
5 mM
1 mM
0.5 mM
0
10
20
30
40
50
pulse duration, ms
C
τ, ms
3500
3000
2500
2000
1500
1000
500
0
1 mM
5 mM
0.5 mM
10
20
30
40
50
pulse duration, ms
D
ADP
ATP
100 pA
2 s
α,β-Methylen ATP
ATP
50 pA
2 s

51c

Figure R-8. Membrane currents induced by pressure application of ATP. A, dependence of amplitude and time course of the current induced by 5 mM ATP on pulse duration (indicated in ms alongside tracings). Arrowhead indicates the time of ATP application. B, dependence of peak current amplitude on pulse duration for 0.5 mM (downward triangles), 1 mM (diamonds), and 5 mM (upward triangles) ATP. Datapoints are from 2-4 cells. C, plot of the timeconstant (τ) of the response monoexponential decay against pulse duration for different concentrations of ATP. Symbols, abbreviations and error bars as in B. D, comparison of effectiveness of ADP and α,β-methylene ATP *versus* that of ATP. Drugs were applied by 20 ms pressure pulses from 5 mM solutions (different cells in left and right panels).

nicotine prior to (left), 30 s after (middle) or 2 min after (right) the conditioning pulse of nicotine. As compared to responses recorded under similar conditions with pipette containing 10 mM BAPTA (Bb), suppression of test response after conditioning pulse was much stronger with fluo-3. On average (Fig. 7I Bc), omission of any exogenous buffer was associated with persistent desensitization as the current was 17±9 % (n=3) of control ($P<0.005$ versus BAPTA-loaded cells; $P=0.06$ versus fluo-3 loaded cells). In this condition recording stability was shortlasting presumably due to the unhindered rise in $[Ca^{2+}]_i$ induced by intracellular dialysis. With BAPTA-containing pipettes desensitization at 30 s was much less since the test current was 81±6 % (n=4; significantly different from 50 ± 9 % of fluo-3 loaded cells, n=10; $P<0.05$).

X. Fast and slow desensitization of P_{2X} receptors on PC12 cells

The process of P_{2X} receptor desensitization which underlies response fading under continuous presence of ATP, is much less studied in comparison with that of nAChRs. Therefore it was described first using conventional whole-cell patch clamp recording and pressure application of ATP.

X-1. Characteristics of membrane currents induced by ATP

At -70 mV holding potential brief (10-50 ms) applications of ATP from pipettes containing 0.5, 1 or 5 mM ATP induced inward currents as shown in Fig. R-8 A for a 5 mM solution. Tracings in Fig. R-8A indicate that the amplitude and time course of ATP-induced currents were related to pulse duration for the same pipette solution. On a sample of 6 cells tested with 20 ms applications from 5 mM solution the currents

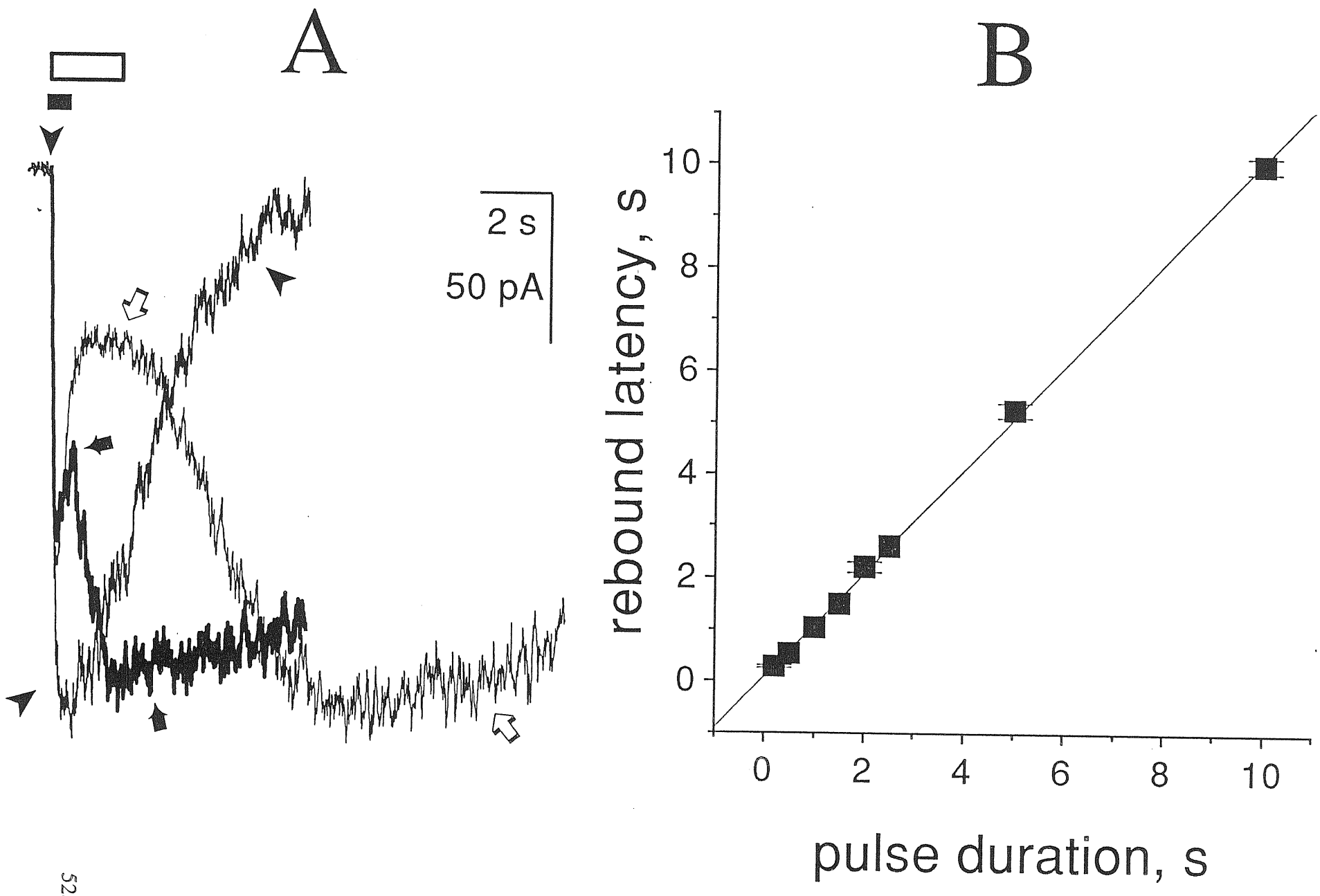
A
2 s
50 pA
B
rebound latency, s
0
2
4
6
8
10
pulse duration, s

Figure R-9. Current fade and rebound with 5 mM ATP pulse longer than 100 ms. A, superimposed tracings of responses evoked by 20 ms (filled arrowheads and medium thickness trace), 200 ms (thick trace and filled arrows), and 2000 ms (thin trace and open arrows) pulses of 5 mM ATP. Above baseline arrowhed indicates time of 20 ms ATP application, while filled and open bars show the duration of 200 ms and 2000 ms pulses, respectively. B, correlation between pulse duration and latency for onset of rebound; latency was measured as the time interval from the beginning of the pulse to the crossover of the rebound current slope with the current level at the end of the pulse. Data points (from 2-4 cells) are fitted with a linear equation where $Y = 0.0887 + 0.9996 * X$ (0.9996 is the correlation coefficient).

displayed a 10-90 % rise time of 163±14 ms and a slower decay (1130±202 ms timeconstant, τ, for monoexponential decline). Application time/effect curves depict the relation obtained when 0.5, 1 or 5 mM solutions were used on a sample of cells (Fig.R-8 B). Under these conditions the largest effects were observed with 50 ms applications from 5 mM ATP solution. Pressure applications from 0.5 or 1 mM solutions evoked comparatively smaller amplitude responses (Fig. R-8 B). The time constant values for monoexponential decay of the inward currents possessed a complex dependence on the pulse duration as shown in Fig. R-8 C: when 0.5 mM solution was used there was no apparent variation, whereas the time constant value grew for increases in duration of pulses with the 1 mM solution and attenuated with the 5 mM one. With pulses >50 ms from a 5 mM solution the current decay became multiexponential (not shown). Pressure applications of 5 mM solutions of either ADP or α,β-methylene ATP produced only weak responses which in the example of Fig. R-8 D were <3 % of those elicited by ATP at the same concentration. The responses to short pulses of ATP were stable and highly reproducible at applications rates as high as 1 every 60 s. On a sample of three cells, ATP induced responses were fully and reversably blocked by bath administration of 10 μM PPADS, the specific antagonist of P_{2X} receptors.

X-2. Current fade and rebound

Fig. R-9 A shows that 20 ms ATP (5 mM) application (filled arrowhead above tracings) induced a large inward current with a rise time of 205 ms. Increasing the duration of the ATP pulse to 200 ms (filled horizontal bar) generated an initial current

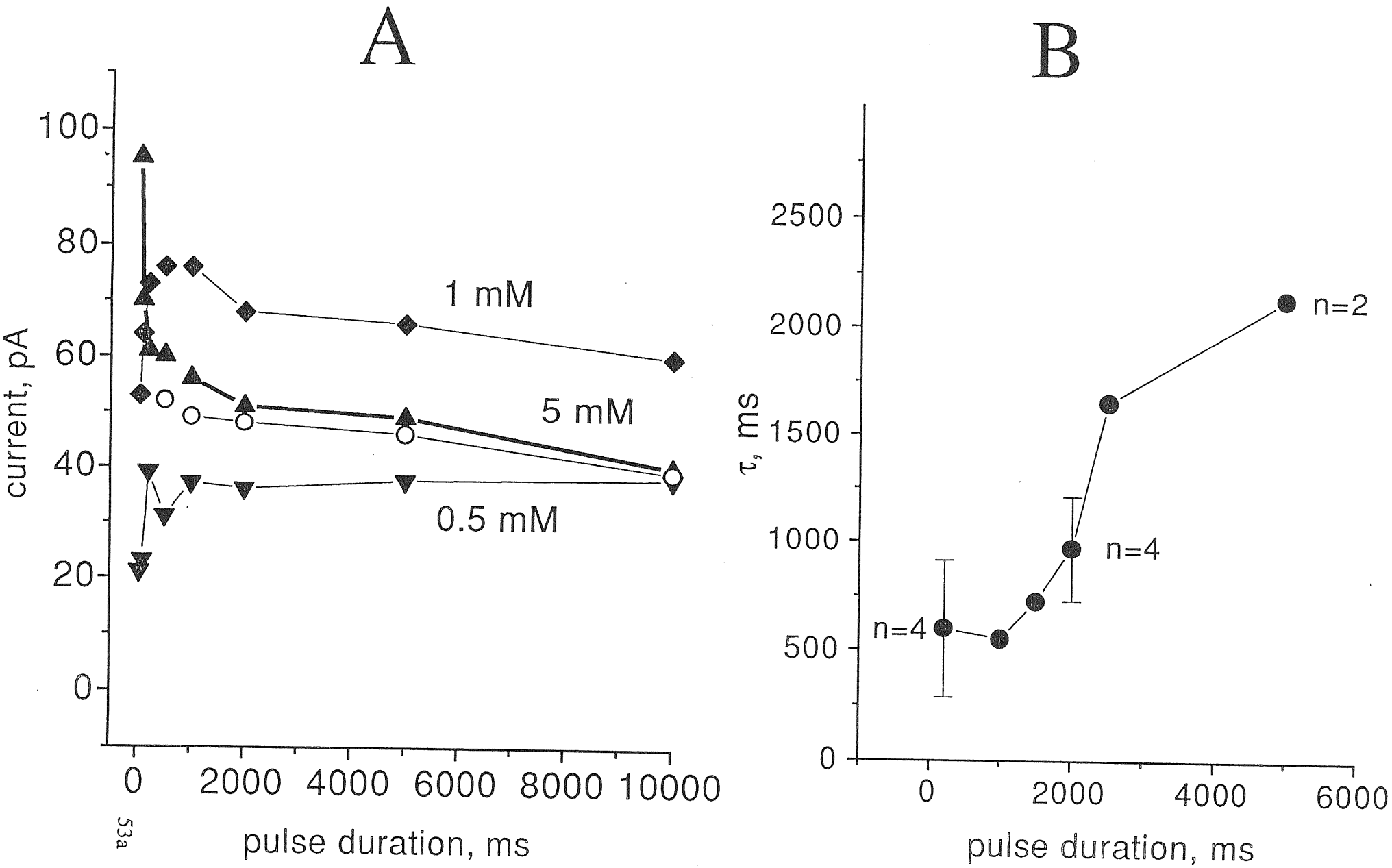
A
B
100
80
60
40
20
0
current, pA
1 mM
5 mM
0.5 mM
0
2000
4000
6000
8000
10000
pulse duration, ms
2500
2000
1500
1000
500
0
τ, ms
n=2
n=4
n=4
0
2000
4000
6000
pulse duration, ms

Figure R-10. Current peak, rebound amplitude and onset of rebound are dependent on ATP pulse duration. A, dependence of current initial peak (filled symbols) and rising phase of the rebound currents (whenever present; open circles) amplitude on pulse duration for three pipette concentrations of ATP (0.5 mM downward triangles; 1mM diamonds; 5 mM upward triangles). All data are from the same representative cell on which responses were usually tested twice; B, dependence of the time constant (τ) of rebound response evoked by 5 mM ATP on pressure pulse duration. n=number of cells.

with smaller peak (see thick tracing; rise time = 130 ms) than that observed with the shorter application (medium thickness tracing; arrowhead) and was followed by fast current fade (see filled arrow). Immediately after the end of 200 ms drug delivery the response rapidly increased (termed rebound) up to the level observed with the 20 ms application (Fig. R-9 A, filled arrow) despite fast superfusion of the cell which rapidly lowered extracellular ATP. When the pressure pulse was 2 s long (open bar above tracings), the initial current peak was the same as with the 200 ms application (rise time was also very similar, i.e. 140 ms) and then faded to a plateau level (open arrow). In such a case the current decline from its peak value could be fitted by two exponentials (τ_1=95±15 ms; τ_2=4.3±0.2 s; n=5). Immediately after the end of the 2 s drug application current rebound also developed. This pattern of current fade and rebound was readily reproduced as long as ATP pulses were applied at 2-3 min intervals. It is also interesting to note that in the example of Fig. R-9 A the τ_1 value for current fade shortened from 1097 to 264 ms when the pressure application time was varied from 0.2 to 2 s, while the corresponding τ value for rebound onset increased from 1148 to 7994 ms. Fig. R-9 B shows the relation between the latency of the rebound (from the start of the pulse) and the pulse duration (0.2-10 s): this was found to be linear and in no instance the rebound developed prior to the end of the application itself. Neither initial peak no rebound current were observed in the presence of 10 μM PPADS (n=3).

X-3a. Current fade in response to Y-tube applied ATP

The unexpected observation of a large current rebound raised the possibility that this

response was somewhat caused by the method of pressure application of the agonist and perhaps its incomplete removal. In order to rule out this potential artefact, ATP (5 mM) was also applied by the Y-tube method (Akaike *et al.*, 1991). Furthermore, it was equally important to check the time course of the signals produced in blank experiments by KCl applied either by pulse pressure or by the Y-tube technique, since these observations can suggest the time profile of agonist presence in the external medium (Zhang *et al.,* 1994). Fig. M-12 (Methods section) shows a representative example of records obtained following pressure application of KCl (Aa) or 5 mM ATP (Ab): the ATP current peak was generated slightly slower than the maximum of the KCl-induced signal while the ATP rebound current appeared when the KCl signal had already dissipated. Fig. M-12 B shows comparative data obtained with the Y-tube application of KCl (Ba) or ATP (5 mM; Bb). Also in this case the ATP-induced current peak had an onset similar to that of the KCl signal and manifested a rebound at the time when the KCl-induced liquid junction change had disappeared. Similar observations were obtained in three cells. These results confirm that the ATP current rebound was observed with two different methods of application and was not dependent on slow agonist washout.

X-3b. Dependence of amplitude and onset of rebound on pulse duration

The relation between ATP-induced peak current and rebound was explored in a more systematic fashion as indicated in Fig. R-10 A which presents the plot of the amplitude of the first peak (filled symbols) and of the rebound (whenever present; open symbols) currents *versus* pulse duration for solutions containing 0. 5, 1 or 5 mM ATP (all data from the same cell). With a 5 mM solution, the largest response was

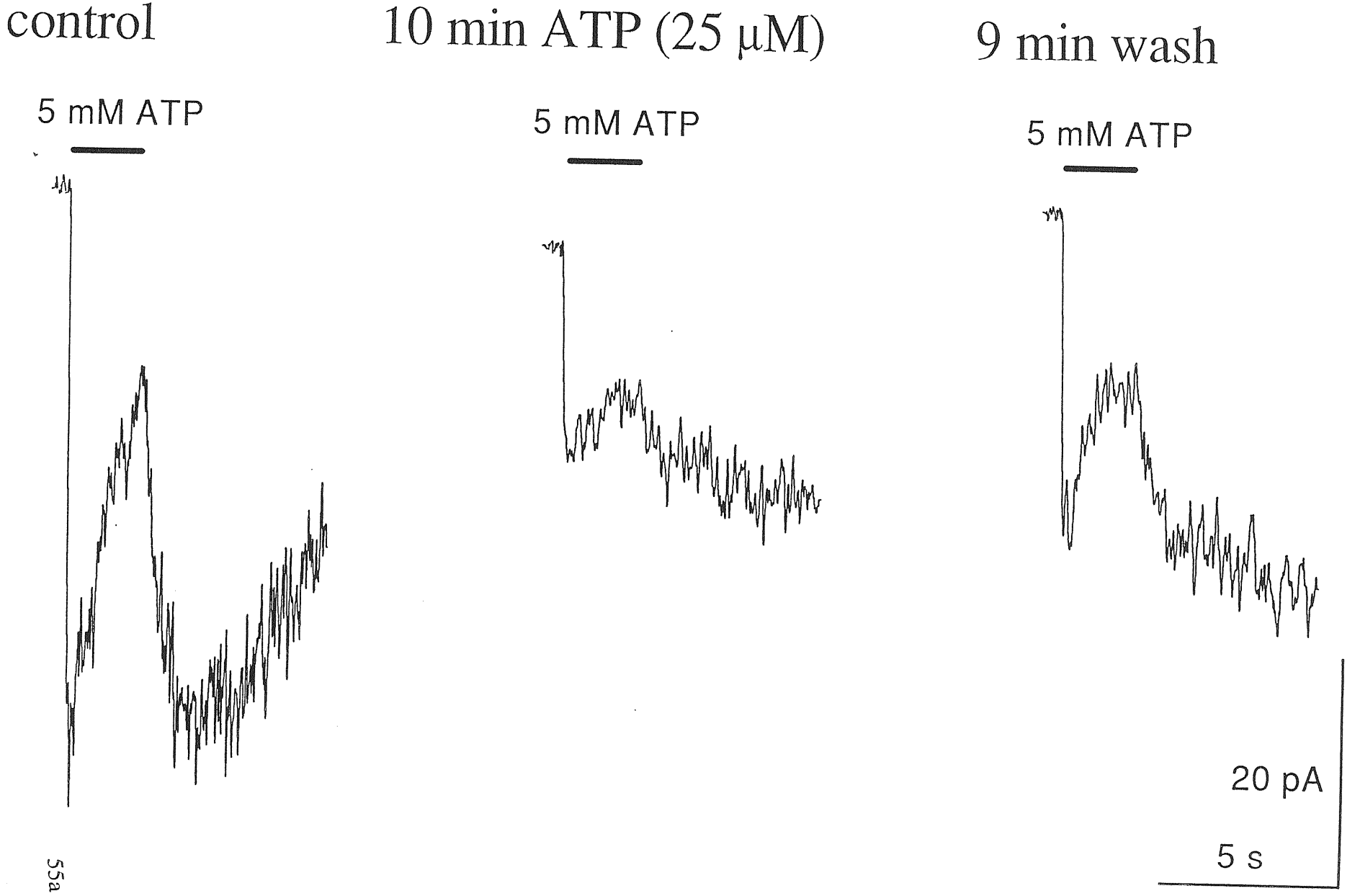
control
10 min ATP (25 μM)
9 min wash
5 mM ATP
5 mM ATP
5 mM ATP
20 pA
5 s
55a

Figure R-11. Bath application of 25 μM ATP affects response to 2 s pressure application of 5 mM ATP. Pressure application duration is indicated by the horizontal bars; the time of wash is calculated from the beginning of bath exchange with control solution. In the presence of 25 μM ATP both initial peak and rebound are reduced while there is a modest downward shift of the baseline indicating a slight inward current due to bath-applied ATP.

found with a 100 ms pulse (which produced no fast fading and rebound) since longer pulses elicited smaller peak responses (see upward triangles) presumably due to fast desensitization which initiated already during the receptor activation process, and were associated with a rebound response of approximately similar amplitude (open circles). On average, on a sample of 7 cells a 2 s pulse (5 mM ATP) induced a current peak of 136±43 pA and a rebound of 99±28 pA, that is the rebound was 75±12 % of the peak current. When pulses were several s long, neither the current peak nor the rebound consistently changed in amplitude, indicating that an apparently steady-state condition had been reached; a small decrease (from 64 pA to 54 pA peak amplitude) between responses to 2 and 10 s could be due to accumulation of slow desensitization (see below, Fig. R-14), even if stimulation frequency was kept as low as once every 3 min.

Responses elicited by 0.5 or 1 mM solutions were not followed by a rebound even if some peak current responses (e.g. those to 0.2-1 s pulses from 1 mM solution), though submaximal in absolute terms, were larger than the ones elicited by the 5 mM solution for equivalent pulse duration. Only in 1/11 cells 0.5 or 1 mM solutions evoked rebound effects. As indicated by the sample tracings of Fig. R-9 A the rate of rise of the rebound wave was faster when the application was 200 ms instead of 2 s. The graph of Fig. R-10 B quantifies this phenomenon by plotting τ values for the rising phase of the rebound current against ATP pulse duration, though the relation was not linear.

X-3c. Effects of bath-appplied ATP on current fade and rebound

Should ATP current fade and rebound have a common origin, they might share similar sensitivity not only to pressure applied ATP but also to bath application of the same substance. In Fig. R-11 this issue was examined by bath-applying a small concentration of ATP (25 μM) which *per se* produced only a minimal inward current (5 pA) that remained stable for about 10 min: subsequent application of a 2 s pulse from a 5 mM ATP solution produced a smaller peak response (37 % of control) and rebound (48 %) although the ratio between rebound and first peak remained essentially similar before (94 %) and during (121%) bath-application of ATP. It is interesting also to note that the current faded to the same absolute level regardless of the presence of bath-applied ATP (13 pA in control solution and 12 pA in ATP solution). In summary then, the rebound wave required duration of pulse application longer than that needed for maximal responses, was similar in size to the first peak with which it shared comparable sensitivity to ambient ATP, and developed more slowly as the pulse length was increased.

X-3. Voltage dependence of ATP-induced inward currents

The inward rectification of the ATP current at holding potentials less negative than -40 mV (see Khakh *et al.,* 1995) prevented a systematic analysis of the voltage sensitivity of the current fade and rebound. Nevertheless, within the apparently linear range of the current/voltage relation the slope conductance (calculated between -80 and -40 mV) was relatively similar, being 2.8±0.4 nS for the first peak and 2.4±0.8 nS for the rebound (n=3). Furthermore, the apparent null potential for the rebound

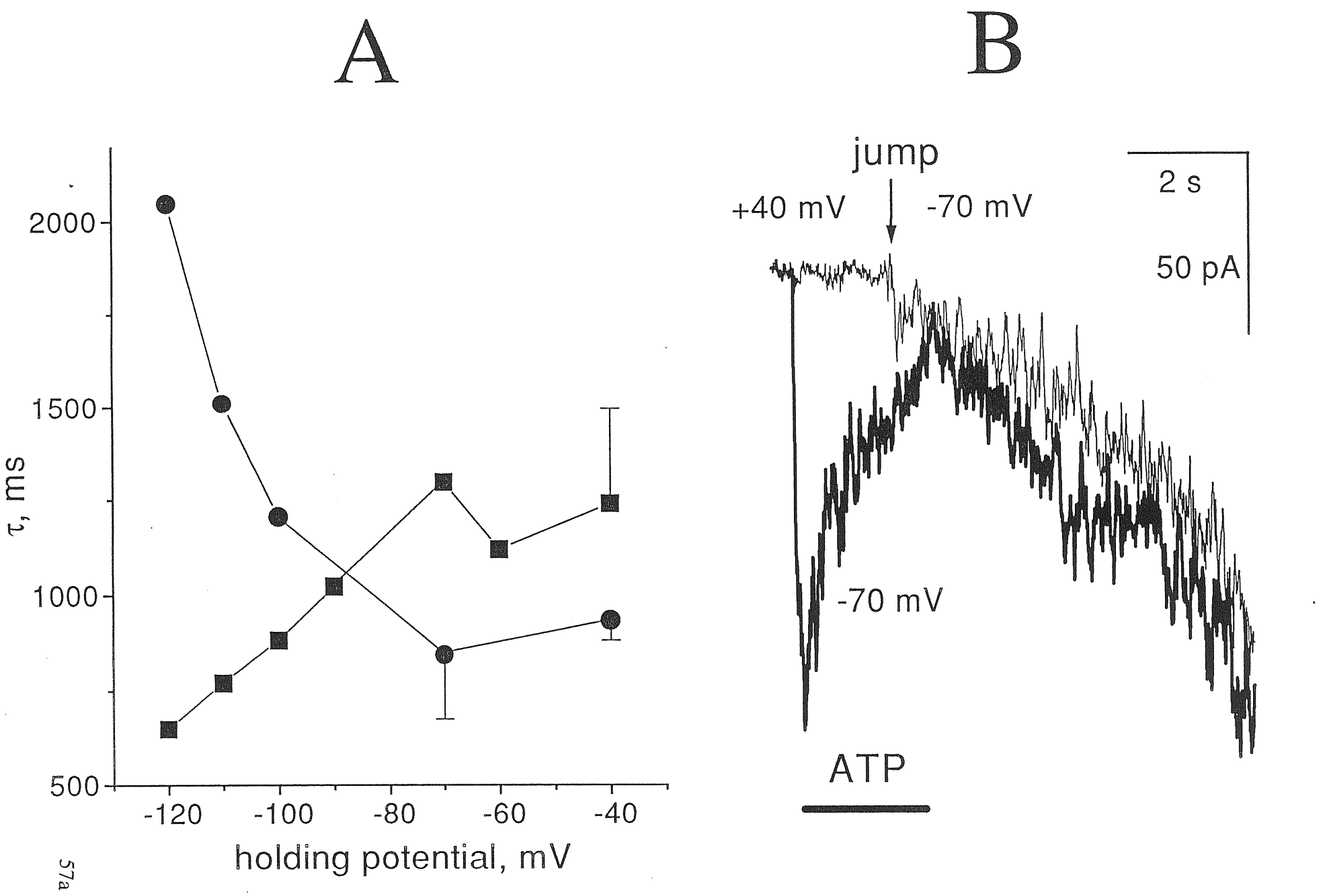
A
B
2000
1500
1000
500
τ, ms
-120
-100
-80
-60
-40
holding potential, mV
jump
+40 mV
-70 mV
2 s
50 pA
-70 mV
ATP

57a

Figure R-12. Voltage dependence of current fade and rebound. A, plot of first time constant of current fade (squares) and time constant of rebound (circles) against holding membrane potential. Data from 2-4 cells. B, thick tracing shows current fade and rebound after 2 s application of 5 mM ATP to a cell clamped at -70 mV, while the thin tracing shows the response from the same cell clamped at +40 mV during the 2 s application of ATP, after which the holding potential was stepwise changed to -70 mV (the time of potential jump is indicated by the arrow). With either holding potential the rebound was similar. The horizontal bar corresponds to the time of pressure application of ATP.

wave was -34.6±4.7 mV, a value close to that found for the first peak (-28.4±6.4; n=4) following a 2 s pulse of ATP. Fig. R-12 A shows a plot of τ_I for peak current fade (filled squares) and of τ for rebound onset (filled circles) *versus* holding membrane potential. These two parameters showed differential dependence on changes in membrane potential only in the range -120 to -90 mV as the τ_I values for current fade grew with depolarization while τ values for rebound decreased. At less negative membrane potentials (from -70 to -40 mV) neither parameter changed. Fig. R-12 B shows the result obtained with a different voltage clamp protocol: ATP was initially applied for 2 s to the cell clamped at -70 mV to produce a fading response followed by rebound (thick current trace); after a recovery of about 3 min the cell was clamped at +40 mV and did not display a response during the application of ATP (owing to strong current rectification). Immediately after the end of ATP delivery the membrane potential was returned to -70 mV (indicated by arrow in Fig. R-12 B) and a rebound similar to that one previously observed became apparent. These data imply that the rebound phenomenon was independent from actual current flow through activated purinoceptors.

X-4. Sensitivity of ATP currents to paired-pulse or repetitive applications

Fig. R-13 shows the effect of a short (20 ms) application of 5 mM ATP either alone (A) or at different intervals (C, D) after a long (2 s) pulse of ATP which produced fade and rebound (B). When the short application (arrowhead) coincided with the developing phase of the rebound (Fig. R-13 C), there was a transient current suppression which lasted for 900-1500 ms and was then followed by the rebound

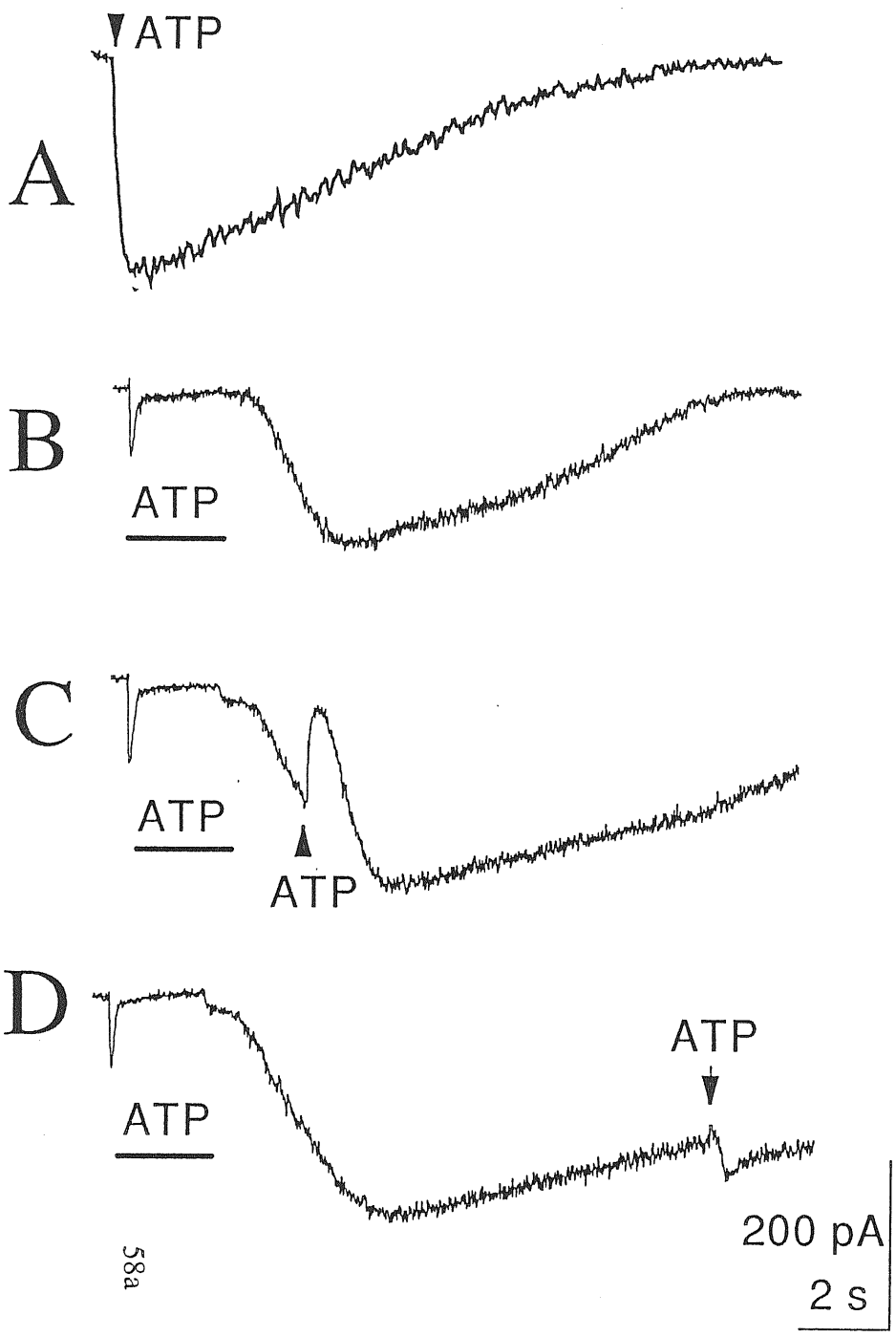
A
ATP
B
ATP
C
ATP
ATP
D
ATP
ATP
200 pA
2 s
58a

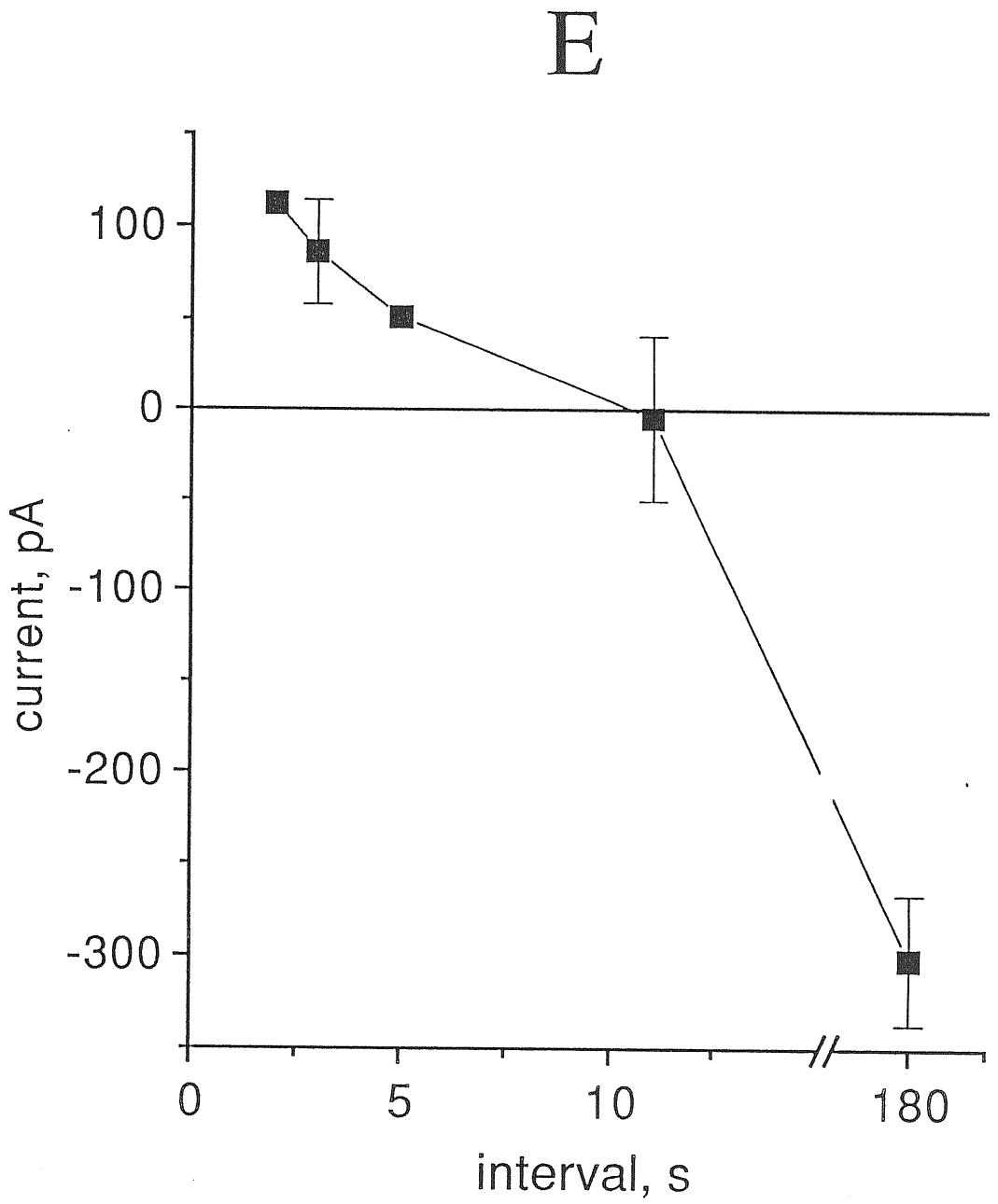
E
100
0
-100
-200
-300
current, pA
0
5
10
180
interval, s

Figure R-13. Brief application of ATP can influence rebound response. A, large, nondecrementing response evoked by 20 ms pulse of ATP (5 mM). The arrowhead indicates the time of application. B, biphasic response evoked by 2 s application of ATP (5 mM) indicated by the horizontal bar. C, 20 ms (arrowhead) pulse of ATP applied 2 s after the end of 2 s application (horizontal bar) transiently suppressed rebound current (observed as a outwardly-directed current after which rebound development continued). D, 20 ms (arrowhead) pulse of ATP applied 11 s after the end of 2 s pulse (horizontal bar) evoked a small inward current. E, responses (expressed in terms of absolute current amplitude with respect to preceding current level) to 20 ms application of ATP are plotted versus the interval between the end of 2 s application and the delivery of 20 ms pulse. Data are repeated measurements (2-4) from the same cell.

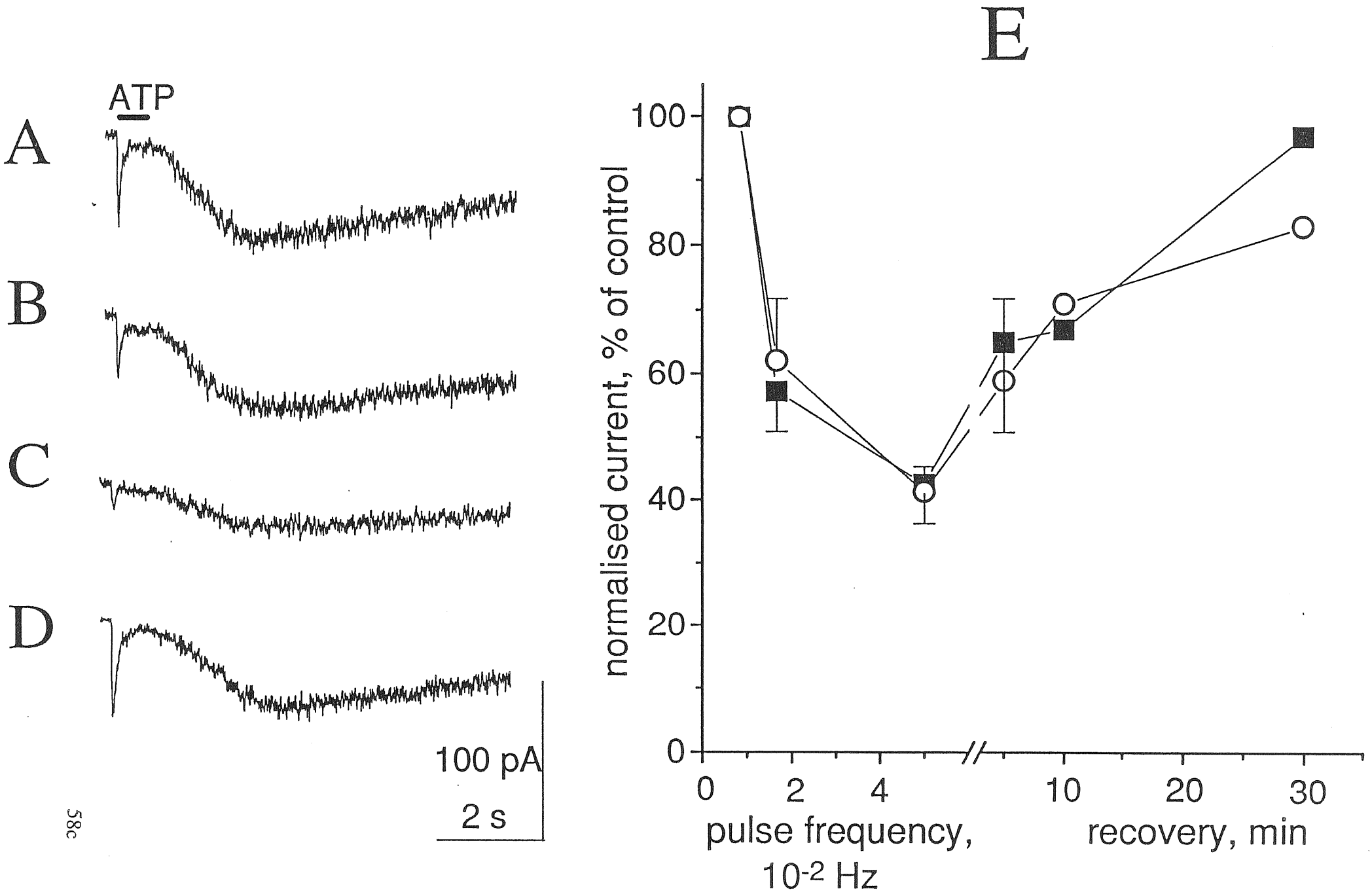
ATP
A
B
C
D
100 pA
2 s
E
normalised current, % of control
100
80
60
40
20
0
0
2
4
10
20
30
pulse frequency,
10-2 Hz
recovery, min

Figure R-14. Responses to repeatitive 2 s applications (indicated by horizontal line) of 5 mM ATP. A-D show progressive decline in inward currents when application interval was changed from 2 min (A) to 1 min (B) and to 20 s (C) with recovery after 30 min wash (D). E, plot of current amplitude (as % of control) against pulse frequency (Hz) between successive applications of 5 mM ATP. Data points after break in graph indicate responses at various intervals after the high frequency tests (recovery; note that abscissa is now in min). Filled squares indicate initial peak currents while open circles are for the rebound currents. Data are from 3-7 cells.

wave. This additional fast current fade presumably reflected high probability of receptor transition back into fast desensitized state during developing phase of rebound wave. When the short pulse of ATP was given during the decay phase of the rebound (arrow in Fig. R-13 D) but at the same absolute current level as before, the response consisted in a small inward current. Hence, the timing of the short application of ATP meant either suppression or non-linear summation of the response: this result is shown in Fig. R-13 E where the absolute current response produced by 20 ms ATP with respect to the preceding current level is plotted as a function of its interval from the long 2 s application. Similar findings were obtained from three cells. In control conditions the standard frequency of 2 s pulse 5 mM ATP applications was one every 2-3 min to prevent gradual decline of the response. In fact, when 10 mM ATP was pressure-applied for 2 s, responses run down even if spaced at 3 min intervals (data not shown). Fig. R-14 presents an example of the progressive change in response to 5 mM ATP (2 s pulse application) when the frequency of application was increased first to once every 60 s (see Fig. R-14 B) and then to once every 20 s (Fig. R-14 C). In the latter case the initial current peak was 28 % of control while the rebound wave was 42 % (recovery was obtained 30 min later; Fig. R-14 D). Fig. R-14 E shows a graph of the time course of peak and rebound currents induced by applying ATP (5 mM) at various intervals: it is apparent that there was a parallel decline (and recovery) for both components of the response.

XI. Role of $[Ca^{2+}]_i$ in P_{2X} receptor desensitization

Having demonstrated two distinct phases of P_{2X} receptor desensitization, namely fast and slow ones of which the first one was followed by a large rebound current (see

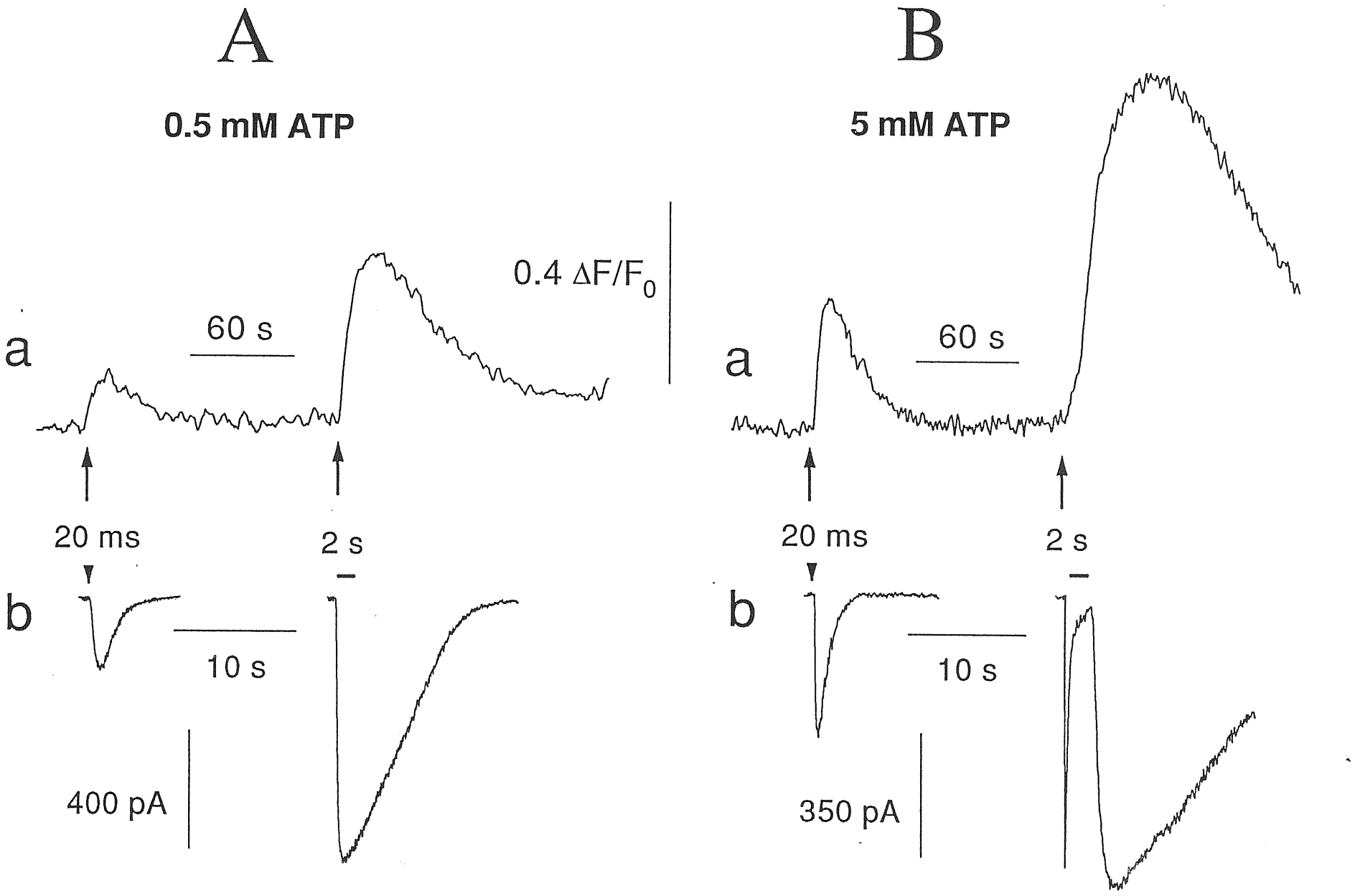
A
0.5 mM ATP
0.4 ΔF/F0
60 s
a
20 ms
2 s
b
10 s
400 pA
B
5 mM ATP
60 s
a
20 ms
2 s
b
10 s
350 pA

Figure R-15. Effects of ATP on $[Ca^{2+}]_i$ transients and membrane currents of PC12 cells. A: combined recording of $[Ca^{2+}]_i$ response (a) and inward current (b) induced by either 20 ms (arrowhead) or 2 s (horizontal bar) application of ATP (0.5 mM). Note different timescale for a and b. ATP applications in a are indicated by arrows. B: Responses produced by 5 mM ATP on a different PC12 cell. Application times and symbols are the same as in A. Timescale in a is much slower than in b. Note that a 2 s application of ATP induces a large peak current which fades during the application and is followed by a large rebound immediately after termination of ATP pressure pulse.

Chapter X), any modulation of these phases by $[Ca^{2+}]_i$ and possible temporal correlation between desensitization and $[Ca^{2+}]_i$ elevation were investigated.

Since long pulses applied from 5 mM ATP solution were reliably capable of inducing rapid receptor desensitization consisting of current fade and rebound (Chapter X), further experiments aimed at investigating the relation between ATP induced currents and $[Ca^{2+}]_i$ were carried out using this concentration of ATP. Nevertheless, it should be noted that, unlike the conventional patch clamp study of PC12 cells reported in Chapter X, for the present experiments with Ca^{2+} imaging it was necessary to omit from the pipette solution Ca^{2+} chelators such as EGTA which would have compromised $[Ca^{2+}]_i$ imaging itself (see Methods). Hence, since long-term changes in $[Ca^{2+}]_i$ could not be prevented, it was decided to measure responses to ATP (in the presence of fluo-3 in the internal solution) for not more than 20 min after the stabilization period of 8 min, during which these responses were as reproducible as those of intact (non-patched) cells loaded with fluo-3 AM (see below).

XI-1. Membrane currents and $[Ca^{2+}]_i$ transients induced by ATP

Membrane currents and associated changes in $[Ca^{2+}]_i$ were studied in combined experiments using whole-cell patch clamp recording and confocal Ca^{2+} imaging. An example of this approach is provided in Fig. R-15, in which at -70 mV holding potential, application of ATP from pipettes containing 0.5 or 5 mM concentrations induced inward currents (Fig. R-15 Ab and Bb) and rises in $[Ca^{2+}]_i$ (Fig. R-15 Aa and Ba) of a PC12 cell. In this case, a 0.5 mM solution of ATP (either 20 ms or 2 s pulse application; arrows show applications for $[Ca^{2+}]_i$ responses while arrowhead or bar shows application for current responses) induced monophasic responses with rapid onset and gradual decline although there was an apparent lag between the peak of

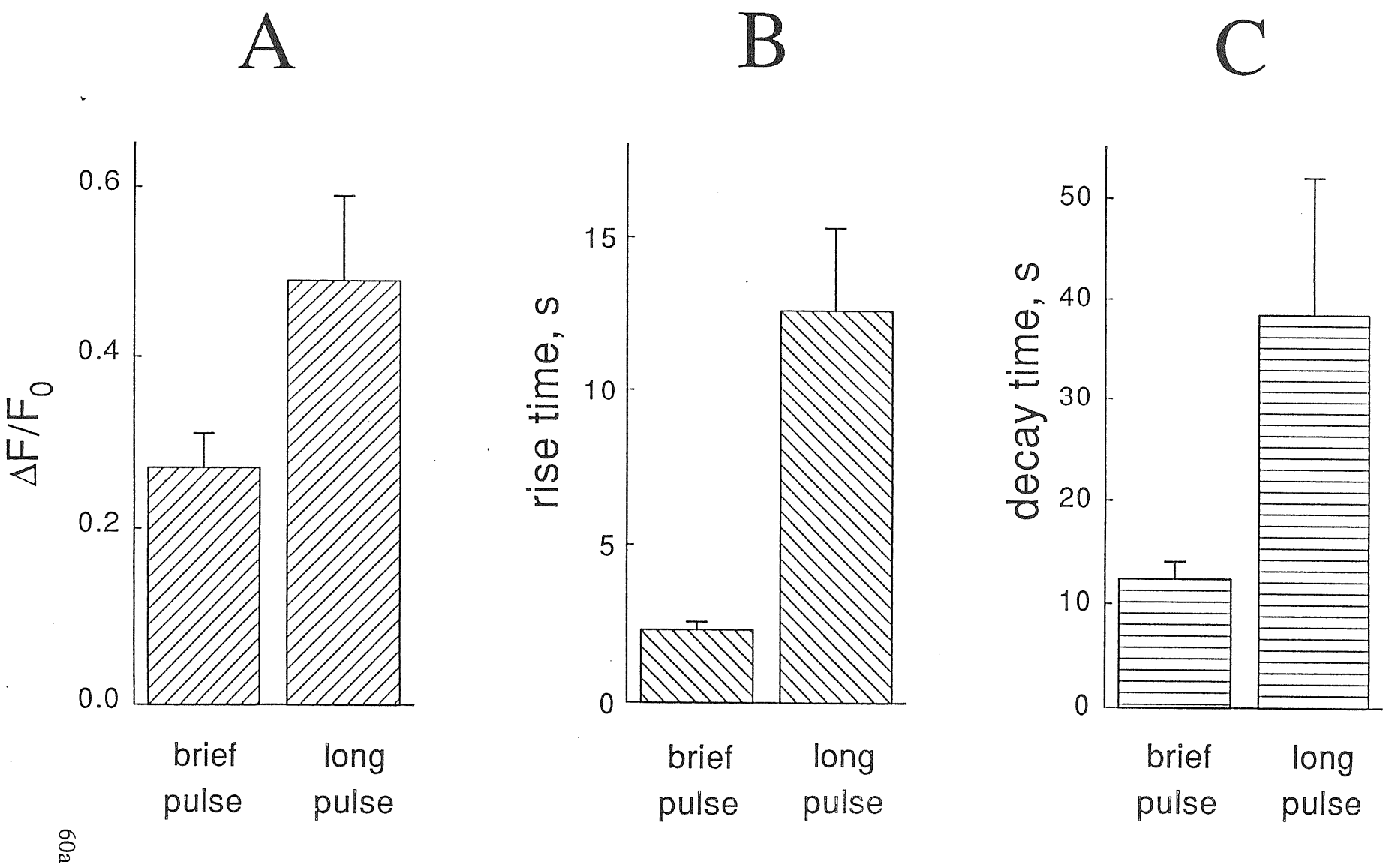
A
B
C
0.6
0.4
0.2
0.0
ΔF/F0
brief pulse
long pulse
15
10
5
0
rise time, s
brief pulse
long pulse
50
40
30
20
10
0
decay time, s
brief pulse
long pulse

60a

Figure R-16. Histograms of $[Ca^{2+}]_i$ changes following brief (20-50 ms) or long (2 s) pulses of 5 mM ATP to patch-clamped PC12 cells. A: fractional changes in peak amplitude of $[Ca^{2+}]_i$ responses. B: time constant of $[Ca^{2+}]_i$ rises. C: decay time constant of $[Ca^{2+}]_i$ transients. Data are from 9 cells. In A, B and C the difference between the pair of histograms was significant ($P<0.05$, 0.005, and 0.05, respectively) when analyzed with ANOVA test (A) or paired *t*-test (B and C).

these inward currents and that of $[Ca^{2+}]_i$ transients (the latter peaking at 6.7 s for 20 ms or 8.3 s for 2 s pulse after current peak; note that the timescale for $[Ca^{2+}]_i$ is much slower than that for membrane currents). When the ATP concentration was 5 mM, a 20 ms pulse application generated a monophasic response comprising a 364 pA inward current and an associated rise (0.32 $\Delta F/F_0$) in $[Ca^{2+}]_i$ (see Fig. R-15 Ba, b; different cell from Fig. R-15 A). When the 5 mM ATP solution was applied for 2 s, the inward current peak (960 pA) quickly faded almost back to baseline level and was followed by a rebound current (1034 pA) immediately after the end of drug application: the latter phenomenon is considered to be due to fast receptor desensitization and recovery (Chapter X). Unlike this biphasic nature of the inward current response, the corresponding $[Ca^{2+}]_i$ rise (although much larger in fractional amplitude and decay time constant, namely 0.64 $\Delta F/F_0$ and 40 s, respectively) had smooth onset and decline (Fig. R-15 Ba; note slower timebase than corresponding currents in Fig. R-15 Bb). It is worth noting that the peak $[Ca^{2+}]_i$ increase occurred with a considerable delay (21 s) with respect to peak and rebound inward currents. Since it has been shown that the development of $[Ca^{2+}]_i$ rise is related more to the current integral rather than its peak amplitude (Rathouz & Berg, 1994), it is not unexpected that the rise in $[Ca^{2+}]_i$ after 2 s ATP pulse was slower than after 20 ms pulse since the long application induced a 157 pC charge transfer during the initial peak *versus* 245 pC charge transfer induced by the brief pulse.

Histograms in Fig. R-16 A-C show, for a sample of 9 cells, that using either brief (10-50 ms) or long (2 s) pulses of 5 mM ATP led to significant differences in the increase in $[Ca^{2+}]_i$, and its rise and decay times. Long pulses elicited responses of larger

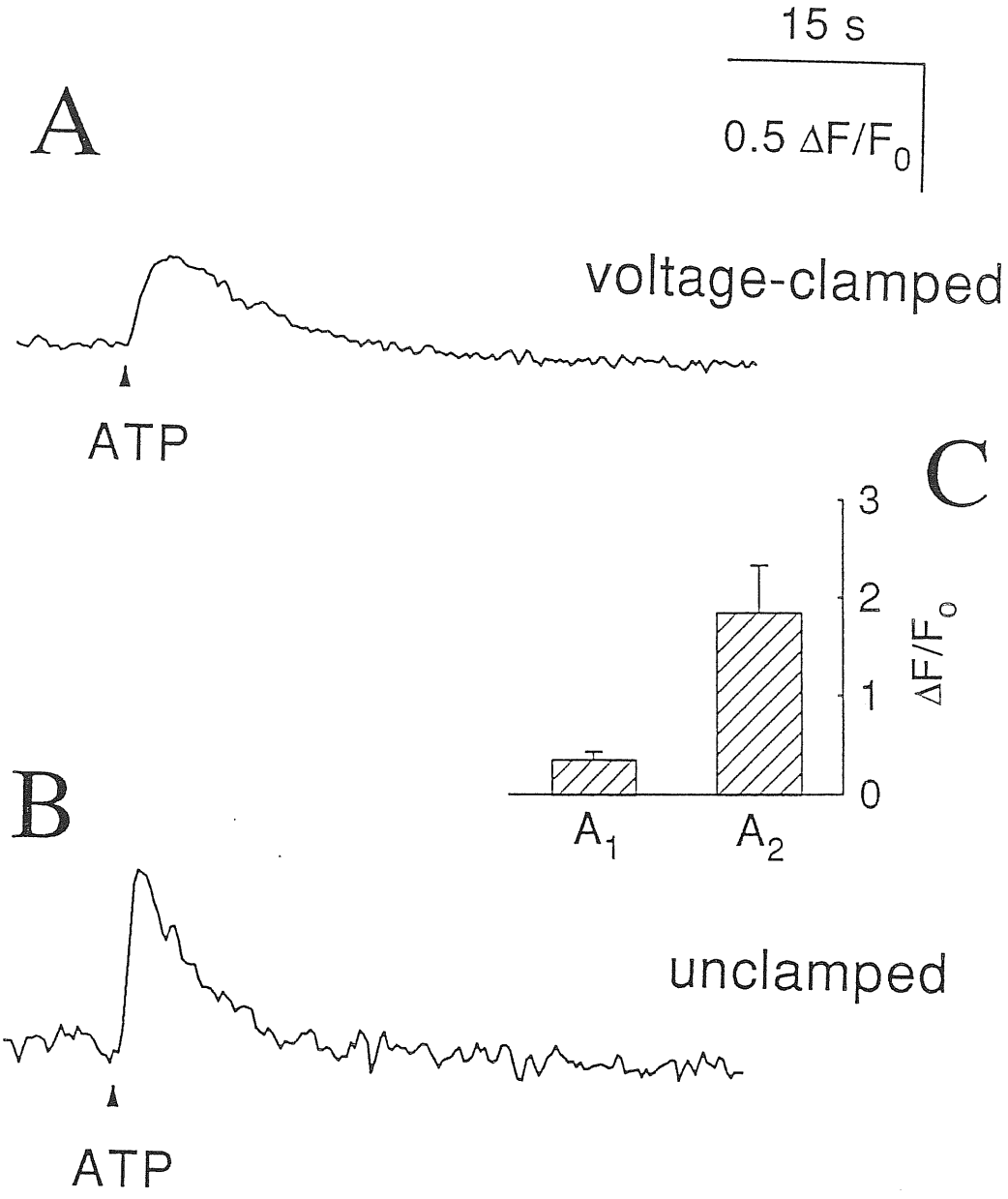
15 s
A
0.5 ΔF/F0
voltage-clamped
ATP
C
3
2
1
0
ΔF/F0
A1
A2
B
unclamped
ATP

Figure R-17. Comparison of $[Ca^{2+}]_i$ transients in patched or intact PC12 cells. A, a response induced by 20 ms ATP (5 mM) pulse in voltage-clamped cell; B, a response induced by 20 ms application of ATP in intact (unclamped) cell. Inset shows histograms of average values for the first (A_1) or the second (A_2) peak of the $[Ca^{2+}]_i$ response of intact cells (n=9; see Fig. M-11 for details).

amplitude (Fig. R-16 A; $P<0.05$), and longer rise time (Fig. R-16 B; $P<0.005$). Interestingly, the parameter which differed most between responses to brief and long pulses was the rise time (see Fig. R-16 B) for $[Ca^{2+}]_i$ transients (5.5 fold increment); this behaviour was the opposite of the one displayed when ATP-induced membrane currents were considered (see for example Fig. R-15 B). Time constant values of $[Ca^{2+}]_i$ transient decay were also significantly different (Fig. R-16 C; $P<0.05$) between brief or long pulses of ATP delivered to the same cells.

XI-2. Source of $[Ca^{2+}]_i$ rise induced by ATP

The relatively slow characteristics of $[Ca^{2+}]_i$ changes produced by ATP raised the possibility that they were caused by the voltage clamp condition which prevented activation of voltage-dependent Ca^{2+} channels by membrane depolarization. It therefore seemed interesting to compare $[Ca^{2+}]_i$ changes in patched or intact cells. This question was explored with 20 ms or 2 s ATP pulses. Fig. R-17 exemplifies the case with brief (20 ms) pulses of ATP (see arrowheads) which induced monophasic $[Ca^{2+}]_i$ responses in both patched and intact (unclamped) cells. The peak amplitude of $[Ca^{2+}]_i$ rise was larger in the intact than in the voltage-clamped cell (0.81 ± 0.23 and 0.27 ± 0.04 $\Delta F/F_0$, respectively, for a sample of 9 cells), and its rate of rise was faster (0.61 ± 0.1 s *versus* 2.82 ± 0.28 s, respectively, n=9).

However, the major difference appeared when comparing responses produced by the 2 s ATP application. This situation is demonstrated in Fig. R-17 and Fig. M-11 (see Methods). ATP application is indicated by horizontal bars in Fig. M-11. In this

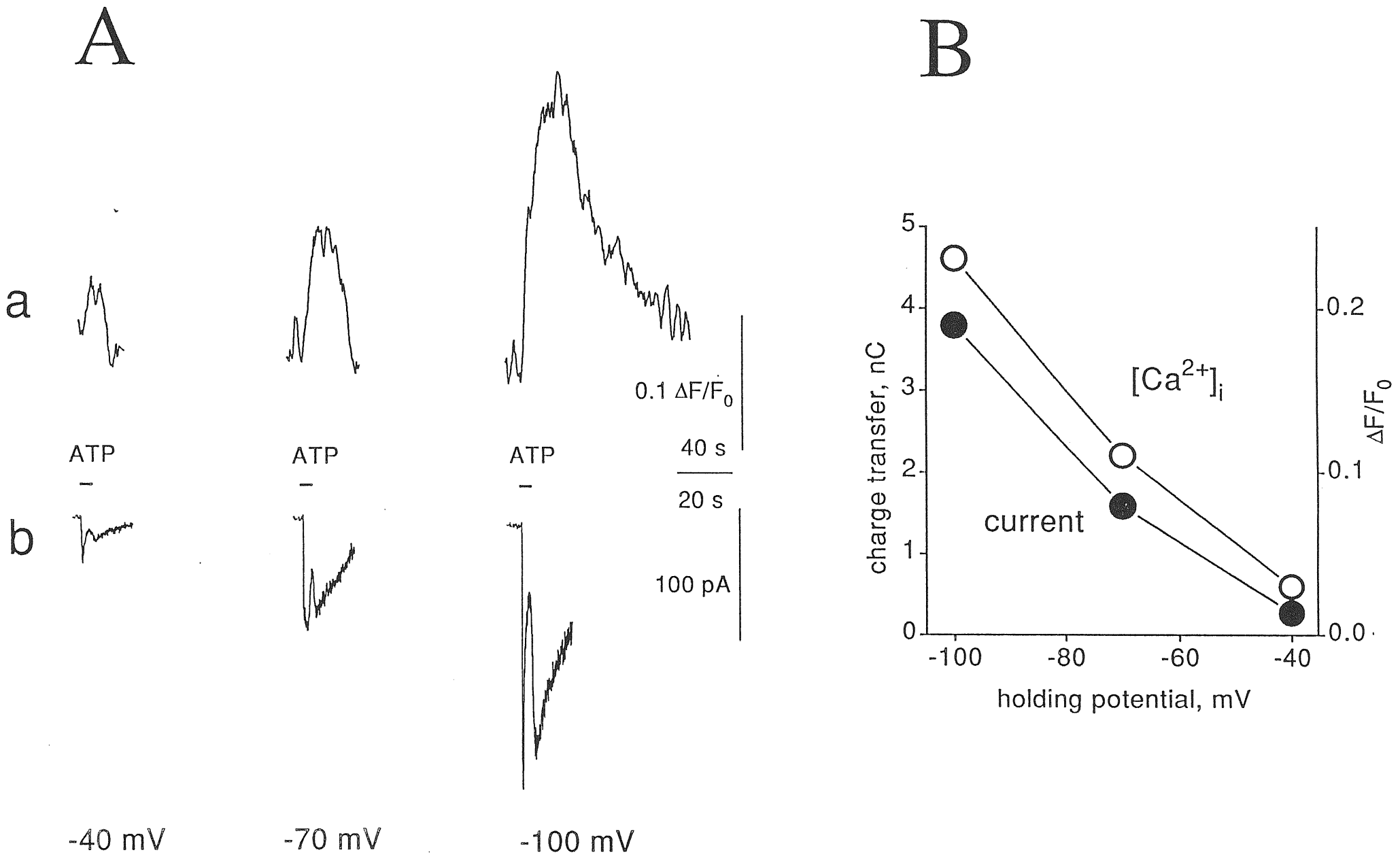
A
a
b
ATP
ATP
ATP
0.1 ΔF/F0
40 s
20 s
100 pA
-40 mV
-70 mV
-100 mV
B
charge transfer, nC
[Ca2+]i
current
ΔF/F0
holding potential, mV
-100
-80
-60
-40
0
1
2
3
4
5
0.0
0.1
0.2

Figure R-18. Effect of changes in holding potential on $[Ca^{2+}]_i$ transients and membrane currents induced by 2 s application of 5 mM ATP. A: simultaneous recording of $[Ca^{2+}]_i$ transients (a) and inward currents (b) at the holding potentials indicated at the bottom of the tracings. Note different timescale in a and b. B: plot of holding potential (abscissa) *versus* the charge transfer (left) of the ATP current or the peak increase in $[Ca^{2+}]_i$ (right). Note approximately linear relation of both sets of response to membrane potential.

experiment, a pair of neighbouring cells (at the same distance from the puffer pipette) were imaged, both loaded with the Ca^{2+}-sensitive dye though only one (shown in Fig. R-17 B and Fig. M-11 B) was patched. In the intact cell there was an initial, rapid rise (labelled as A_1 in Fig. M-11 B) in $[Ca^{2+}]_i$ followed by a decline and a much larger and slower increase (labelled as A_2 in Fig. M-11 B). On the other hand, the response of the adjacent, patched cell had monophasically slow onset and offset (Fig. M-11 A). The intact cell displayed a much larger peak rise in $[Ca^{2+}]_i$ (1.9 *versus* 0.76 $\Delta F/F_0$) although in either cell the time from the beginning of ATP pulse to the maximum increase in $[Ca^{2+}]_i$ was approximately the same (4.3 s *versus* 4.7 s). The inset C to Fig. R-17 shows that the initial peak (A_1) was consistently smaller that the second one (A_2) for a sample of 9 intact cells. It is worth noting that the amplitude of the maximal peak (A_2) evoked by 2 s ATP pulse was significantly ($P<0.05$) larger (by 73%) than the corresponding peak of patch clamped cells (see Fig. R-16 A), although the decay time constant of $[Ca^{2+}]_i$ transient was the same (27.1±9.1 *versus* 30.6±8.1; n=9). The difference between the amplitudes of $[Ca^{2+}]_i$ rises in intact *versus* patched cells suggested that the response measured from intact cells partly comprised a component due to voltage-dependent Ca^{2+} channels possibly activated by ATP-induced depolarization. On the other hand, the similar decay time course indicated that it was not determined by voltage activated channels, and that systems responsible for removal of $[Ca^{2+}]_i$ following a long pulse of ATP were not substantially disturbed in patch clamped cells.

XI-2a. [Ca2+]i rises induced by membrane depolarization

A more controlled way to assess the role of voltage-dependent Ca^{2+} channels in the persistent rise in $[Ca^{2+}]_i$ was to apply depolarizing voltage steps to patched cells. For this purpose 5 s long voltage commands from -70 mV holding potential to -20 mV test potential were used (which should be sufficient to activate high threshold Ca^{2+} currents; Di Virgilio *et al.*, 1987; Fasolato *et al.*, 1990). Under these conditions (n=3 cells) the $[Ca^{2+}]_i$ rise displayed monotonic, rapid (0.88±0.21 s) increase to a peak level ($\Delta F/F_0$ 0.46±0.13) from which it recovered with a decay time constant of 9.6±2.1 s. These responses from patched cells had onset/offset kinetics similar to those of the $[Ca^{2+}]_i$ rise observed in unclamped cells either with a brief ATP pulse or early during a 2 s ATP pulse (A_1 peak). These data imply that, while membrane depolarization by ATP could raise $[Ca^{2+}]_i$ via activation of voltage-dependent Ca^{2+} channels in intact cells, this phenomenon could not be detected when cells were clamped at -70 mV holding potential.

XI-2b. Dependence of $[Ca^{2+}]_i$ rise on holding potential and on $[Ca^{2+}]_o$

It seemed therefore feasible that the increase in $[Ca^{2+}]_i$ observed under patch clamp conditions following ATP application resulted from Ca^{2+} permeation through influx via activated P2-receptors, intracellular Ca^{2+} release, or a combination of the two. If the rise in $[Ca^{2+}]_i$ depended exclusively on Ca^{2+} release from the intracellular compartment, one might expect it to be relatively insensitive to changes in membrane potential (Sugasawa *et al.*, 1996) which, on the other hand, should influence transmembrane Ca^{2+} influx by changing its driving force (Reber *et al.*, 1992). Fig. R-18 shows an experiment in which a 2 s application of ATP was performed on a cell

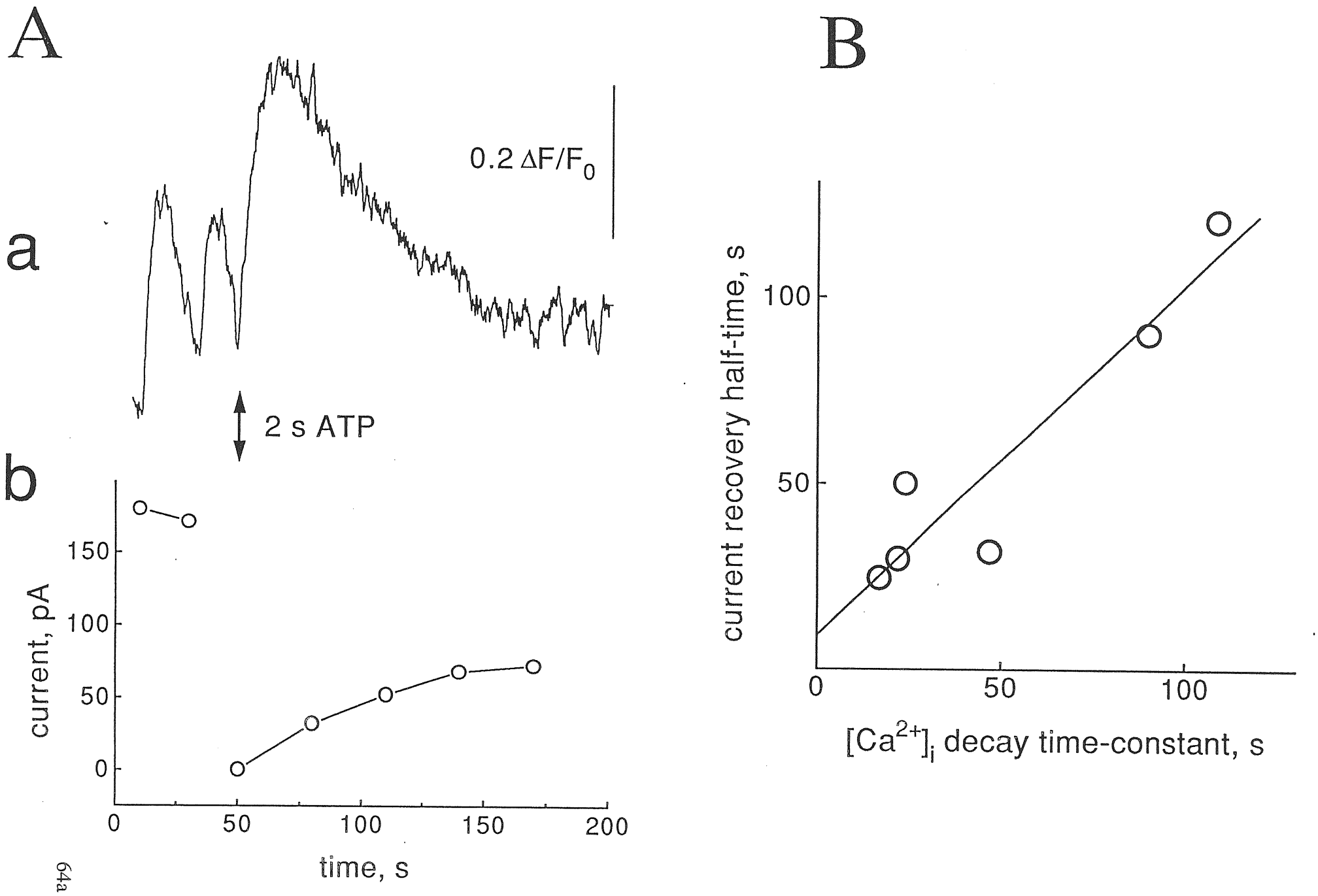
A
a
0.2 ΔF/F0
2 s ATP
b
current, pA
150
100
50
0
0
50
100
150
200
time, s
B
current recovery half-time, s
100
50
0
50
100
[Ca2+]i decay time-constant, s

Figure R-19. Changes in $[Ca^{2+}]_i$ level and inward currents produced by ATP (5 mM). A: a), $[Ca^{2+}]_i$ transients induced by 20 ms pulses of ATP before and after a 2 s ATP pulse (doubleheaded arrow); b), corresponding current amplitudes recorded from the same cell following the same protocol as above. Current amplitudes are expressed in absolute values disregarding their polarity. Timescale in b applies also to a. B: plot of time constant of $[Ca^{2+}]_i$ decay *versus* half-time of current recovery (obtained from graphs such as the one in Ab). Datapoints refer to different cells.

clamped at -40, -70 or -100 mV holding potential. As the holding potential was made more negative, there was a progressive increase in $[Ca^{2+}]_i$ (see Fig. R-18 Aa) and in the inward current (Fig. R-18 Ab). Plotting the integral of the membrane current (which is related to the changes in $[Ca^{2+}]_i$; *cf* Rathouz & Berg, 1994) or the peak amplitude of $[Ca^{2+}]_i$ against holding potential (Fig. R-18 B) yielded an approximately linear relation for both parameters, suggesting that the magnitude of the $[Ca^{2+}]_i$ transient was dependent on membrane voltage and thus perhaps related to Ca^{2+} influx. This notion was confirmed in another set of experiments measuring changes in $[Ca^{2+}]_i$ in control or Ca^{2+}-free external solution using either intact or patched cells. After 4 min removal of external Ca^{2+} (plus addition of 10 mM EGTA to the superfusion solution) the peak $[Ca^{2+}]_i$ rise induced by 2s pulse of ATP was reduced from 1.84 ± 0.49 to 0.083 ± 0.032 (n=9) $\Delta F/F_0$ in intact cells, and from 0.49±0.1 to 0.04±0.02 (n=3) $\Delta F/F_0$ in patch clamped cells. These results indicate that in intact or patched PC12 cells the increase in $[Ca^{2+}]_i$ was predominantly dependent on extracellular Ca^{2+}.

XI-3. Role of $[Ca^{2+}]_i$ in ATP receptor desensitization

It was previously observed that ATP receptors apparently possess two distinct types of desensitization (see Chapter X). In order to study how changes in $[Ca^{2+}]_i$ developed during desensitization, brief pulses of ATP were repetitively applied at time intervals (15-60 s) which allowed reproducibility of responses and were then followed by a 2 s long, desensitizing application of ATP after which the brief pulse sequence recommenced. With this protocol it was advantageous to study the characteristics of slow desensitization. Conversely, because the apparent $[Ca^{2+}]_i$ increase *during* the 2 s

application of ATP was too small in voltage-clamped cells (see Fig. R-15 Ba and Fig. M-11 B) to study role of $[Ca^{2+}]_i$ in fast desensitization, the latter process was investigated with an alternative approach (based on intracellular Ca^{2+} buffering) as described later.

XI-3a. Time correlation between $[Ca^{2+}]_i$ changes and receptor desensitization

In the example of Fig. R-19 Aa $[Ca^{2+}]_i$ transients followed the inward currents evoked by repetitive ATP pulses (see plot in Fig. R-19 Ab showing absolute amplitude values of membrane current on the same time scale) up to the application of a long pulse of ATP. The latter was associated with a large rise in $[Ca^{2+}]_i$ which in this cell declined with a 109 s time constant and was accompanied by a persistent depression in inward currents and $[Ca^{2+}]_i$ changes. Fig. R-19 B plots the relation between the time constant for the $[Ca^{2+}]_i$ increase *versus* the half-time for recovery of the inward currents due to repetitive brief applications of ATP after a long pulse of the same (n=6). Data could be fitted by a linear relation with r=0.963. These observations thus indicated that there was an association between recovery from slow desensitization of P2-receptors and $[Ca^{2+}]_i$.

XI-3b. Effects of $[Ca^{2+}]_i$ chelators on desensitization

In order to study the influence of $[Ca^{2+}]_i$ on fast desensitization, various Ca^{2+} chelators (applied intracellularly via the patch electrode) were used during measurements of membrane currents induced by ATP. As an index of fast desensitization the time constant of the fast fading of the membrane current to the 2 s pulse of 5 mM ATP was

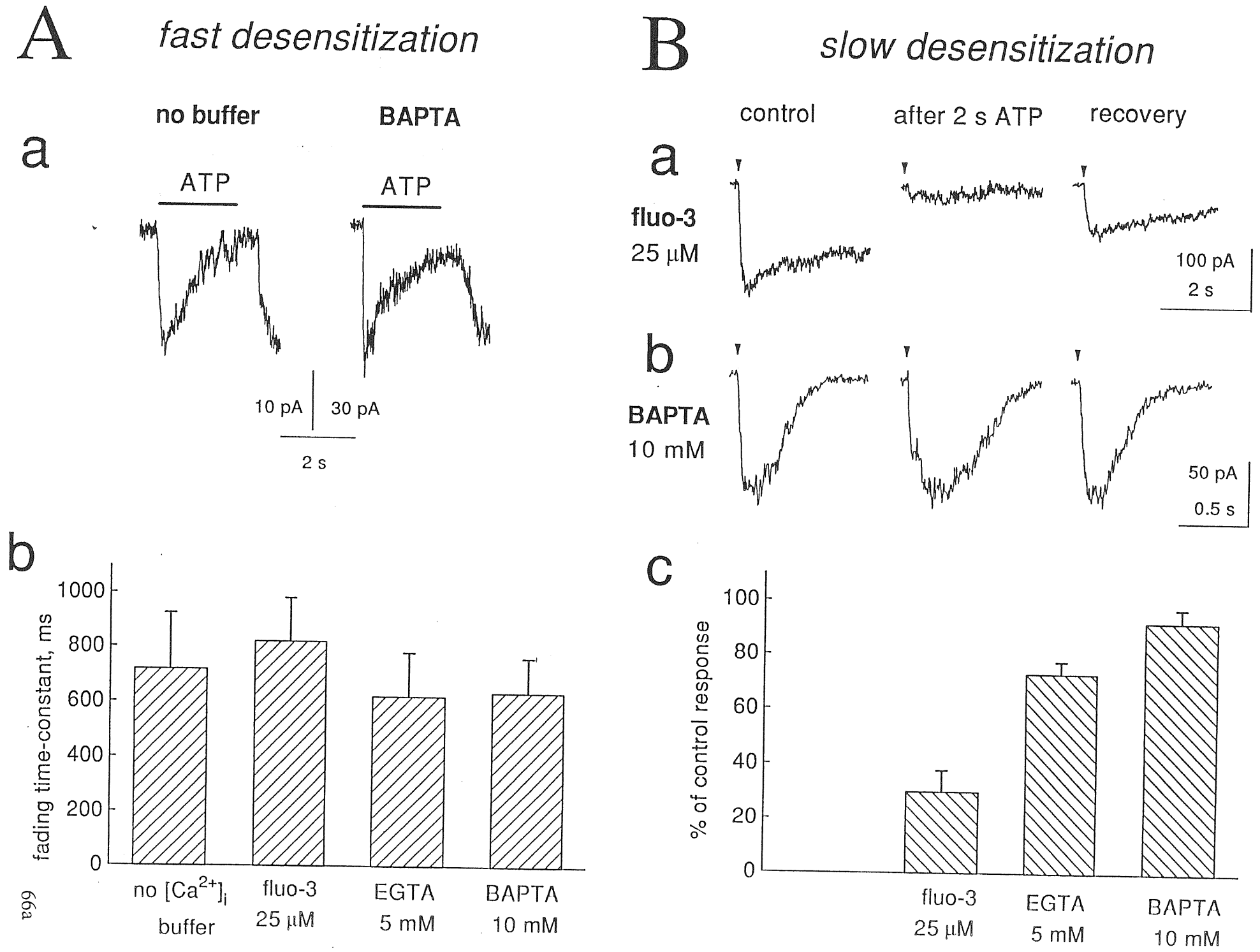
A
fast desensitization
no buffer
BAPTA
a
ATP
ATP
10 pA
30 pA
2 s
b
fading time-constant, ms
1000
800
600
400
200
0
no [Ca2+]i
buffer
fluo-3
25 μM
EGTA
5 mM
BAPTA
10 mM
B
slow desensitization
control
after 2 s ATP
recovery
a
fluo-3
25 μM
100 pA
2 s
b
BAPTA
10 mM
50 pA
0.5 s
c
% of control response
100
80
60
40
20
0
fluo-3
25 μM
EGTA
5 mM
BAPTA
10 mM

Figure R-20. Influence of $[Ca^{2+}]_i$ buffers on membrane currents induced by 5 mM ATP. A: a), comparison of current fading evoked by 2 s ATP pulse (horizontal bar) recorded in a cell without adding $[Ca^{2+}]_i$ buffers (left) *versus* a cell recorded with a BAPTA containing pipette (right). Note similar fading process during ATP application; b), histograms of time constant of peak current fading from cells recorded without addition of intracellular buffers (n=7), or with indicated buffers (fluo-3 n=13; EGTA n=16; BAPTA n=18). Note similar results despite different pipette solutions. B: a), responses to 20 ms ATP pulse before (control), 30 s after a 2 s ATP pulse (middle), and 2 min recovery (right) recorded from a cell patch clamped with a fluo-3 containing pipette; b), comparable data obtained from another cell patch clamped with a BAPTA containing pipette; c), histograms depicting degree of slow desensitization (expressed as % of response to 20 ms ATP 30 s after 2 s ATP pulse) of cells recorded with fluo-3 (n=7), EGTA (n=3) or BAPTA (n=7) containing pipettes. Note that slow desensitization is minimal in the presence of BAPTA and very large in the presence of fluo-3. The average value for fluo-3 was significantly different from the one for EGTA ($P<0.05$) and BAPTA ($P<0.05$), while the difference between BAPTA and EGTA data was not significant ($P>0.05$).

used. Sample tracings are shown in Fig. R-20 Aa in which responses observed in control solution (with no internal buffers added) were essentially similar to those observed after at least 8 min whole-cell patch recording with electrode containing 10 mM BAPTA. Histograms of Fig. R-20 Ab show that the fading time constant of the initial peak current was approximately the same either in the presence of 25 μM fluo-3, 5 mM EGTA or 10 mM BAPTA, or when no internal chelators were applied.

We also investigated the process of slow desensitization when minimal (with 25 μM fluo-3) or strong (with 5 mM EGTA or 10 mM BAPTA) Ca^{2+} buffering was used. Slow desensitization was taken as % depression of the test inward current (elicited by 20 ms ATP pulse) at 30 s from the start of 2 s desensitizing pulse when the rebound current had fully dissipated. Fig. R-20 Ba, b shows an example of tracings of current responses induced by a 20 ms pulse before (left), 30 s (middle), or 2 min (right) after a 2 s pulse of ATP. When the pipette contained fluo-3 the test current was almost suppressed (on average it was reduced to 30.0±7.6 % of the first pulse current; n=7; see histogram in Fig. R-20 Bc), while with BAPTA-containing pipettes the test current was not reduced (on average 92.2± 5.1 %; n=5; Fig. R-20 Bc). With an EGTA-containing pipette the test current was slightly reduced to 73±4.6 % of the first response (Fig. R-20 Bc; n=3). Since recording stability with pipettes containing no Ca^{2+} buffers was often brief, it was difficult to obtain comparable observations when $[Ca^{2+}]_i$ was allowed to rise without introducing intracellular chelators.

XII. Role of substance P in P_{2X} receptor desensitization

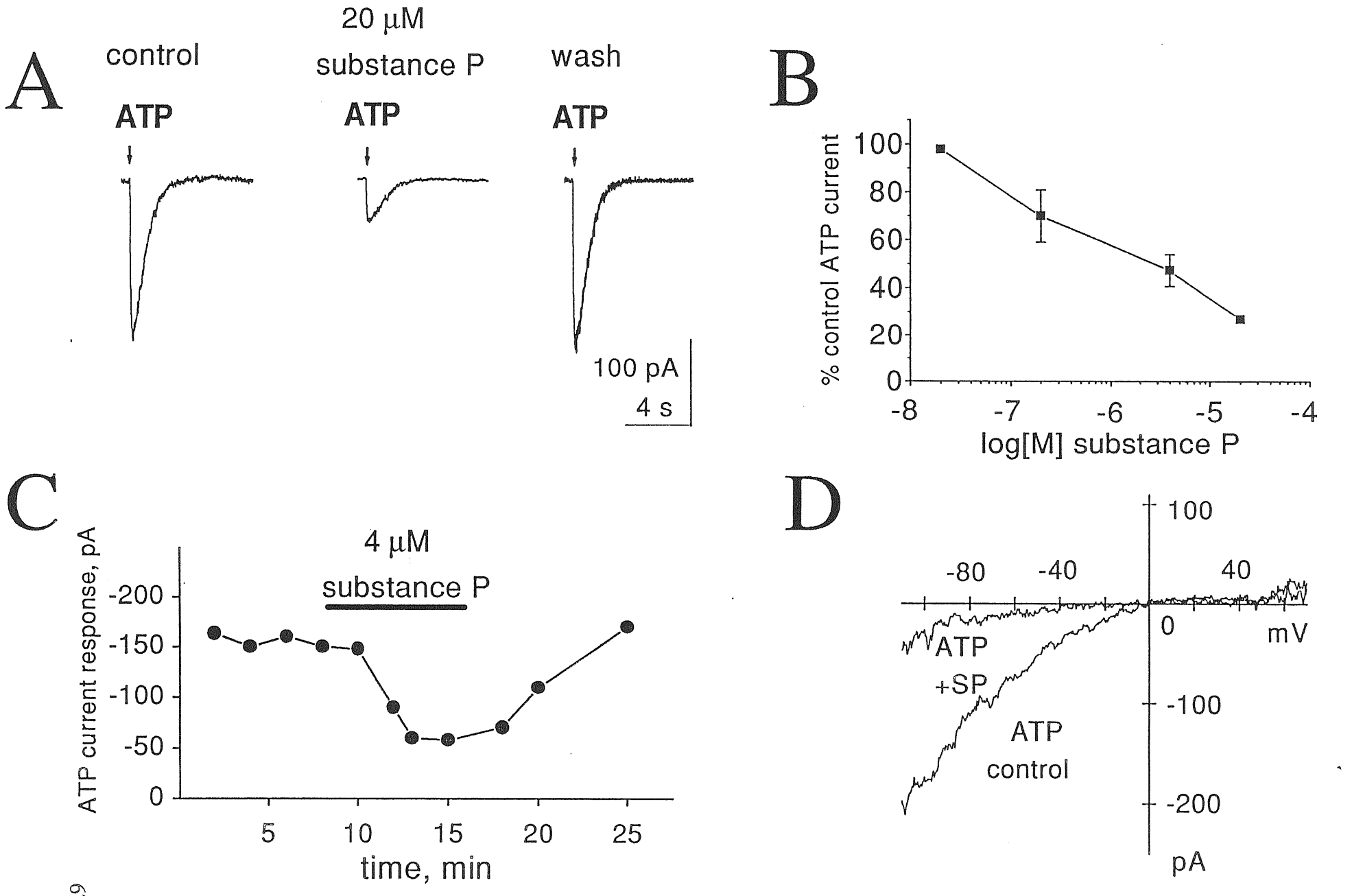
A
control
20 μM
substance P
wash
ATP
ATP
ATP
100 pA
4 s
B
% control ATP current
100
80
60
40
20
0
-8
-7
-6
-5
-4
log[M] substance P
C
4 μM
substance P
ATP current response, pA
-200
-150
-100
-50
0
5
10
15
20
25
time, min
D
100
-80
-40
40
0
mV
ATP
+SP
ATP
control
-100
-200
pA

Figure R-21. Depression of ATP-induced currents by bath-applied substance P. A, effect of substance P (20 μM) on currents evoked by a 20 ms pressure pulse of 5 mM ATP (indicated by arrowheads); B, plot of substance P depressant effect (measured as percent of control ATP current, ordinate) *versus* log substance P concentration (abscissa). Error bars indicate s.e.m. for 4 cells; C, plot showing the timecourse of ATP-current depression induced by bath application of 4 μM substance P and subsequent recovery after washout; D, current-voltage relation for ATP currents in control conditions or in the presence of 4 μM substance P. Membrane potential was changed with a continuous voltage ramp (400 mV/s) from -130 to +40 mV at the peak of ATP-induced currents.

While allosteric effects of substance P on nAChRs are well known (Livett *et al.*, 1979; Akasu *et al.*, 1983) and have been shown to consist in promoting receptor desensitization (Clapham and Neher, 1984), the action of this peptide on ATP receptors remains to be studied. This issue was addressed by combining electrophysiological recording of ATP-induced membrane currents and confocal microscopy imaging of $[Ca^{2+}]_i$.

XII-1. Depressant effect of bath-applied substance P

The database of this study comprises 30 PC12 cells clamped at -70 mV holding potential. When patch clamp alone was used, 5 mM EGTA was added to the pipette solution. In some experiments, when patch clamping was combined with confocal Ca^{2+} imaging, EGTA was omitted while 25 μM fluo-3 was added. Figure R-22 A shows an example of the inward current induced by a brief (20 ms) pulse of ATP (5 mM; arrowheads point to pressure application) which, under these conditions, is known to elicit halfmaximal responses (Chapter X). Bath-applied substance P (20 μM; 5 min) was ineffective on baseline current but it strongly depressed the ATP peak current (by 73 %), an effect which was reversible after 7 min washout. The depressant action of substance P was dose-dependent as indicated by the graph of Fig. R-21 B although even at 20 μM concentration a residual response to ATP persisted. The dose-effect curve was found to be linear (on semi-logarithmic scale) in the concentration range studied. On average substance P (4 μM) reversibly decreased the current amplitude induced by 20 ms pulses of ATP from 185±44 to 90±25 pA (51 % reduction; n=6). Fig. R-21 C shows a typical example of the time profile of the

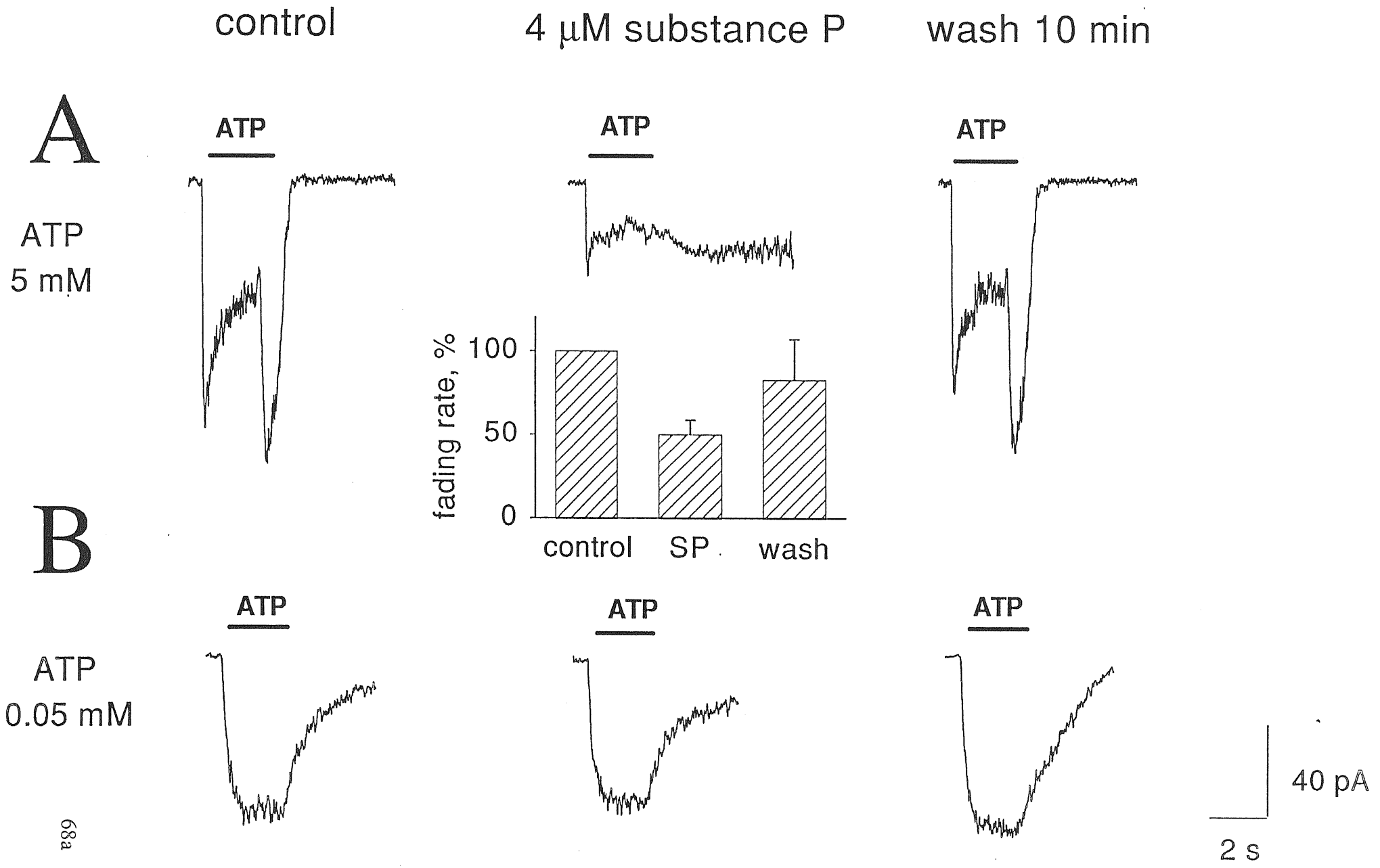
control
4 μM substance P
wash 10 min
A
ATP
5 mM
ATP
ATP
ATP
fading rate, %
100
50
0
control
SP
wash
B
ATP
0.05 mM
ATP
ATP
ATP
40 pA
2 s

Figure R-22. Effects of bath-applied substance P on membrane currents induced by long (2 s) pulses of ATP. A, in control solution (left) a 2 s pulse of 5 mM ATP evokes biphasic response with initial peak followed by fade and rebound currents (period of pressure application is indicated by the horizontal bars). All components of the response are reversibly depressed by substance P (see centre and right panels); inset shows histograms for the changes in the time-constant of peak inward current decay (fading rate expressed as % of control one) in the presence of substance P (n=6); B, 2 s pulses of 0.05 mM ATP (horizontal bars) evoke non-desensitizing inward currents which are virtually insensitive to substance P.

depressant action of substance P which developed after 3 min superfusion, reached a maximum at 7 min and gradually recovered upon washout over the next 10 min. Subsequent applications of substance P usually led to tachyphylaxis of its depressant action: for this reason bath-applied substance P was routinely administered only once to each culture dish. The action of substance P was not due to a change in the reversal potential of the ATP-induced current as shown by the superimposed current/voltage tracings of Fig. R-21 D obtained by applying voltage ramps (400 mV/s) from -110 to +70 mV before and during application of substance P (4 μM). Since the two traces are leak-subtracted, it is possible to observe that there was an equivalent degree of reduction in ATP-induced responses throughout the test potential range. This finding was confirmed in 6 experiments by normalisation and scaling of the two current/voltage curves which became virtually identical, indicating that the depressant action of substance P was voltage-independent.

XII-2. Effects of bath-applied SP on responses to long pulses of ATP

Long pulses (2 s) of ATP (5 mM) evoked inward currents which first peaked to a value smaller than the maximum, rapidly faded and were followed by a large current rebound immediately after the end of ATP delivery (see example in left-hand side panel of Fig. R-22 A; *cf.* Chapter X). The initial peak amplitude was reduced by 4 μM substance P from 151±30 to 65±13 pA (n=6), corresponding to a 56 % reduction comparable to the one found when 20 ms applications were used. This effect is exemplified in Fig. R-22 A which also shows that the rebound current was similarly depressed in a reversible manner. The rapid fade of the inward current during long

pulses of ATP has been interpreted as due to fast receptor desensitization (Chapter X) and may be quantified by measuring its decay time constant which was nearly halved by substance P (see inset to Fig. R-22 A). When inward currents were evoked using 2 s long pulses of rather diluted ATP concentrations (50 μM) as depicted in Fig. R-22 B, the depressant action of 4 μM substance P was very small (16 %) even if the peak amplitude of the ATP current was comparable (134±46 pA; n=3) to the one induced by 5 mM ATP.

XII-3. Action of SP on recovery from slow desensitization of P_{2X} receptors

Previous experiments have suggested that a slowly developing form of P_{2X}-receptor desensitization is manifested as transient reduction in currents elicited by 20 ms ATP (5 mM) after a conditioning 2 s pulse of the same agonist (Chapter X): since currents are usually restored after 30 s if the patch pipette contains strong Ca^{2+} buffers (Chapter XI), this time can be taken as an end-point for recovery from desensitization. Fig. R-23 Aa shows that the inward current produced by 20 ms ATP was recovered to 83 % of its initial value 30 s after a conditioning pulse of 2 s ATP with complete recovery 2 min later. On a sample of 3 cells full recovery to test pulses of ATP in control solution took 47±22 s. When the same protocol was repeated on the same cell in the presence of 4 μM substance P (Fig. R-23 Ab) the initial test response to ATP was inhibited by 29 %. Thirty s after the conditioning pulse of ATP the responses was more severely depressed (by 92 %) with partial recovery 2 min later. In fact, full recovery to test pulses was only observed 150±13 s later. The

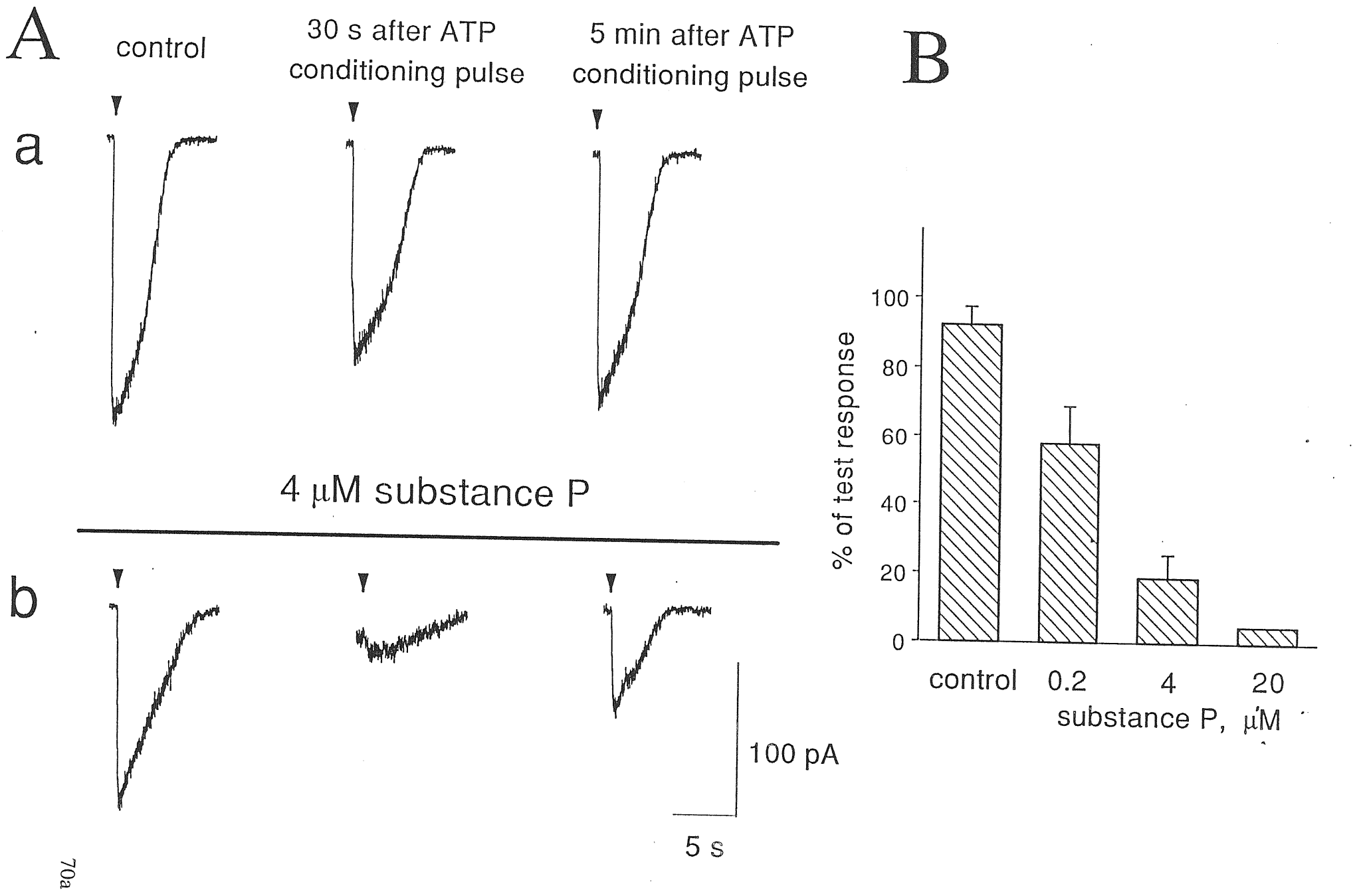
A
control
30 s after ATP conditioning pulse
5 min after ATP conditioning pulse
a
4 μM substance P
b
100 pA
5 s
B
% of test response
100
80
60
40
20
0
control
0.2
4
20
substance P, μM

Figure R-23. Effect of bath-applied substance P on recovery from desensitization induced by 2 s conditioning pulse of 5 mM ATP. A, brief (20 ms) pressure application of 5 mM ATP (arrowheads) evokes an inward current in control solution (a; left). After a 2 s conditioning pulse of the same pipette concentration of ATP which produces P2X-receptor desensitization, the response to the test application of ATP recovers to 83 % of control amplitude (center; 30 s later) with complete recovery after 5 min (right); b, addition of 4 μM substance P to the superfusion solution leads to a 30 % decrease in the test response amplitude (left; compared with control trace in Aa) and slows down recovery of ATP current from the desensitization induced by the ATP conditioning pulse so that after 30 s the response is only 8 % of control and even 5 min later it is 55 %; B, histograms showing dose dependence of the substance P effect on recovery of ATP current from desensitization (measured as % of test response) 30 s after the conditioning pulse in control solution or in the presence of increasing concentrations of substance P (error bars represent s.e.m. for 3-4 cells).

histograms in Fig. R-23 B show the dose-dependent intensification by substance P of the depression of test ATP responses by conditioning pulses of ATP.

XII-4. Depression by SP of membrane currents and $[Ca^{2+}]_i$ rises

My previous experiments have shown that ATP induces a transient rise in $[Ca^{2+}]_i$ proportional to the charge transfer operated by P_{2X}-receptor activation and capable of promoting slow receptor desensitization (Chapter XI). In the present experiments combined patch clamp recording and $[Ca^{2+}]_i$ imaging were thus performed in order to ascertain if substance P itself was changing baseline $[Ca^{2+}]_i$ and if it interfered with $[Ca^{2+}]_i$ rises produced by ATP. 25 μM fluo-3 was added to the pipette solution, while EGTA was omitted (see Methods). Fig. R-24 shows simultaneous increases in $[Ca^{2+}]_i$ (A) and membrane inward current (B; note faster timebase) during 20 ms applications of ATP (5 mM). Substance P (20 μM; pressure-applied via a separate pipette for 1 min) did not change $[Ca^{2+}]_i$ or current baseline but strongly depressed the rise in $[Ca^{2+}]_i$ and inward current elicited by ATP (81 % and 69 % depression, respectively). After 5 min wash recovery of the ATP current was complete while the one for the $[Ca^{2+}]_i$ transient was 54 %. The inset to Fig. R-24 shows the histograms for the reduced size of the $[Ca^{2+}]_i$ and current amplitude following pressure application of substance P to six cells. No direct action of substance P on $[Ca^{2+}]_i$ or current baseline was observed on the same group of cells.

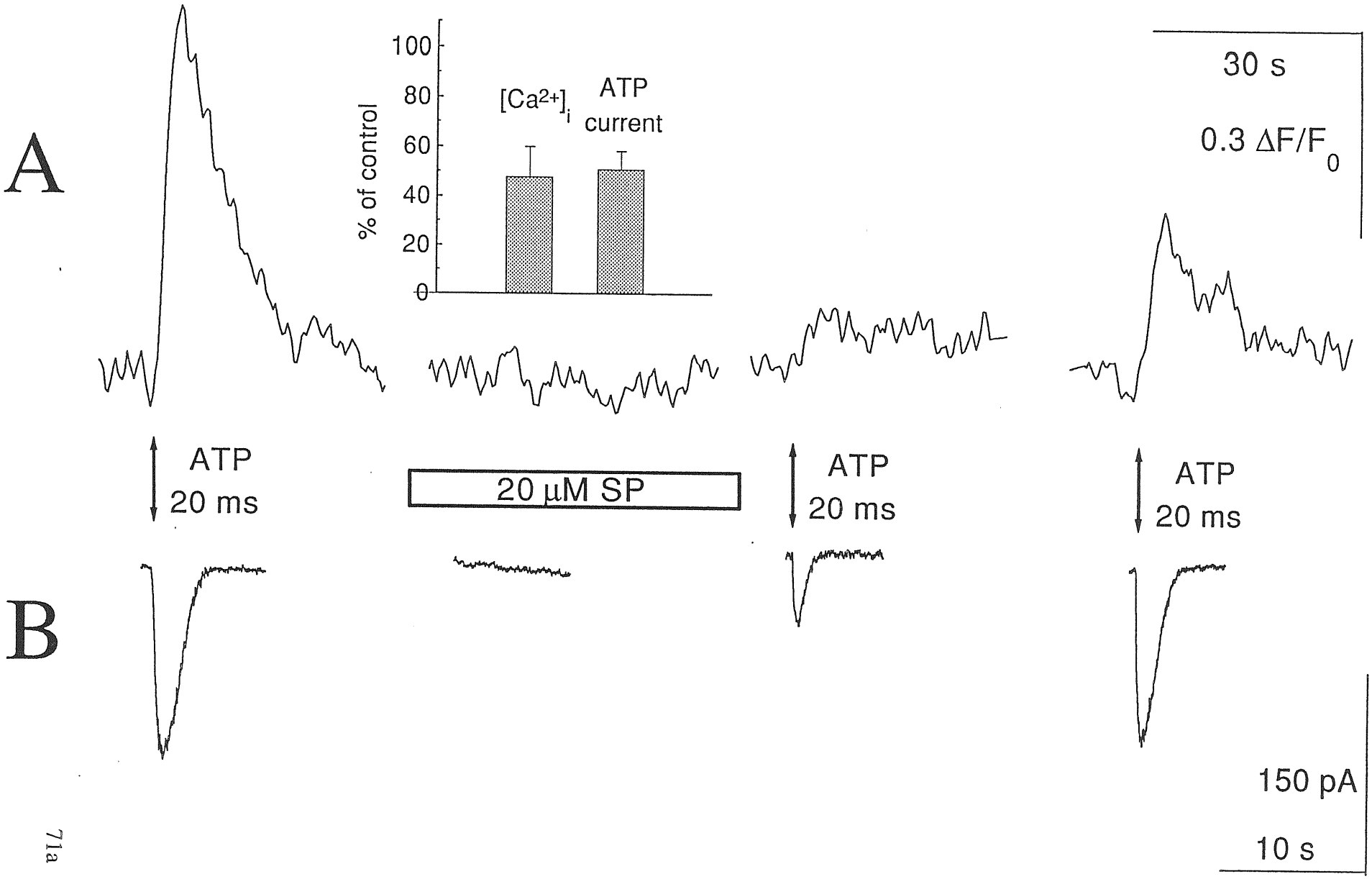
A
B
100
80
60
40
20
0
% of control
[Ca2+]i
ATP
current
30 s
0.3 ΔF/F0
ATP
20 ms
20 μM SP
ATP
20 ms
ATP
20 ms
150 pA
10 s

Figure R-24. Pressure application of substance P produces depression of simultaneously recorded ATP-evoked membrane currents and $[Ca^{2+}]_i$ transients. A and B show responses to brief (20 ms; doubleheaded arrows) pulses of 5 mM ATP recorded as $[Ca^{2+}]_i$ increases (A) and membrane currents (B). Note different time calibration for A and B. Pressure application of 20 μM substance P for 1 min (open bar) does not change either $[Ca^{2+}]_i$ level or baseline current. Test pulse of the same concentration of ATP applied immediately after the substance P treatment elicit largely depressed responses both in terms of $[Ca^{2+}]_i$ transient amplitude and membrane current. Upon 5 min washout recovery of current amplitude is full while the one of the $[Ca^{2+}]_i$ response is incomplete. Inset shows the histograms for depression (measured as % of control) of $[Ca^{2+}]_i$ transient and current amplitude induced by pressure application of substance P (n=6).

Discussion

The principal findings of this project are the following:

- first, the desensitization of nAChRs of rat chromaffin cells and that of P_{2X} receptors of PC12 cells was described and compared. The complex time-course of currents evoked by long applications of the agonists comprising rapid fading and subsequent rebound (which was more pronounced with ATP applications) was studied. Fading and rebound of P_{2X} receptor currents were attributed to their newly described fast desensitization (and to recovery from it). Fading of nAChRs currents was in part due to receptor desensitization with an additional contribution of open channel block by nicotine (with unblocking-produced rebound);
- second, combined patch-clamp and confocal microscopy experiments on neuronal nAChRs of rat chromaffin cells revealed correlation between the speed of recovery of neuronal AChRs from desensitization with the time-course of $[Ca^{2+}]_i$, while the development of desensitization was apparently independent of $[Ca^{2+}]_i$;
- third, the combined experiments on PC12 cells demonstrated the dissimilar role of $[Ca^{2+}]_i$ in fast and slow desensitization of P_{2X} receptors: a close association between $[Ca^{2+}]_i$ and slow desensitization was observed while no correlation for fast desensitization with $[Ca^{2+}]_i$ could be found;
- fourth, the novel demonstration of strong depressant action of the neuropeptide substance P on ATP-evoked responses: this phenomenon seemed to be due to enhancement of both fast and slow desensitization of P_{2X} receptors without exerting any measurable action on $[Ca^{2+}]_i$.

These results suggest not only that $[Ca^{2+}]_i$ plays an important role in desensitization of both neuronal nAChRs and P_{2X} receptors, but that this role can vary at different stages of desensitization and recovery from it. On the other hand, the present results also imply the existence of $[Ca^{2+}]_i$-independent mechanisms of modulation of receptor desensitization, such as the one mediated by substance P on P_{2X} receptors.

XIII. Choice of cell model for studying nAChRs and P_{2X} receptors desensitization

P_{2X} receptors and nAChRs are often co-expressed on the membrane of same peripheral and central neurons, while ACh and ATP are stored together in some presynaptic vesicles (Rogers *et al.,* 1997). In their recent study, Rogers *et al.* (1997) have used cultured sympathetic neurons to address the issue of interactions caused by the two agonist types and their possible cross-desensitization. They have found that only half of rat sympathetic neurons responded to both ATP and nicotine, indicating differences in expression of the two receptor types. Unlike heterogenous cultures of sympathetic neurons, rat chromaffin cells are a useful model to study electrically excitable cells (Fenwick *et al.,* 1982). Embriologically originating from the neural crest, these cells share many properties of autonomic neurons such as voltage-activated Na^+ and K^+ permeabilities and responsiveness to specific stimuli (Biales *et al.,* 1976). In particular, they can be excited by ACh released from the splanchnic nerve fibers (Feldberg *et al.,* 1934). A direct cancer derivation of rat chromaffin cells, the pheochromocytoma (PC12) cell line, also possesses both ATP- and nicotine-activated receptors (Simasko *et al.*, 1987; Nakazawa *et al.*, 1990).

Initially, PC12 cells (which were routinely available in the lab) were used for the present studies of both nicotinic and ATP-receptors. Since ATP-induced currents were reproducible and stable, these cells continued to be used throughout this project to study P_{2X} receptors they express. Conversely, nicotine-induced responses were more variable and eventually so unreliable to suggest insufficient number of nAChRs after a certain time in culture. Therefore, rat chromaffin medullary cells in culture were set up in the lab (Brandt *et al.,* 1976) to obtained a more stable model histologically very similar to PC12 cells. In fact, being a cloned rat cell line, PC12 cells retain a number of chromaffin cell characteristics, such as synthesis and secretion of catecholamines (Margioris *et al.*, 1992). Moreover, PC12 cells can be induced to differentiate to sympathetic neurones, after exposure to nerve growth factor, or to mature chromaffin cells (Mizrachi *et al.,* 1990). Data on nAChRs were therefore based on chromaffin cell experiments while data on ATP receptors originated from PC12 cells.

XIV. Desensitization and recovery of nAChRs: role of $[Ca^{2+}]_i$

XIV-1. Time-course of desensitization and recovery

To study desensitization of nAChRs on rat chromaffin cells nicotine, the selective agonist of nicotinic nAChRs, was used in order to avoid activation of muscarinic ACh receptors. Since the actions of nicotine were blocked by *d*-tubocurarine and insensitive to α-bungarotoxin (see also Fenwick *et al.,* 1982; Vernino *et al.,* 1994; Nooney & Feltz, 1995), it appears that they were mediated by conventional nAChRs

present on chromaffin cells. Currents evoked by 20 ms applications of nicotine were clearly submaximal in amplitude and were not depressed when paired pulse intervals were 5 s, suggesting that if with the paired pulse protocol there was any desensitization of nAChRs it recovered in less than such a time.

Sustained applications (2 s) of nicotine induced inward currents which rapidly faded with a biexponential time course. Two mechanisms may be responsible for this current fading: block of the open channel of the nAChR by ACh itself (Ogden & Colquhoun, 1985; MacOnochie & Knight, 1992; see also Vlachova *et al.*, 1987 for excitatory amino acids, and Bertrand *et al.*, 1992 for the agonist action of *d*-tubocurarine on mutant ACh receptors) or nAChR desensitization (Katz & Thesleff, 1957). Several pieces of evidence suggest that this current fading was mainly due to desensitization. First, no shifts in reversal potential were detected, indicating that the current fading was not due to changes in channel permeability and/or its ion selectivity. Second, no unusual voltage-dependence of the response was observed during voltage ramp tests (slope conductance did not change), making more likely the desensitization hypothesis rather than that of open channel block which has been shown to be highly dependent on membrane potential (Adams, 1976; Sine & Steinbach, 1984; Ogden & Colquhoun, 1985). In fact, Dudel *et al.*(1992) have found significant open channel block by ACh of nicotinic receptors only at potentials more hyperpolarized than -80 mV. Channel-blocking action of nicotine could not, however, be completely excluded since a small rebound current was sometimes observed upon cessation of the agonist pulse, similar to that reported by MacOnochie and Knight (1992) for channels expressed by bovine chromaffin cells and attributed as due to open channel blocking-unblocking mechanism. The latter could contribute to current

fading, although presumably not a major component since in the present experiments membrane potential was clamped at -70 mV. The mechanism of nicotine current fading was not specifically addressed in this project but it was assumed that it was at least partly due to desensitization.

A 2 s conditioning application of nicotine was selected as a suitable one for further studies of nAChR desensitization. The ratio (R_{2s}) between residual current at 2 s and peak current provided a simple index of the extent of such a desensitization. Since return of membrane current to baseline levels after a conditioning dose of nicotine was a slow process developing over >10 s, an interval of 30 s was used for test pulses of nicotine. This approach did not allow to estimate the time profile for any desensitization of test currents, which in any case would have been compounded by the rebound response, but it did provide a standard time-point to assess how the return to control amplitude proceeded. Thirty s after a conditioning dose test currents were largely reduced to about half of control, and then gradually recovered at 60 s or 90 s after the conditioning pulse. Thus, the present protocol allowed to adequately follow the rather slow recovery process.

The nAChRs desensitization reported in the present study was similar to that previously observed on the same receptors expressed by bovine chromaffin cells (Fenwick *et al.,* 1982) or by the PC12 cell line (Boyd, 1987) as far as concentration- and time-dependence, fast biexponential onset and relatively slow recovery time-course are concerned. The test pulse protocol with 30 s interval chosen to follow receptor recovery from desensitization did not provide enough time resolution to study polyexponentiality of the recovery process. However, results seem to be consistent

with the general cyclic kinetic scheme proposed by Katz and Thesleff (1957; see equation 1 in Chapter XI) and extended by Boyd (1987). Besides, two distinct desensitization states have been also proposed for muscle type nAChRs (reviewed by Changeux and Revah, 1987). Each state is part of a complex cycle of closed-open-desensitized-closed steps with different affinity to the agonist. In particular, following application of high concentration of the agonist, the low-affinity desensitized state would be the first one to appear, and then the high-affinity one would develop more slowly.

The observed nAChRs desensitization can also be compared to that of NMDA receptors of hippocampal neurones which have recently been studied using a similar experimental approach, namely combination of patch-clamping with fluo-3 based confocal $[Ca^{2+}]_i$ imaging (Medina *et al.,* 1996). These authors have applied test pulses prior and after the long conditioning pulse of NMDA and found a transient decrease in receptor sensitivity with a recovery that comprised two phases, with the slow one closely correlated with the time-constant of $[Ca^{2+}]_i$ decay. The present experiments on nAChRs revealed a very similar relation between $[Ca^{2+}]_i$ levels and receptor recovery from desensitization, as discussed in the following section.

XIV-2. Dissimilar role of Ca^{2+} at different desensitization stages

The $[Ca^{2+}]_i$ transients evoked by 20 ms nicotine applications developed together with membrane currents but grew with a slower time-course which was related to the amount of charge passing through open nAChRs (Vernino *et al.*, 1994). The $[Ca^{2+}]_i$ signals were mainly due to influx of Ca^{2+} through nAChRs since they were blocked by

d-tubocurarine, were prevented in calcium free media and shared the same sensitivity to membrane potential and pressure application of nicotine as the inward currents. Previous studies of rat chromaffin cells have shown that about 5 % of the nAChR current is carried by Ca^{2+} (Vernino *et al.*, 1994): this observation would explain why in Ca^{2+} free solution there was insignificant depression of membrane currents.

In order to study the effects of $[Ca^{2+}]_i$ on desensitization, imaging changes in $[Ca^{2+}]_i$ as well as manipulating the extracellular concentration of this ion and varying the degree of $[Ca^{2+}]_i$ buffering were used. The latter approach is of course indirect but it helps to address this question over rather fast observation times which are below the limits of $[Ca^{2+}]_i$ imaging of the present study (320 ms for whole cell sampling). There are other limitations to $[Ca^{2+}]_i$ imaging with the method used in the present study. For example, the fluorescent dye fluo-3 (which is active in the visible light range) does not permit ratiometric measurements of $[Ca^{2+}]_i$ concentrations analogous for instance to those based on fura-2 fluorescence: hence, variations in $[Ca^{2+}]_i$ can only be expressed as fractional changes from a reference fluorescence value (baseline or peak). Using fluo-3 did however allow applying low concentrations of the dye which did not apparently interfere with $[Ca^{2+}]_i$ dynamics (see Helmchen, *et al.*, 1996) since results were quantitatively similar to those obtained electrophysiologically from unbuffered cells. Conversely, the use of fura-2 loading of chromaffin cells requires not only that resting $[Ca^{2+}]_i$ is very low but also that during nAChR activation it does not rise above 400 nM (Vernino *et al.*, 1994): these experimental constraints may limit the ability of studying changes in $[Ca^{2+}]_i$ during the intense receptor stimulation required to produce sustained desensitization.

During a 2 s conditioning application of nicotine, the timecourse of current fading as well as desensitization ratio R_{2s} bore no relation to $[Ca^{2+}]_i$ changes or removal of $[Ca^{2+}]_o$, which suggests that this cation was not the prime factor responsible for desensitization under the present experimental conditions. This view was supported by experiments in which similar R_{2s} values were found when recording with pipettes containing BAPTA or no buffers. When the current faded (and rebounded; *cf* MacOnochie & Knight, 1992) the $[Ca^{2+}]_i$ increase leveled off as the charge transfer through nAChRs was complete: this finding accords with the linear relation between $[Ca^{2+}]_i$ rise and charge transfer previously observed on chromaffin cells (Vernino *et al.*, 1994). Thirty s after a conditioning dose test current reduction was not correlated with the fractional increase in $[Ca^{2+}]_i$ over baseline at that time-point but it was strongly correlated with the % fall in $[Ca^{2+}]_i$ from its peak: in practice, as long as $[Ca^{2+}]_i$ remained elevated the test current (evoked by a 20 ms pulse which only slightly raised $[Ca^{2+}]_i$) was attenuated. This correlation extended for 60 s after the conditioning dose and was then lost. In parallel electrophysiological experiments using BAPTA in the pipette the test current had almost completely recovered at 30 s while it remained depressed if no buffer was added to the pipette solution. These findings collectively indicate that a persistent rise in $[Ca^{2+}]_i$ was an important factor in controlling the recovery of nAChRs from desensitization.

Why did $[Ca^{2+}]_i$ not appear to influence the development of desensitization over 2 s continuous application of nicotine? We can only speculate that Ca^{2+} probably triggered a metabolic process which required a certain degree of $[Ca^{2+}]_i$ rise which in the case of 2 s application peaked after the current recovery. One potential candidate

for this slow metabolic process is receptor phosphorylation by Ca^{2+} dependent protein kinases (Levitan, 1994): in fact, protein kinase C activators only potentiate nAChR desensitization when applied for at least 1 min before ACh while ineffective when co-applied with the agonist (Downing & Role, 1987). Nevertheless, the identification of the metabolic process triggered by elevated $[Ca^{2+}]_i$ and responsible for receptor desensitization requires further studies.

Why did paired test pulses (spaced at 5 s) not produce detectable desensitization despite an increase in $[Ca^{2+}]_i$ after the first pulse which decayed with a time constant of approximately 9 s? Presumably the process of desensitization develops fully when there is prolonged exposure of receptor to the agonist, a condition not met in paired pulse experiments. Furthermore, in order to influence desensitization the rise in $[Ca^{2+}]_i$ should perhaps be longer than 10 s as discussed above.

XIV-3. Functional role of nAChRs desensitization and its modulation by $[Ca^{2+}]_i$

In isolated adrenals stimulated via splanchnic nerve fibers, desensitization of nAChR of chromaffin cells is minimal even when synaptic potentials are sufficiently large to generate spikes (Holman *et al.*,1994). This observation may imply that, during neurosecretion simply elicited by presynaptic nerve activity, even voltage-activated influx of Ca^{2+} is insufficient to trigger nAChR desensitization. Nonetheless, it has recently become apparent that, in addition to nerve stimulation, $[Ca^{2+}]_i$ of chromaffin cells can be strongly increased by a variety of endogenous substances such as bradykinin (D'Andrea *et al.*, 1993), a neutrophil derived-factor (Shibata *et al.*, 1996) or pituitary adenylate cyclase-activating polypeptide (PACAP; Przywara *et al.*, 1996),

all of which can release catecholamines. As suggested by Przywara *et al.* (1966) such large and sustained rises in $[Ca^{2+}]_i$ might facilitate nAChR desensitization and transform catecholamine release from a pulsatile event linked to splanchnic nerve impulses to a longer lasting phenomenon less dependent on AChR activity.

On the other hand, other mechanisms have been shown to modulate cell responsiveness to nicotinic agonists by affecting nAChRs desensitization. One of such substances is the neuropeptide substance P which was shown to modulate nAChRs via an allosteric site (Stafford *et al.,* 1994) without interfering with ion permeation or channel activation (Clapham & Neher, 1984). Being well established for nicotinic receptors, the modulatory role of substance P is much less studied for other receptor types and was therefore addressed in the present study in the case of P_{2X} receptors (see below).

XV. Desensitization of P_{2X} receptors: modulation by $[Ca^{2+}]_i$ and substance P

Whereas fast and slow components of desensitization of neuronal nAChRs on rat chromaffin cells have been previously reported (Feltz & & Trautmann, 1982; Boyd, 1987), P_{2X2} receptors on PC12 cells have been described as displaying little or no fast desensitization (Humphrey *et al.,* 1995). New evidence in favour of fast and slow desensitization of P_{2X2} receptors is provided below.

XV-1. Current fade and rebound due to fast desensitization of P_{2X} receptors

XV-1a. Membrane currents evoked by long applications of ATP on PC12 cells

The complex ATP-induced currents evoked by long applications of ATP might have been due to either heterogeneity of purinoceptors or distinct kinetic states of a single receptor type. On single smooth muscle cells ATP activates complex macroscopic current responses via ligand-gated (P_{2X} subtype) and G-protein coupled (P_{2Y} subtype) receptors (Xiong *et al.*, 1991). Previous studies of PC12 cells have reported that these cells, although endowed with G-protein coupled purinoceptors (Grohovaz *et al.*, 1991), typically display ATP-induced inward currents via activation of ligand-gated receptors (Nakazawa *et al.*, 1990; Nakazawa & Inoue, 1992; Brake *et al.*, 1994). In the present experiments on PC12 cells the current peak and rebound induced by ATP were probably caused by activation of a single type of ligand-gated receptor (presumably of the P_{2X2} class) for the following reasons: i) both current components exhibited similar voltage-sensitivity; ii) the biphasic current response was not reproduced by ADP or α,β-methylene ATP which have different degree of effectiveness on P_{2X} receptors of various tissues (Kim & Rabin, 1994; Surprenant *et al.*, 1995); iii) in control solution the rebound always appeared after the end of the pulse application even if the delivery time varied by one order of magnitude, thus making unlikely that the rebound was due to delayed, concentration-dependent activation of a separate receptor system; iv) the initial peak and the rebound wave decreased approximately to the same extent in the presence of bath-applied ATP; v) currents evoked by both brief and long pulses of ATP were reversibly blocked by 10 μM PPADS.

XV-1b. Characteristics of fading and rebound of ATP-induced currents

ATP current rebound has not apparently been described before. Previous studies of native or cloned PC12 forms of purinoceptors (Nakazawa *et al.*, 1990; Nakazawa & Inoue, 1992; Brake *et al.*, 1994; King *et al.*, 1996) did not detect current rebound probably because lower ATP concentrations and slow rates of ATP application (e.g. by bath superfusion) were used. In the present experiments current rebound was observed with ATP pipette concentrations >1 mM and pulse duration ≥200 ms (15-20 ms solution exchange time). A similar rebound effect has been observed in ACh-activated channels from bovine adrenal chromaffin cells with >1 ms agonist application (MacOnochie & Knight, 1992). The present data suggest that fading and rebound of ATP currents originated from some common mechanism. In fact, the latency and the onset time constant of the rebound were proportional to the ATP pulse duration which also determined the extent of current fading. Furthermore, the rate of rebound development was inversely related to the fading rate of the first peak response.

XV-1c. Fading and rebound are due to receptor desensitization

In the light of the above mentioned considerations it seems interesting to discuss first why responses to ATP faded since this approach might provide a unitary hypothesis to account for the fade and rebound phenomena of P_2 receptors. As it was mentioned before (see Chapter XII-1), there are two possible mechanisms for current fading under the action of high concentrations of agonist, namely desensitization (Katz & Thesleff, 1957) and open channel block (Sine & Steinbach, 1984; Ogden &

Colquhoun, 1985). For example, fading and rebound of ACh receptor activity was attributed by MacOnochie and Knight (1992) to blocking and unblocking of open channels. In the present study some arguments stand against open channel block/unblock as the most plausible explanation for current fading and rebound induced by ATP. First, it is known that the action of open channel blockers is highly voltage-dependent (Adams, 1976; Neher & Steinbach, 1978; Sine & Steinbach, 1984; Ogden & Colquhoun, 1985). On PC12 cells the τ_1 value for peak current fading (and τ for rebound onset) did not vary for membrane potentials less negative than -70 mV. Moreover, the rebound phenomenon was the same when the cell was clamped at +40mV or at -70 mV during the ATP application. It means that the rebound phenomenon was independent of current flow through ATP-activated channels. Second, ATP molecules are negatively charged and thus unlikely to be attracted to cationic channels (see for example Neher, 1983). These findings thus favour fast desensitization as the main mechanism for current fading in the presence of high concentrations of ATP.

Assuming that desensitization was the predominant process, the onset of the rebound phenomenon at the end of ATP application might have reflected the recovery from fast desensitization of purinoceptors. Fast desensitization was observed not only as quick current fading during continuous application of a high concentration of ATP but also when a short (20 ms) pulse of ATP (applied during the onset of the rebound) rapidly suppressed the slowly-developing inward current. Short application during the decline of the rebound current did not produce any profound, additional desensitization but only a small inward current. It seems likely that the different

responses induced by short pulses of ATP reflected the dissimilar concentration of ATP at receptor level immediately before these brief applications.

In addition to such a process of fast desensitization which developed quickly within hundreds of ms, slow desensitization (over a span of some min in terms of onset and recovery) was also present: this phenomenon would be analogous to the one reported for nicotinic receptors (Sakmann *et al.*, 1980) and, in the present study, was manifested as a reversible decrease in responses induced by 5 mM ATP after bath application of low doses of the same agonist (*cf.* Katz & Thesleff, 1957) or when ATP was applied repetitively (0.05 Hz). These data are also in agreement with observations by Nakazawa *et al.* (1990) who, using a slow drug application system, reported slow rate of desensitization and recovery in these cells.

XV-1d. A kinetic scheme for receptor activation and desensitization

The present data can be described by a model which takes into account the experimental observations of rapid fade and rebound of the ATP current plus the classical description of desensitization according to Katz & Thesleff (1957; see equation 1 in Chapter XI). It should be emphasized that this is only an operational scheme to provide a framework for further studies. Accordingly:

$$\begin{array}{ccccc} A + R & \leftrightarrow & AR^{*} & \leftrightarrow & AD_1 \\ \uparrow\downarrow & & \uparrow\downarrow & & \\ A + D_2 & \leftrightarrow & AD_2 & & \end{array} \qquad (3)$$

where A is the agonist (ATP), R and R^* are the resting and activated receptors, and D_1 and D_2 are receptors in fast and slow desensitized states, respectively. For sake of simplicity this scheme implies that one ATP molecule is sufficient for receptor activation and that ATP-bound receptors are either in an active conformation or desensitized.

According to Equation 3, in the presence of large concentrations of ATP, the ATP-activated receptor (AR^*) might quickly turn to the AD_1 state (experimentally observed as rapid current fading) from which recovery to the AR^* state (experimentally observed as current rebound developing with an order of magnitude slower than the initial fading) would ensue only after ATP delivery in view of fast superfusion which aided removal of free agonist molecules. The rebound phenomenon might therefore be based on reopening of channels as they dwell in an active state before entering a resting state. Interestingly, when a brief pulse of agonist (which under resting conditions would evoke an inward current) was applied during developing phase of rebound wave, it actually appeared as an outward current (or channel closure) which levelled off at the same level as the steady-state desensitized current. Presumably, the probability for the channel to return to the fast desensitized state (D_1) was higher than at rest. Since high concentrations of ATP were required to observe rapid desensitization and rebound, D_1 probably represents a low-affinity receptor conformation. This property would explain why with pipette concentrations of ATP $\leq$ 1 mM current fading and rebound were very rarely seen. Fast desensitization (D1) thus appeared to be the predominant phenomenon under the action of high

concentrations of ATP as the model implies fast transition to and from the D_1 state. On the other hand, the D_2 state might be induced by the continuous presence of low concentrations of ATP activating only a small fraction of channels. This phenomenon would be typically observed following sustained bath application of low doses of ATP which depressed peak and rebound currents evoked by a large concentration of ATP to a similar degree by reducing the number of available receptors for ATP binding. Hence, the D_2 state would represent a high-affinity receptor conformation. Might the D_2 state have a role in shaping responses to low concentrations of pressure-applied ATP? This seems unlikely because with the lowest pipette concentration of ATP tested (0.5 mM) the inward current declined monoexponentially with the same τ value even if the pulse duration (and thus the agonist concentration) was more than doubled (see, however, data with substance P; Chapter XVI). Curiously, when the pipette solution was 1 mM, the τ of current decline increased with a longer pulse application (50 ms): perhaps this phenomenon reflected recruitment of distant receptors by an increasing dose of agonist. Further dose increments reduced the τ value presumably as desensitization limited the response duration.

XV-2. Ca^{2+}-dependence of fast and slow desensitization

The novel fast desensitization described in the present study was further studied in terms of $[Ca^{2+}]_i$ changes. The main result of this work is the demonstration of a close association between $[Ca^{2+}]_i$ and slow desensitization of P2-receptors activated by high doses of ATP in PC12 cells. Conversely, the process of fast desensitization of the same receptors appeared to be independent of $[Ca^{2+}]_i$.

XV-2a. $[Ca^{2+}]_i$ changes in response to brief and long ATP application

Brief applications of ATP elicited monophasic $[Ca^{2+}]_i$ rises in intact as well as patch clamped cells; this response was consistently slower in the latter. 2 s Applications of ATP to intact cells induced biphasic time course of the changes in $[Ca^{2+}]_i$. Under voltage clamp conditions when this initial $[Ca^{2+}]_i$ rise was absent, the current peak fading and rebound were reliably present. It seems likely that the fast increase in $[Ca^{2+}]_i$ was due to influx of this ion via voltage gated Ca^{2+} channels which are known to be activated by depolarization during ATP application (Di Virgilio *et al.*, 1987). This conclusion is supported by the fast temporal characteristics of the initial peak of $[Ca^{2+}]_i$ transient in intact cells which resembled rapid rise and decay of $[Ca^{2+}]_i$ responses to voltage steps applied to patch clamped cells.

Several factors might determine the decay of $[Ca^{2+}]_i$ transients such as Na^+/Ca^{2+} exchange, Ca^{2+} pumps, and intracellular Ca^{2+} sequestration (Neher & Augustine, 1992; Markram *et al.*, 1995; Park *et al.*, 1996). It is worth noting, however, that the time course of $[Ca^{2+}]_i$ transient decay after a long pulse of ATP was similar for patch clamped and intact cells, indicating that Ca^{2+} removal mechanisms in the cells under patch clamp conditions (with a 25 μM fluo-3 containing pipette) were not disrupted.

XV-2b. Origin of ATP-induced $[Ca^{2+}]_i$ rises

While the main part of $[Ca^{2+}]_i$ rise in intact cells appeared to be due to influx through

voltage-gated Ca^{2+} channels activated by ATP-induced depolarization, the remaining component constituting $[Ca^{2+}]_i$ responses in patch clamped cells might have been caused either by influx of this cation via ionotropic P2-receptors (Nakazawa & Inoue, 1992; Reber *et al.,* 1992; Raha *et al.,* 1993), or by its release from intracellular Ca^{2+} stores (Grohovaz *et al.,* 1991; Zacchetti *et al.*, 1991), or by a combination of the two. In our experiments $[Ca^{2+}]_i$ elevation in both intact and patch clamped cells was dependent on extracellular Ca^{2+}, as suggested by the near absence of $[Ca^{2+}]_i$ increase in the cells superfused with Ca^{2+}-free external solution (see also Nakazawa & Inoue, 1992; Reber *et al.*, 1992). This observation suggests the predominant role of transmembrane Ca^{2+} influx and, while not excluding intracellular Ca^{2+} release (previously reported for these cells; Grohovaz *et al.*, 1991; Zacchetti *et al.*, 1991), it implies that if the latter took place, it must have been dependent on Ca^{2+} influx. The steep, linear dependence of $[Ca^{2+}]_i$ transients on holding potential of patch clamped cells (see present study and Reber *et al.*, 1992) indicates, however, a minimal contribution by intracellular Ca^{2+} release which is expected to be voltage independent (Sugasawa *et al.*, 1996).

XV-2c. $[Ca^{2+}]_i$ changes during fast and slow desensitization of ATP receptors

There are several lines of evidence which suggest that fast desensitization of ATP-gated channels of PC12 cells took place independently of $[Ca^{2+}]_i$ variations. First, using combined Ca^{2+} imaging and patch clamp recording, there was only a negligible $[Ca^{2+}]_i$ rise during fading of membrane current corresponding to fast desensitization. Second, even stronger evidence was provided by experiments on $[Ca^{2+}]_i$ buffering with different (or no) Ca^{2+} chelators. In this case, the onset of fast desensitization

(measured as fading rate of the current induced by 2 s pulse of ATP) was the same in a large sample of cells dialysed with various Ca^{2+} buffers such as the fast acting BAPTA (Tsien, 1981), the relatively slow acting EGTA, a low concentration of the BAPTA derived fluorescence dye fluo-3, or even with no exogenous buffers.

Unlike the fast one, slow desensitization was found to be highly Ca^{2+}-dependent. This conclusion is supported by the same arguments used to discard a major role of $[Ca^{2+}]_i$ in fast desensitization. In fact, as indicated by simultaneous recording of $[Ca^{2+}]_i$ and membrane currents induced by ATP, the time-course of $[Ca^{2+}]_i$ after a desensitizing application of this agent developed over the same time scale which might have allowed Ca^{2+} to interact with desensitized receptors. An important finding was the high correlation between the decay of ATP-induced $[Ca^{2+}]_i$ transients and the recovery from relatively long-lasting desensitization in a sample of cells in which these two phenomena always varied in a similar fashion. The role of Ca^{2+} in slow desensitization was further supported by experiments in which slow desensitization was evaluated in the presence of different intracellular Ca^{2+} chelators. Thus, the degree of sensitivity loss after a 2 s pulse of ATP was the largest with a low concentration of fluo-3 (which presumably allowed more Ca^{2+} to interact with P2-receptors from the cytoplasmic side) than with EGTA or BAPTA. The Ca^{2+} independence of fast desensitization, on the one hand, and the high Ca^{2+} dependence of slow desensitization, on the other hand, accord with a similar role of $[Ca^{2+}]_i$ in the fast and slow phases of desensitization of ACh receptors on skeletal muscle (Cachelin & Colquhoun, 1989).

One might consider two possible hypotheses for the precise mechanism of Ca^{2+} action on slow desensitization. Firstly, Ca^{2+} might switch on various protein kinases which

can influence receptor activity by phosphorylation of certain subunits (Kozawa *et al.*, 1995). Alternatively, if the temporal overlap between the persistence of $[Ca^{2+}]_i$ rise (after 2 s pulse of ATP) and the changes in receptor sensitivity is taken into consideration, a direct action of intracellular Ca^{2+} on the sensitivity of P2-receptors without intervention of other second messengers would be possible. On PC12 cells, single-channel currents induced by ATP could be blocked by Ca^{2+} applied either externally or internally. This phenomenon was also present with other divalent cations such as Cd^{2+}, Ba^{2+} or Mg^{2+} (Nakazawa & Hess, 1993). This suppressant action was proposed to be due to Ca^{2+} blocking Na^+ influx through ATP-activated channels. The molecular mechanism appears to be complex since such a phenomenon could not be described by a simple one-binding site model with symmetric energy barriers.

The work by Nakazawa and Hess (1993) was carried out using single-channel recordings in cell-attached or inside-out configuration. The potency of external Ca^{2+} in reducing Na^+ influx was not high since its EC_{50} was 6 mM, a value three times larger than the standard Ca^{2+} concentration of the medium used in the present experiments. The potency of internal Ca^{2+} was not quantitatively estimated by Nakazawa and Hess who, however, reported a concentration of 0.6 mM as necessary to produce a voltage-dependent block of Na^+ permeation. While $[Ca^{2+}]_i$ in the present experiments was not directly measured, ionomycin-based calibration experiments indicated that maximum $[Ca^{2+}]_i$ rises were in the order of μM. Hence, it is unlikely that $[Ca^{2+}]_i$, even in restricted subcellular regions, might have reached the levels necessary to block ATP receptors as reported by Nakazawa and Hess (1993). This suggestion is supported also by the fact that in Ca^{2+}-free media ATP currents were found to be only slightly changed and that internally applied BAPTA did not significantly alter peak currents induced by ATP.

Further experiments will, however, be necessary to resolve the question of whether Ca^{2+} is acting directly or indirectly (via intracellular second messengers) on ATP receptors of PC12 cells.

XV-3. Physiological role of fast and slow desensitization of P2X receptors

The rebound process observed in our experiments can be regarded as a novel manifestation of ATP buffering by desensitized receptors. Such a buffering might be observed with either exogenously-applied agonists or endogenous transmitter. Thus, agonist buffering by desensitized $GABA_A$ receptors has been shown with exogenously-applied GABA (Jones & Westbrook, 1995) and has led to the proposal that reopening of GABA channels after desensitization may be the physiological mechanism which produces a long-lasting component of the transmitter-induced inhibitory current. This changes in time-course due to desensitization would, however, depend on factors such as receptor affinity, and efficiency of any agonist breakdown mechanism. In the case of purinoceptors the ATP current rebound might be expected to prolong purinergic synaptic currents when the ATP concentration reaches the mM range, a phenomenon which would be enhanced as a result of any impairement of ecto-ATPase activity. Such a current rebound might then be an amplifying mechanism to support sustained Ca^{2+} influx through the ATP-gated channels which are permeable to this cation (Humphrey *et al.*, 1995).

In contrast to fast desensitization, slow desensitization might serve as an efficient process to limit excitability of neurons during repetitive stimulation of ATP releasing nerve fibers. The functional role of Ca^{2+} in slow desensitization of P2-receptors of

PC12 cells was probably underestimated by the present study because voltage clamping prevented a more substantial $[Ca^{2+}]_i$ rise via voltage activated Ca^{2+}-channels. In many patch clamp studies concerning P_{2X} receptors (Bean, 1990; Nakazawa *et al.*, 1990; Nakazawa & Inoue, 1992; Valera *et al.*, 1994; Khakh *et al.*, 1995), whole-cell patch clamping used pipettes containing relatively high levels of Ca^{2+} buffers. It is likely that this condition has also led to underestimation of slow desensitization. These considerations therefore reinforce the important role of Ca^{2+} in regulating slow desensitization in physiological conditions. Since $[Ca^{2+}]_i$ levels can be influenced by a variety of intracellular second messengers, it seems plausible that the process of $[Ca^{2+}]_i$ dependent slow desensitization is modulated according to different functional states of the cell.

XVI. Desensitization modulation: depression of ATP currents by substance P

Once the role of $[Ca^{2+}]_i$ in regulation of P_{2X} receptor desensitization and recovery was established, it seemed of interest to study if desensitization might have been regulated by endogenous substances and in what way this would occur. Thus, the neuropeptide substance P known to regulate desensitization of nAChRs (Clapham & Neher, 1984) was tested. It was found that substance P, without exerting any measurable action on baseline current or $[Ca^{2+}]_i$, strongly depressed only those responses which were produced by high concentrations of ATP. These results are interpreted as due to facilitation by substance P of ATP induced receptor desensitization.

XVI-1. Substance P depressed ATP responses

No effect of substance P *per se* on PC12 cells in terms of changes in either baseline current or $[Ca^{2+}]_i$ was observed indicating that it had no agonist activity on these cells. This observation confirms that PC12 cells do not possess tachykinin receptors (Simmons *et al.,* 1990). Previous experiments indicated that brief applications of ATP to PC12 cells induce membrane currents and associated $[Ca^{2+}]_i$ rises via activation of a homogeneous population of P_{2X}-receptors (See Results, Chapters X and XI). The depressant action of substance P on ATP-induced currents was dependent on the dose of the peptide, had slow onset and offset, and was unaffected by changes in membrane potential. Likewise, substance P reduced the $[Ca^{2+}]_i$ transients evoked by ATP in parallel with the decrease in membrane currents. It is worth noting that the ability of substance P to depress ATP-induced currents was clearly related to the concentration of ATP. Short applications (20 ms) of 5 mM ATP evoked rapid inward currents which were readily reduced by substance P: an analogous reduction was also apparent when the application of ATP induced strong fading and rebound of the response. However, currents induced by small doses of ATP (0.05 mM for 2 s) were minimally affected by substance P even if their amplitude was comparable to that of currents observed after larger doses of ATP. Furthermore, substance P significantly slowered recovery of ATP currents after a conditioning application of ATP.

XVI-2. Possible mechanisms of depression of ATP currents by substance P

No direct action of substance P, either in terms of current or $[Ca^{2+}]_i$ changes, on PC12 cells was observed (in keeping with their lack of tachykinin receptors; Simmons *et al.,* 1990). Thus, it is likely that substance P exerted a modulatory role on P_{2X}-receptor activity. This phenomenon might have involved block of P_{2X}-receptors (or of their open channels), or facilitation of their desensitization. If substance P was a competitive antagonist of P_{2X}-receptors, its inhibitory effect should have been proportionally the same regardless of the ATP concentration. Against this interpretation, it was observed that substance P preferentially blocked ATP responses induced by large doses of this agonist. Such a depressant activity was unlikely to be due to an open channel block process, even if substance P molecule is positively charged. In fact, while open channel block is usually a voltage-dependent phenomenon (see Clapham & Neher, 1984), the action of substance P was the same despite wide variations in membrane potential and did not involve any change in the reversal potential or slope conductance for the ATP currents. Since these findings make improbable open channel block as the mechanism of action of substance P (see also analogous conclusions for the effect of substance P on nicotinic receptors; Stafford *et al.,* 1994), it seems worth considering the possibility of facilitation by the peptide of P_{2X}-receptor desensitization.

XVI-3. How might substance P interfere with P_{2X}-receptor desensitization?

Substance P is known to potentiate desensitization of nicotinic acetylcholine receptors via allosteric site modulation (Stafford *et al.,* 1994) without interfering with channel activation or ion permeation (Clapham & Neher, 1984). The precise molecular mechanism is still uncertain although it appears to require the presence of

the β receptor subunit (Stafford *et al.,* 1994): one possibility is that substance P allosterically binds to the nicotinic receptor and stabilizes its desensitized state which may be present even in the absence of substance P (Clapham & Neher, 1984). As far as P_{2X}-receptors are concerned, single channel recordings of their activity during substance P application will be necessary to cast light on this phenomenon. However, in analogy with the interpretation applied to nicotinic receptor data, the present results may be explained by facilitation of P_{2X}-receptor desensitization by substance P presumably bound to an unidentified subunit of the P_{2X}-receptor. In favor of this interpretation is the observation that desensitized responses were largely depressed by substance P which also delayed recovery of ATP responses from desensitization.

Our previous experiments suggested that on PC12 cells P_{2X}-receptor desensitization is a heterogeneous process including distinct fast and slow states. According to this notion fast desensitization is typically manifested during ATP application as rapid current fade with 100 ms time-constant which in the present study was significantly reduced by substance P. Slow desensitization is observed as a persistent depression of current peak amplitude after exposing the cell membrane to sustained application of ATP and is correlated with a rise in $[Ca^{2+}]_i$. Also in this case substance P enhanced slow desensitization and prolonged recovery from it.

Some observations of the present study are, nevertheless, apparently in contrast with the view that substance P facilitated P_{2X}-receptor desensitization. First, the response peak to short pulses of high doses of ATP was depressed even if there was no manifest desensitization: perhaps these control responses were already limited by a degree of "occult desensitization" (Werman, 1976; Nistri & Constanti, 1979)

enhanced by the peptide application. It seems less likely that substance P merely converted closed channels to a desensitized state since relatively large amplitude currents induced by low doses of ATP were unaffected. Secondly, since in the presence of substance P ATP-induced $[Ca^{2+}]_i$ transients were smaller, one might actually expect less slow desensitization which is related to $[Ca^{2+}]_i$ (See Chapter XI), a prediction not borne out by the experimental data. As the size of the $[Ca^{2+}]_i$ transient is strongly dependent on the charge transfer of the ATP current through the membrane (See chapter XI), it is not surprising that the substance P-induced current depression led to smaller $[Ca^{2+}]_i$ rises. Persistence of slow desensitization despite reduced amplitude of $[Ca^{2+}]_i$ transients suggests that $[Ca^{2+}]_i$ was only one element of the multifactorial process of slow desensitization of P_{2X2} receptors.

These novel data raise the interesting possibility that this peptide might control the neurotransmitter action of ATP, even though the present report does not identify the precise mechanism responsible for the substance P/ATP interaction,. Future studies might explore any modulation by substance P of the neurotransmitter function of ATP for example on the dorsal horn neurons of the spinal cord (Burnstock & Wood, 1996) or on chromaffin cells of the adrenal gland (Nakazawa *et al.*, 1990), since both tissues contain endogenous substance P (Otsuka & Yoshioka, 1993).

XVII. Comparison of desensitization of P2X receptors with that of nAChRs

It seemed interesting to compare the two systems of ligand-gated receptors which were studied in the present thesis in terms of their desensitization time-course, its $[Ca^{2+}]_i$ dependence and modulation. This comparison may be done from the point of

view of the time-course of desensitization onset and recovery, modulation of these stages by $[Ca^{2+}]_i$, and proposed receptor kinetic scheme.

XVII-1. Time-course of desensitization of nAChRs and ATP receptors

Since pressure application of ATP or nicotine (using similar micropipettes and perfusion conditions) induced membrane currents which faded in the presence of the agonist, it is possible for the two receptors to compare the time-course of desensitization onset which in both cases can be fitted by bi-exponential curves (*cf* Feltz & Trautmann, 1982; Boyd, 1987) with time-constants of 145 ms and 1.4 s for nAChRs, and 95 ms and 4.3 s for P_{2X} receptors. The most apparent difference in the time-course of responses to nicotine and ATP was, however, a more pronounced return of the ATP-activated currents after the end of application as compared to that of nicotinic receptors. In fact, at the end of the ATP pulse the rebound current had even larger amplitude and a much longer duration than the peak current, whereas the amplitude of the nicotine-induced rebound current was less than half of its initial peak.

The rate of recovery of test pulse amplitude was faster for nicotine-induced currents under similar conditions (i.e., with the same interval between the pulses and similar degree of $[Ca^2]_i$ buffering with the fluo-3 in the patch pipette). It seems worth noticing that the slow component of the desensitization onset was about three-fold faster for nAChRs than for P_{2X} receptors, suggesting direct relation between rate of desensitization development and that of recovery form it (*cf* Boyd, 1987).

XVII-2. Kinetic schemes for nAChRs and ATP receptors

Equations 1 and 3 (Chapter I-1b) schematically represent the current understanding of activation and desensitization of nAChRs and P_{2X} receptors, respectively. In spite of apparent similarities between macroscopic currents induced by 2 s applications of ATP or nicotine (both fade rapidly during the agonist pulse and rebounce after it), the proposed kinetic schemes have some principal differences. In fact, according to Katz & Thesleff (1957) and Boyd (1987), there is only one, cyclic desensitization for nAChRs (see Equation 1) in which channel conformation changes from closed to open state and subsequently to the bound and then unbound desensitized states, from which it returns to the closed state again. The scheme is oversimplified and should probably include additional consecutive step(s) (see Boyd, 1987) since the time-course of current fading is better described by a biexponential curve (Feltz & Trautmann, 1982). However, even assuming the four-state model (comprising two desensitized states with increasing affinity to the agonist; Changeux & Revah, 1987), one should notice the cyclic process of transitions into both desensitized states, implying a higher probability of returning from the desensitized state to the resting rather to the open one. On the other hand, a component of open channel block has been reported (MacOnochie & Knight, 1992), as is also suggested by occasional rebound current which could be due to unblocking mechanism. Nevertheless, the comparatively small size of nAChRs rebound current implies that the fading prior to it is largely due to receptor desensitization.

The kinetic scheme for P_{2X} receptors (see Equation 3 in Chapter XV-1d) has and additional conformational state (D1, with closed channel and agonist-bound receptor) which is different form the one of conventional cyclic desensitization (D2). This difference from the nAChRs kinetic scheme (Equation 1 in Chapter I-1b) could explain the dissimilarity in receptor behavior after the end of agonist application. In fact, P_{2X} receptors in PC12 cells show reopening after the cessation of ATP pulse which is revealed as rebound current that can reach higher levels than initial peak and is attributed to receptor desensitization. Conversely, fading of nAChRs-driven currents is not consistently followed by a substantial rebound current. The nAChRs seem more likely to pass into closed state before becoming re-activable again (see equation 1).

XVII-3. Modulation of desensitization by $[Ca^{2+}]_i$: nAChRs *vs* P_{2X} receptors

Onset of desensitization (measured as time-course of current fade during the agonist application) appeared to be independent of $[Ca^{2+}]_i$ for both receptors studied, since it was not different with either strong or no Ca^{2+} buffering in the pipette. However, a difference between the two systems appeared when the time-course of the membrane currents was compared with that of associated $[Ca^{2+}]_i$ rises. In the case of nicotinic receptors, the increase in $[Ca^{2+}]_i$ initiated simultaneously with the current (within the 320 ms resolution of the confocal imaging) and persisted during current fade and rebound until the end of charge transfer through the membrane. Conversely, during rise and fading of P_{2X}-mediated current there were no detectable increase in $[Ca^{2+}]_i$ which grew slowly after the end of the ATP pulse during rebound current. This delay was absent, however, in non-clamped cells where a biphasic $[Ca^{2+}]_i$ response was

observed presumably due to opening of Ca^{2+} produced by membrane depolarization. This difference could be explained by a comparatively small charge transfer through the open ATP receptors during the initial peak and fast fading as compared to that during the rebound current, while in the case of nicotinic receptors the substantial part of charge passed through the receptor by the fading current rather than by the relatively small rebound one. The larger charge transfer by the fading nicotine-induced current is also suggested by the slower first time-constant of desensitization for nAChRs than that of P_{2X} receptors.

For both receptors, recovery from desensitization, although different between the receptors, was found to be strongly dependent on the time-course of $[Ca^{2+}]_i$ changes. Thus, 30 s after the conditioning pulse of the agonist, the high correlation between $[Ca^{2+}]_i$ and recovery from desensitization was observed for both nAChRS and P_{2X} receptors, although fine details differed (namely, the degree of nAChRs recovery was related to the % fall of $[Ca^{2+}]_i$ from its peak rather than to the % $[Ca^{2+}]_i$ rise over baseline as in the case of P_{2X} receptors). Similar dependence of recovery rate on $[Ca^{2+}]_i$ buffering was observed for the two receptors, too. Thus, both for nAChRs and P_{2X} receptors the role of $[Ca^{2+}]_i$ is more pronounced on the stage of recovery rather than during the onset of receptor desensitization.

Bibliography

1. ABBE, E. (1884) Note on the proper definition of the amplifying power of a lens or a lens-system, *J. R. Microsc. Soc.* **4**, 348-351.

2. ADAMS, P.R. (1976). Drug blockade of open end-plate channels. *J. Physiol.*, **260**, 531-552.

3. AKAIKE, N., SHIRASAKI, T. & YAKUSHIJI, T. (1991). Quinolones and fenbuten interact with $GABA_A$ receptor in dissociated hippocampal cells of rat. *J.Neurophysiol.*, **66**, 497-504.

4. AKASU, T., KOJIMA, M. & KOKETSU, K. (1983). Substance P modulates the sensitivity of the nicotinic receptor in amphibian cholinergic transmission. *Br. J. Pharmacol.*, **80**, 123-131.

5. ANDERSON, C.R., & STEVENS, C.F. (1973) Voltage clamp analysis of acetylcholine produced end-plate current fluctations at frog neuromusculat junction. *J. Physiol.*, **235**, 655-691.

6. ANDJUS, P.R., KHIROUG, L., YAKEL, J. L., CHERUBINI, E. & NISTRI, A. (1996a). Changes in intracellular calcium induced by NMDA in cultured rat hippocampal neurones require exogenous glycine. *Neurosci. Lett.*, **210**, 1-4.

7. ANDJUS, P.R., KHIROUG, L., NISTRI, A., CHERUBINI, E. (1996b) ALS IgGs suppress $[Ca^{2+}]_i$ rise through P/Q type calcium channels in central neurones in culture. *NeuroReport*, 7, 1914-1916.

8. ANDJUS, P.R., KHIROUG, L., NISTRI, A., CHERUBINI, E. (1996c) Effects of amyotropic lateral sclerosis IgGs on calcium homeostasis in neural cells. In: *Immunoregulation in Health and Disease*, Ed: Lukic M.L., Colic M., Stojkovic M.M., & Cuperlovic K., Academic Press, London, pp.173-180.

9. AMOS, W.B., WHITE, J.G. & FORDHAM, M. (1987) Use of confocal imaging in the study of biological structures. *Appl. Opt.* **26**, 3239-3243.

10. ARMSTRONG, C.M. & GILLY, W.F. (1992) Access resistance and space clamp problems associated with whole-cell patch clamping. *Meth. Enzymol.* **207**, 100-122.

11. ASLUND, N., CARLSSON, K., LILJEBORG, A. & MAJLOF, L. (1983) PHOIBOS, a microscope scanner deseigned for micro-fluorometric applications, using laser-induced fluorescence. In: *Proc. of the 3rd Scandinavian Conf. on Image Analysis, Studentlliteratur,* Lund, p. 338.

12. BEAN, B.P. (1990). ATP-activated channels in rat and bullfrog sensory neurones: Concentration dependence and kinetics. *J. Neurosci.,* **10**, 1-10.

13. BEAN, B. & FRIEL, D.D. (1990) ATP-activated channels in excitable cells. In: *Ion*

Channels, **2** Ed: T. Narahashi, Plenum Press, New York.

14. BERRIDGE, M.J. (1993) Inositol trisphosphate and calcium signalling. *Nature,* **361**, 315-325.

15. BERTRAND, D., DEVILLERS-THIERY, A., REVAH, F., GALZI, J.-L., HUSSY, N., MULLE, C., BERTRAND, S., BALLIVET, M., & CHANGEUX, J.-P. (1992). Unconventional pharmacology of a neuronal nicotinic receptor mutated in the channel domain. *Proc. Nat. Acad. Sci. USA*, **89**, 1261-1265.

16. BEZPROZVANNY, I., WATRAS, J. & EHRLICH, B.E. (1991) Bell-shaped calcium-response curves of Ins(1,4,5)P3- and calcium-gated channels from endoplasmic reticulum of cerebellum. *Nature* **351**, 751-754.

17. BETZ, W.J. & BEWICK, G.S. (1992) Optical analysis of synaptic vesicle recycling at the frog neuromuscular junction. *Science,* **255**, 200-203.

18. BIALES, B., DICHTER, M. & TISCHLER, A. (1976) Eliectrical excitability of cultured adrenal chromaffin cells. *J. Physiol.,* **262**, 743-753.

19. BLITON, A.C. & LECHLEITER, J.D. (1995) Optical considerations at ultraviolet wavelengths in confocal microscopy. In: *Handbook of Biological Confocal Microscopy,* Ed: J. B. Pawley, Plenum Press, New York.

20. BOYD, N.D. (1987). Two distinct kinetic phases of desensitization of acetylcholine receptors of cloned rat PC12 cells. *J. Physiol.,* **389**, 45-67.

21. BRAKE, A.J., WAGENBACH, M.J. & JULIUS, D. (1994). New structural motif for ligand-gated ion channels defined by an ionotropic ATP receptor. *Nature*, **371**, 519-523.

22. BRANDT, B.L., HAGIWARA, S., KIDOKORO, Y., MIYAZAKI, S. (1976). Action potentials in the rat chromaffin cell and effects of acetylcholine. *J. Physiol.*, **263**, 417-439.

23. BURNSTOCK, G. (1990). Purinergic mechanisms. *Ann. N. Y. Acad. Sci.,* **603**, 1-17.

24. BURNSTOCK, G. & WOOD, J.N. (1996). Purinergic receptors: their role in nociception and primary afferent neurotransmission. *Curr. Opin. Neurobiol.,* **6**, 526-532.

25. CACHELIN, A.B. & COLQUHOUN, D. (1989). Desensitization of the acetylcholine receptor of frog end-plates measured in a vaseline-gap voltage clamp. *J. Physiol.,* **415**, 159-188.

26. CAMPOS-CARO, A., SMILLIE, F.I., DOMINIQUEZ DEL TORO, E., ROVIRA, J.C., VICENTE-AGULLO, F., CHAPULI, J., JUIZ, J.M., SALA, S., SALA, F., BALLESTA, J.J. & CRIADO, M. (1997) Neuronal nicotinic acetylcholine receptors on bovine

chromaffin cells: cloning, expression, and genomic organization of receptor subunits. *J. Neurochem.* **68**, 488-497.

27. CARLSSON, K., DANIELSSON, P., LENZ, R., LILJEBORG, A., MAJLOF, L. & ALSUND, N. (1985) Three-dimensional microscopy using a confocal laser scanning microscope. *Opt. Lett.,* **10**, 53-55.

28. CHANGEUX, J-P. (1990) Functional architecture and dynamics of the nicotinic acetylcholine receptor: An allosteric ligand-gated ion channel, in: *1988-1989 Fidia Research Foundation: Neuroscience Award Lectures,* **4**, 21-168.

29. CHANGEUX, J-P. & REVAH, F. (1987) The acetylcholine receptor molecule: allosteric sites and the ion channel. *Trends in Neurosci.,* **6**, 245-249.

30. CLAPHAM, D. E., & NEHER, E. (1984). Substance P reduces acetylcholine-induced currents in isolated bovine chromaffin cells. *J. Physiol.,* **347**, 255-277.

31. CLARKE, P.B. (1992) The fall and rise of neuronal alpha-bungarotoxin binding proteins. *Trends. Pharmacol. Sci.,* **13**, 407-413.

32. CLEMENTI, F. & SHER, E. (1985) Antibody induced internalization of acetylcholine nicotinic receptor: kinetics, mechanism and selectivity. *Eur. J. Cell. Biol.,* **37**, 220-228.

33. COLLO, G., NORTH, A.N., KAWASHIMA, E., MERLO-PICH, E., NEIDHART,

C., SURPRENANT, A. & BUELL, G. (1996). Cloning of $P2X_5$ and $P2X_6$ receptors and the distribution and the properties of an extended family of ATP-gated ion channels. *J. Neurosci.*, **16**, 2495-2507.

34. CRIADO, M., ALAMO, L. & NAVARRO, A. (1992). Primary structure of an agonist binding subunit of the nicotinic acetylcholine receptor from bovine adrenal chromaffin cells. *Neurochemistry Research*, **17**, 281-287.

35. D'ANDREA, P., ZACCHETTI, D., MELDOLESI, J. & GROHOVAZ, F. (1993). Mechanism of $[Ca^{2+}]_i$ oscillations in rat chromaffin cells. *Journal of Biological Chemistry,* **268**, 15213-15220.

36. DEL CASTILLO, J. & KATZ, B. (1957) Interaction at endplate receptors between different choline derivatives. *Proc. R. Soc. Lond. B,* **146**, 369-381.

37. DI VIRGILIO, F., MILANI, D., LEON, A., MELDOLESI, J. & POZZAN, T. (1987). Voltage-dependent activation and inactivation of calcium channels in PC12 cells. Correlation with neurotransmitter release. *J. Biol. Chem.*, **262**, 9189-9195.

38. DOUGLAS, W.W. & RUBIN, R.P. (1961). The role of calcium in the secretory response of the adrenal medulla to acetylcholine. *Journal of Physiology*, **159**, 40-57.

39. DOWNING, J.E.G. & ROLE, L.W. (1987). Activators of protein-kinese C enhance acetylcholine receptor desensitization in sympathetic ganglion neurons. *Proceeding of the National Academy of Sciences USA,* **84**, 7739-7743.

40. DUDEL, J., FRANKE, C. & HATT, H. (1992). Rapid activation and desensitization of transmitter-liganded receptor channels by pulses of agonists. In: *Ion Channels.* Ed: T. Narahashi, vol. 3, pp.207-260, Plenum, New York.

41. EDWARDS, F.A., GIBB, A.J. & COLQUHOUN, D. (1992)ATP receptor-mediated synaptic currents in the central nervous system. *Nature* **359**, 144-147

42. EVANS, R.J., DERKACH, V. & SURPRENANT, A. (1992) ATP mediates fast synaptic transmission in mammalian neurons. *Nature* **357,** 503-505.

43. EVANS RJ, LEWIS C, BUELL G, VALERA S, NORTH RA, SURPRENANT A (1995) Pharmacological characterization of heterologously expressed ATP-gated cation channels (P2x purinoceptors). *Mol. Pharmacol.,* **48**, 178-183.

44. FABIATO, A. (1985) Effects of ryanodine in skinned cardiac cells. *Fed. Proc.* **44**, 2970-2976.

45. FASOLATO, C., PIZZO, P. & POZZAN, T. (1990). Receptor-mediated calcium influx in PC12 cells. ATP and bradykinin activate two independent pathways. *J. Biol. Chem.,* **265**, 20351-20355.

46. FELDBERG, W., MINZ, B., & TSUDZIMURA, H. (1934). The mechanism of the nervous discharge of adrenaline. *Journal of Physiology*, **81**, 286-304.

47. FELTZ, A. & TRAUTMANN, A. (1982) Desensitization at the frog muscular junction: a biphasic process. *J. Physiol.*, **322**, 257-272.

48. FENWICK, E.M., MARTY, A. & NEHER, E. (1982). A patch-clamp study of bovine chromaffin cells and of their sensitivity to acetylcholine. *Journal of Physiology*, **331**, 577-597.

49. GINIATULLIN, R., KHIROUG, L., TALANTOVA, M. & NISTRI, A. (1996). Fading and rebound of currents induced by ATP on PC12 cells. *Br. J. Pharmacol.*, **119**, 1045-1053.

50. GREENE, L.A., & TISCHLER, A.S. (1976) Establishment of a noradrenergic clonal line of rat adrenal pheochromocytoma cells which respond to nerve growth factor. *Proc. Natl. Acad. Sci. U.S.A.* **73**, 2424-2428.

51. GROHOVAZ, F., ZACCHETTI, D., CLEMENTI, E., LORENZON, P., MELDOLESI, J. & FUMAGALLI, G. (1991). $[Ca^{2+}]_i$ imaging in PC12 cells: multiple response patterns to receptor activation reveal new aspects of transmembrane signalling. *J. Cell Biol.*, **113**, 1341-1350.

52. GRYNKIEVICZ, G., POENIE, M. & TSIEN, R.Y. (1985) A new generation of Ca^{2+} indicators with greatly improved fluorescence properties. *J. Biol. Chem.*, **260**, 3440-3450.

53. GURNEY, E. & LESTER, I. (1987) Light-flash physiology with synthetic photosensitive compounds. *Physiol. Rev.* **67**, 583-616.

54. HAMILL, O.P., MARTY, A., NEHER, E., SAKMANN, B. & SIGWORTH, F.J. (1981) Improved patch-clamp techniques for high-resolution current recording from cells and cell-free membrane patches. *Pflugers Arch.* **391**, 85-100.

55. HARDWICK, J.C. & PARSONS, R.L. (1996) Activation of the protein phosphatase calceneurin during carbachol exposure decreases the extent of recovery from end-plate desensitization. *J. Neurophysiol.* **76**, 3609-3616.

56. HODGKIN, A.L., HUXLEY, A.F. & KATZ, B. (1952) Measurement of current-voltage relations in the membrane of the giant axon of loligo. *J.Physiol*, **116**, 424-448.

57. HAUGLAND, R.P. (1996) Handbook of fluorescent probes and research chemicals. 6th edition, Molecular Probes, Eugene, USA.

58. HEIDMANN, T. & CHANGEUX, J.P. (1979) Fast kinetic studies on the interaction of a fluorescent agonist with the membrane-bound acetylcholine receptor from Torpedo marmorata. *Eur. J. Biochem.* **94**, 255-279.

59. Time-resolved photolabelling by the noncompetitive blocker chloropromazine of the acetylcholine receptor in its transiently open and closed ion-channel conformation. *Proc. Natl. Acad. Sci. USA,* **81**, 1897-1901.

60. HELMCHEN, F., IMOTO, K. & SAKMANN, B. (1996). Ca^{2+} buffering and action potential-evoked Ca^{2+} signaling in dendrites of pyramidal neurons. *Biophysical Journal,* **70**, 1069-1081.

61. HILLE, B. (1992) Ionic Channels of Excitable Membranes. - 2nd ed. Sinauer Associates Inc.

62. HOLMAN, M.E., COLEMAN, H.A., TONTA, M.A. & PARKINGTON, H.C. (1994). Synaptic transmission from splanchnic nerves to the adrenal medulla of guinea-pigs. *Journal of Physiology,* **478**, 115-124.

63. HOPKINS, H.H., & BARHAM, P.M. (1950) The influence of condensor on microscopic resolution. *Proc. Roy. Soc. Lond.* **63B**, 737-744.

64. HOTH, M. & PENNER, R. (1992) Depletion of intracellular calcium stores activates a calcium current in mast cells. *Nature* **355**, 353-356.

65. HUGANIR, R.L. & GREENGARD, P. (1983) cAMP-dependent protein kinase phosphorylates the nicotinic acetylcholine receptor. *Proc Natl Acad Sci USA,* **80**, 1130-1134

66. HUGANIR, R.L., MILES, K. & GREENGARD, P. (1984) Phosphorylation of the nicotinic acetylcholine receptor by an endogenous tyrosine-specific protein kinase. *Proc. Natl. Acad. Sci. USA,* **81**, 6968-6972

67. HUME, R.I. & HONIG, M.G. (1986) Excitatory action of ATP on embrionic chick muscle. *J. neurosci.,* **6**, 681-690.

68. HUMPHREY, P.P.A., BUELL, G., KENNEDY, I., KHAKH, B.S., MICHEL, A.D., SUPRENANT, A. & TREZISE, D.J. (1995). New insights on P_{2X} purinoceptors. *Naunyn-Schmiedeber's Arch. Pharmacol.*, **352**, 585-596.

69. INOUE, K., NAKAZAWA, K., FUJIMORI, K. & TAKANAKA, A. (1989). Extracellular adenosine 5'-triphosphate-evoked norepinephrine secretion not related to voltage-gated Ca^{2+} channels in pheochromocytoma PC12 cells. *Neurosci. Lett.,* **106**, 294-299.

70. INOUE, S. (1995) Foundations of confocal scanned imaging in light microscopy. In: *Handbook of Biological Confocal Microscopy,* Ed: J. B. Pawley, Plenum Press, New York.

71. JARAMILLO, F. & SCHUETZE, S.M. (1988) Kinetic differences between embryonic- and adult-type acetylcholine receptors in rat myotubes. *J. Physiol.,* **396**, 267-296.

72. JONES, M.V. & WESTBROOK, G.L. (1995). Desensitized states prolong

$GABA_A$ channel responses to brief agonist pulses. *Neuron*, **15**, 181-191.

73. KAPLAN, L.H. & SOMLYO, A.P. (1989) Flash photolysis of caged compounds: New tools for cellular physiology. *Trends Neurosci.* **12**, 54-59.

74. KAO, J.P., HAROOTUNIAN, A.T. & TSIEN, R.Y. (1989). Photochemically generated cytosolic calcium pulses and their detection by fluo-3. *J. Biol. Chem.*, **264**, 8179-8184.

75. KATZ, B. & THESLEFF, S. (1957). A study of the "desensitization" produced by acetylcholine at the motor end-plate. *J. Physiol.*, **138**, 63-80.

76. KHAKH, B.S., HUMPHREY, P.P.A. & SURPRENANT, A. (1995). Electrophysiological properties of P_{2X}-purinoreceptors in rat superior cervical, nodose and guinea-pig coeliac neurones. *J. Physiol.*, **484**, 385-395.

77. KHIROUG, L. (1994) Temporal-spatial analysis of Ca^{2+} oscillations in rat chromaffin cells studied with confocal microscopy. // EMBO Course on Optical Probes for Intracellular Signalling in Living Cells. - Babraham, Cambridge, England.

78. KHIROUG, L., GINIATULLIN, R., TALANTOVA, M. & NISTRI, A. (1997a). Role of intracellular calcium in fast and slow desensitization of P_2-receptors in PC12 cells. *British Journal of Pharmacology,* **120**, 1552-1560.

79. KHIROUG, L., GINIATULLIN, R., TALANTOVA, M. & NISTRI, A. (1997b). The effect of the neuropeptide substance P on desensitization of ATP receptors of PC12 cells. *British Journal of Pharmacology,* **120**, in press.

80. KHIROUG, L., GINIATULLIN, R., TALANTOVA, M. & NISTRI, A. (1997c). Confocal imaging of intracellular calcium during desensitization of nicotinic acetylcholine receptors of rat chromaffin cells. *Journal of Physiology,* submitted.

81. KIM, W.K., & RABIN, R.A. (1994). Characterization of the purinergic P2 receptors in PC12 cells. Evidence for a novel subtype. *J. Biol. Chem.*, **269**, 6471-7.

82. KING, B.F., ZIGANSHINA, L.E., PINTOR, & BURNSTOCK, G. (1996). Full sensitivity of $P2X_2$ purinoceptor to ATP revealed by changing extracellular pH. *Br.J.Pharmacol.*, **117**, 1371-1373.

83. KOZAWA, O., SHINODA, J. & SUZUKI, A. (1995). Genestein inhibits Ca^{2+} influx by extracellular ATP in PC12 pheochromocytoma cells. *Horm. Metab. Res.*, **27**, 272-274.

84. KRISHTAL, O.A. & PIDOPLICHKO, V.I. (1980) A receptor for protons in the nerve cell membrane. *Neuroscience* **5**, 2325-2327.

85. KRISHTAL, O.A., MARCHENKO, S.M. & PIDOPLICHKO, V.I. (1983) Receptor for ATP in the membrane of mammalian sensory neurons. *Neurosci. Lett.*, **35**, 41-45.

86. LECHLESTER, J.D. & CLAPHAM, D.E. (1992) Molecular mechanisms of intracellular calcium excitability in X. laevis oocytes. *Cell* **69**, 283-294.

87. LEVITAN, I.B. (1994). Modulation of ion channels by protein phosphorylation and dephosphorylation. *Annual Review of Physiology*, **56**, 193-212.

88. LINDSTROM, J., ANAND, R., PENG, X., GERZANICH, V., WANG, F., & LI, Y. (1995) Neuronal nicotinic receptor sutypes. *Ann. N.Y. Acad. Sci.* **757**, 100-116.

89. LINDSTROM, J. (1996) Neuronal nicotinic acetylcholine receptors. In: *Ion Channels,* Ed: T. Narahashi, Plenum Press, New York.

90. LIPP, P. & NIGGLI, E. (1993) Ratiometric confocal Ca(2+)-measurements with visible wavelength indicators in isolated cardiac myocytes. *Cell Calcium* **14**, 359-372.

91. LIPP, P. & NIGGLI, E. (1996) A hierarchical concept of cellular and subcellular Ca(2+)-signalling. *Prog Biophys Mol Biol* **65**, 265-296.

92. LIPP, P. & NIGGLI, E. (1996b) Submicroscopic calcium signals as fundamental events of excitation-contraction coupling in guinea-pig cardiac myocytes. *J. Physiol.*, **492**, 31-38.

93. LIPP, P., POTT, L., CALLEWAERT, G. & CARMELIET, E. (1990) Simultaneous recording of Indo-1 fluorescence and Na^+/Ca^{2+} exchange current reveals two components of Ca^{2+}-release from sarcoplasmic reticulum of cardiac atrial myocytes. *FEBS Lett.* **275**, 181-184.

94. LIVETT, B.G., KOZOUZEK, V., MIZOBE, F., & DEAN, D.M. (1979). Substance P inhibits nicotinic activation of chromaffin cells. *Nature,* **278**, 256-257.

95. LUSCHER, C., LIPP, P., LUSCHER, H.R. & NIGGLI, E. (1996) Control of action potential propagation by intracellular Ca2+ in cultured rat dorsal root ganglion cells. *J. Physiol.* **490**, 319-324.

96. MACONOCHIE, D.J. & KNIGHT, D.E. (1992). A study of the bovine adrenal chromaffin nicotine receptor using patch clamp and concentration-jump techniques. *J. Physiol.*, **454**, 129-153.

97. MAGAZANIK, L.G. & VYSKOCIL, F. (1970). Dependence of acetylcholine receptor desensitization on the membrane potential of frog muscle fiber and on the ionic changes in the medium. *J. Physiol.*, **210**, 507-518.

98. MALGAROLI, A. & TSIEN, R.W. (1992) Glutamate-induced long-term potentiation of the frequency of miniature synaptic currents in cultured hippocampal neurons. *Nature* **357**, 134-139.

99. MANTHEY, A.A. (1966). The effect of calcium on the desensitization of membrane receptors at the neuromuscular junction. *Journal of General Physiology*, **49**, 963-975.

100. MARGIORIS, A.N., MARKOGIANNAKIS, E., MAKRIGIANNAKIS, A. & GRAVANIS, A. (1992) PC12 rat pheochromocytoma cells synthesize dynorphin. Its secretion is modulated by nicotine and nerve growth factor. *Endocrinology* **131**, 703-709.

101. MARKRAM, H., HELM, P.J. & SAKMANN, B. (1995). Dendritic calcium transients evoked by single back-propagating action potentials in rat neocortical pyramidal neurons. *J. Physiol.*, **485**, 1-20.

102. MARLEY, P.D. (1988). Desensitization of the nicotinic secretory response of adrenal chromaffin cells. *Trends in Pharmacological Science*, **9**, 102-107.

103. MEDINA, I., FILIPPOVA, N., BAKHRAMOV, A. & BREGESTOVSKI, P. (1996) Calcium-induced inactivation of NMDA receptor-channels evolves independently of run-down in cultured rat brain neurones. *J. Physiol.*, **495**, 411-427.

104. MILEDI, R. (1980). Intracellular calcium and desensitization of acetylcholine receptors *Proc. Roy. Soc. Lond. B.*, **209**, 447-452.

105. MINSKY, M. (1988) Memoir on inventing the confocal scanning microscope. *Scanning*, **10**, 128-138.

106.MINTA, A., KAO, J.P. & TSIEN, R.Y (1989). Fluorescent indicators for cytosolic calcium based on rhodamine and fluorescein chromophores. *J. Biol. Chem.,* **264**, 8171-8178.

107.MISHINA, M., KUROSAKI ,T., TOBIMATSU, T., MORIMOTO, Y., NODA, M., YAMAMOTO, T., TERAO, M., LINDSTROM, J., TAKAHASHI, T., KUNO, M. & SAKMANN, B. (1984) Expression of functional acetylcholine receptor from cloned cDNAs. *Nature,* **307**, 604-608.

108.MIZRACHI, Y., NARANJO, J.R., LEVI, B.Z., POLLARD, H.B. & LELKES, P.I. (1990) PC12 cells differentiate into chromaffin cell-like phenotype in coculture with adrenal medullary endothelial cells. *Proc. Natl. Acad. Sci. USA,* **87**,6161-6165

109.MOLLARD, P., SEWARD, E.P. & NOWYCKY, M.C. (1995). Activation of nicotinic receptors triggers exocytosis from bovine chromaffin cells in the absence of membrane depolarization. *Proceedings of the National Academy of Sciences USA,* **92**, 3065-3069.

110.MULLE, C., CHOQUET, D., KORN, H. & CHANGEUX, J.-P. (1992). Calcium influx through nicotinic receptor in rat central neurons: its relevance to cellular regulation. *Neuron,* **8**, 135-143.

111.NAKAZAWA, K., FUJIMORI, K., TAKANAKA, A. & INUE, K. (1990). An ATP-activated conductance in pheochromocytoma cells and its suppression by

extracellular calcium. *J. Physiol.*, **428**, 257-272.

112.NAKAZAWA, K., & HESS, P. (1993). Block by calcium of ATP-activated channels in pheochromocytoma cells. *J. Gen. Physiol.*, **101**, 377-392.

113.NAKAZAWA, K. & INOUE, K. (1992). Roles of Ca^{2+} influx through ATP-activated channels in catecholamine release from pheochromocytoma PC12 cells. *J. Neurophysiol.*, **68**, 2026-2032.

114.NEHER, E. (1983). The charge carried by single-channel currents of rat cultured muscle cells in the presence of local anaesthetics. *J. Physiol.*, **339**, 663-678.

115.NEHER, E. & AUGUSTINE, G.J. (1992). Calcium gradients and buffers in bovine chromaffin cells. *J. Physiol.*, **450**, 273-301.

116.NEHER, E., & SAKMANN, B. (1976) Single channel currents recorded from membrane of denervated frog muscle fibres. *Nature,* **260**, 799-801.

117.NEHER, E. & STEINBACH, J.H. (1978). Local anesthetics transiently block currents through single acetylcholine-receptor channels. J. Physiol., **277**, 153-176.

118.NICHOLLS, J. G., MARTIN, A. R., & WALLACE, B.G. (1992) From Neuron to Brain: A Cellular and Molecular Approach to the Function of the Nerous System. - 3rd ed. Sinauer Associates.

119.NISTRI, A., & CONSTANTI, A. (1979). Pharmacological characterization of different types of GABA and glutamate receptors in vertebrates and invertebrates. Prog. Neurobiol., **13**, 117-235.

120.NOBLE, M.D., BROWN, T.N. & PEACOCK., J.H. (1978) Regulation of acetylcholine receptor levels in mouse muscle cell cultures. *Proc. Nat. Acad. Sci. USA,* **75**, 3488-3492.

121.NODA, M., TAKAHASHI, H., TANABE, T., TOYOSATO, M., FURUTANI, Y., IROSE, T., ASAI, M., INAYAMA, S., MIYATA, T. & NUMA, S. (1982) Primary structure of α-subunit precursor of *Torpedo californica* acetylcholine receptor deduced from cDNA sequence. *Nature*, **299**, 793-797.

122.NOONEY J.M. & FELTZ A. (1995). Inhibition by cyclothiazide of neuronal nicotinic responses in bovine chromaffin cells. *British Journal of Pharmacology*, **114**, 648-655.

123.NUMA, S., NODA, M., TAKAHASHI, H., TANABE, T., TOYOSATO, M., FURUTANI, Y. & KIKYOTANI, S. (1983) Molecular structure of the nicotinic acetylcholine receptor. *Cold Spring Harbor Symp. Quant. Biol.,* **48**, 57-69.

124.OCHOA, E.L., CHATTOPADHYAY, A. & MCNAMEE, M.G. (1989) Desensitization of the nicotinic acetylcholine receptor: molecular mechanisms and effect of

modulators. *Cell. Mol. Neurobiol.,* **9**, 141-178.

125.OGDEN, D.C. & COLQUHOUN, D. (1985). Ion channel block by acetylcholine, carbachol and suberyldicholine at the frog neuromuscular junction. *Proc. R. Soc. Lond. B*, **225**, 329-355.

126.ORCHARD, C.H., BOYETT, M.R., FRY, C.H., AND HUNTEN, M. (1991) The use of electrodes to study cellular Ca^{2+} metabolism. In: *Cellular Calcium: A Practical Approach.* Ed: J.G. McCormack, P.H. Cobbold. Oxford University Press, Oxford, New York, Tokyo.

127.OTSUKA, M. & YOSHIOKA, K. (1993). Neurotransmitter functions of mammalian tachykinins. *Physiol. Rev.,* **73**, 229-307.

128.PARK, Y.B., HERRINGTON, J., BABCOCK, D.F. & HILLE, B. (1996). Ca^{2+} clearance mechanisms in isolated rat adrenal chromaffin cells. *J. Physiol.,* **492**, 329-346.

129.PEPER, K., BRADLEY, R.J. & DREYER, F. (1982) The acetylcholine receptor at the neuromuscular junction. *Physiol. Rev.* **62,** 1271-1340.

130.PLANT, T.D., EILERS, J. & KONNERTH, A. (1995) Patch-clamp technique in brain slices. In: *Neuromethods, vol. 26, Patch-clamp applications and protocols.* Ed: A.Boulton, G.Baker, & W.Walz. Humana Press, New Jersey.

131.PRZYWARA, D.A., GUO, X., ANGELILLI, M.L., WAKADE, T.D. & WAKADE, A.R. (1996). A non-cholinergic transmitter, pituitary adenylate cyclase-activating polypeptide, utilezes a novel mechanism to evoke catecholamine secretion in rat adrenal chromaffin cells. *Journal of Biological Chemistry*, **271**, 10545-10550.

132.RAHA, S., de SOUZA, L.R. & REED, J.K. (1993). Intracellular signalling by nucleotide receptors in PC12 pheochromocytoma cells. *J. Cell. Physiol.*, **154**, 623-630.

133.RATHOUZ, M.M. & BERG, D.K. (1994). Synaptic-type acetylcholine receptors raise intracellular calcium levels in neurons by two mechanisms. *J. Neurosci.*, **14**, 6935-6945.

134.REBER, F.X., NEUHAUS, R. & REUTER, H. (1992). Activation of different pathways for calcium elevation by bradykinin and ATP in rat pheochromocytoma (PC12) cells. *Pflugers Arch.*, **420**, 213-218.

135.REVAH, F., BERTRAND, D., GALZI, J.L., DEVILLERS-THIERY, A., MULLE, C., HUSSY, N., BERTRAND, S., BALLIVET, M. & CHANGEUX, J.P. (1991) Mutations in the channel domain alter desensitization of a neuronal nicotinic receptor. *Nature* **353**, 846-849

136.ROBERTSON, S.J., RAE, M.G., ROWAN, E.G. & KENNEDY, C. (1996). Characterization of a P_{2X}-purinoceptor in cultured neurones of the rat dorsal root

ganglia. *Br. J. Pharmacol.*, **118**, 951-956.

137.ROGERS, M., & DANI, J.A. (1995). Comparison of quantitative calcium flux through NMDA, ATP, and ACh receptor channels. *Biophys. J.,* **68**, 501-506.

138.ROGERS, M., COLQUHOUN, L.M., PATRICK, J.W. & DANI, J.A. (1997) Calcium flux through predominantly independent purinergic ATP and nicotinic acetylcholine receptors. *J. Neurophysiol,* **77**, 1407-1417

139.ROLE, L. (1992) Diversity in primary structure and ufnction of neuronal nicotinic acetylcholine receptor channels. *Curr. Opin. Neurobiol.,* **2**, 254-262.

140.SAFRAN, A., PROVENZANO, C., SAGI-EISENBERG, R. & FUCHS, S. (1989) Phosphorylation of membrane-bound acetylcholine receptor by protein kinase C: characterization and subunit specificity. *Biochem.* **29**, 6730-6734.

141.SAKMANN, B., PATLAK, J. & NEHER, E. (1980). Single acetylcholine activated channels show burst-kinetics in the presence of desensitizing concentrations of agonists. *Nature*, **286**, 71-73.

142.SARGENT, P. (1993) The diversity of neuronal nicotinic acetylcholine receptors. *Annu. Rev. Neurosci.,* **16**, 403-443.

143.SHIBATA, K., MORITA, K., KITAYAMA, S., OKAMOTO, H. & DOHI, T. (1996). Ca^{2+} entry induced by calcium influx factor and its regulation by protein kinase C in rabbit neutrophils. *Biochemical Pharmacology,* **52**, 167-171.

144.SIMASKO, S.M., DURKIN, J.A., & WEILAND, G.A. (1987). Effects of substance P on nicotinic acetylcholine receptor function in PC12 cells. *J. Neurochem.,* **49**, 253-260.

145.SIMMONS, L.K., SHUETZE, S.M. & ROLE, L.W. (1990). Substance P modulates single-channel properties of neuronal nicotinic acetylcholine receptors. *Neuron,* **2**, 393-403.

146.SINE, S. (1988) Functional properties of human skeletal muscle acetylcholine receptors expressed by the TE671 cell line, *J.Biol.Chem.,* **263**, 18052-18062.

147.SINE, S.M. & STEINBACH, J.H. (1984). Agonists block currents through nicotine acetylcholine receptor channels. *Biophys. J.*, **46**, 277-283.

148.SONTHEIMER, H. (1995) Whole-cell patch-clamp recordings. In: *Neuromethods, vol. 26, Patch-clamp applications and protocols.* Ed: A.Boulton, G.Baker, & W.Walz. Humana Press, New Jersey.

149.STAFFORD, G.A., OSWALD, R.E., & WEILAND, G.A. (1994). The β subunit of neuronal nicotinic acetylcholine receptors is a determinant of the affinity for

substance P inhibition. *Mol. Pharmacol.,* **45**, 758-762.

150.SUGAZAWA, M., EROSTEGUI, C., BLANCHET, C. & DULON, D. (1996). ATP activates non-selective cation channels and calcium release in inner hair cells of the guinea-pig cochlea. *J. Physiol.,* **491**, 707-718.

151.SURPRENANT, A., BUELL, G. & NORTH, R.A. (1995). P_{2X} receptors bring new structure to ligand-gated ion channels. *Trends Neurosci.,* **18**, 224-229.

152.THOMAS, R.C. (1978) Ion selective microelectrodes: how to make and use them. In: *Biological Techniques* series. Academic Press, New York and London.

153.TSIEN, R.Y. (1981). A non-disruptive technique for loading calcium buffers and indicators into cells. *Nature,* **290**, 527-528.

154.UNWIN, N., TOYOSHIMA, C. & KUBALEK, E. (1988) Arrangement of acetylcholine receptor subunits in the resting and desensitized states, determined by crolelectron microscopy of crystallized *Torpedo* postsynaptic membranes. *J. Cell Biol.,* **107**, 1123-1138.

155.VALERA, S., HUSSY, N., EVANS, R., ADAMI, N., NORTH, R.A., SURPRENANT, A. & BUELL, G. (1994). A new class of ligand-gated ion channel defined by P_{2X} receptor for extracellular ATP. *Nature,* **371**, 516-519.

156.VERNINO, S., ROGERS, M., RADCLIFFE, K.A. AND DANI, J.A. (1994). Quantitative measurement of calcium flux through muscle and neuronal nicotinic acetylcholine receptors. *Journal of Neuroscience*, **14**, 5514-5524.

157.VLACHOVA, V., VYKLICKY, L., VYKLICKY, L.Jr. & VYSKOCIL, F. (1987). The action of excitatory amino acids on chick spinal cord neurones in culture. *J. Physiol.*, **386**, 425-438.

158.WALZ, W. (1995) Perforated patch-clamp techniques. In: *Neuromethods, vol. 26, Patch-clamp applications and protocols.* Ed: A.Boulton, G.Baker, & W.Walz. Humana Press, New Jersey.

159.WERMAN, R. (1976). Desensitization and stoichiometry of transmitter-receptor interactions. In: *Electrobiology of Nerve, Synapse and Muscle,* pp. 45-60. Eds. J.P.REUBEN, D.P. PURPURA, M.V.L. BENNETT & E.R. KANDEL, Raven Press, New York.

160.XIONG, Z., KITAMURA, K. & KURIYAMA, H. (1991). ATP activates cationic currents and modulates the calcium current through GTP-binding protein in rabbit portal vein. *J. Physiol.*, **440**, 143-165.

161.ZACCHETTI, D., CLEMENTI, E., FASOLATO, C., LORENZON, P., ZOTTINI, M., GROHOVAZ, F., FUMAGALLI, G., POZZAN, T. & MELDOLESI, J. (1991). Intracellular Ca^{2+} pools in PC12 cells. *J. Biol. Chem.*, **266**, 20152-20158.

162.ZHANG, Z., VIJAYARAGHAVAN, S. & BERG, D.K. (1994). Neuronal acetylcholine receptors that bind α-bungarotoxin with high affinity function as ligand-gated ion channels. *Neuron*, **12**, 167-177.

Aknowledgements

I should like to express my gratitude to:

- My supervisor Professor Andrea **Nistri**, for his excellent, professional and kind help in my research and education;
- Professor Rashid A. **Giniatulin** (Kazan Medical University, Russia), for his most valuable collaboration and leadership;
- Doctor Paola **D'Andrea** (University of Trieste, Italy), for giving me the first lessons during the initial steps in my research work;
- Doctor Pavle **Andjus** (University of Belgrade, F.R.Yugoslavia), for being an example of hard-work in science;
- Doctor Jerrel L. **Yakel** (NIEHS, NC, U.S.A.), for teaching me to always search the Truth;
- Doctor Massimo **Righi** and Doctor Isabella **Masi**, for being very helpful and prompt with cell cultures;
- Doctor Maria **Talantova** and Doctor Elena **Sokolova** (Kazan Medical University, Russia), for the pleasent time spent doing experiments together;
- Doctor Dmitri **Smirnov** and Doctor Maria **Kouznetsova**, for their friendly attitude and valuable discussions of the project-related problems;
- All my SISSA collegues whom I cannot name for space reasons (sorry!), for the beautiful friendly and collaborative atmosphere that aided essentially the research -

Thank you all!

JOURNAL ARTICLES

Giniatullin, R.A., **Kheeroug**, L.S. (1993) Comparative study of kinetics of pre- and postsynaptic processes in the neuromuscular synapse using original model of endplate current. *Neurophysiology,* **1**(2), 126-132.

Giniatullin, R.A., **Kheeroug**, L.S., Vyskocil, F. (1995) Modelling endplate current: dependence on quantum secretion probability and postsynaptic miniature current parameters. *European Biophysical Journal,* **23**, 443-446.

Andjus, P.R., **Khiroug**, L., Yakel, J.L., Cherubini, E., Nistri, A. (1996) Changes in intracellular calcium induced by NMDA in cultured rat hippocampal neurones reguire exogenous glycine. *Neurosci. Letters*, **210**, 25-28.

Andjus, P.R., **Khiroug**, L., Nistri, A., Cherubini, E. (1996) ALS IgGs suppress [Ca2+]i rise through P/Q type calcium channels in central neurones in culture. N*euroReport*, **7**, 1914-1916.

Andjus, P.R., **Khiroug**, L., Nistri, A., Cherubini, E. (1996) Effects of amyotropic lateral sclerosis IgGs on calcium homeostasis in neural cells. In: *Immunoregulation in Health and Disease*, Lukic M.L., Colic M., Stojkovic M.M., and Cuperlovic K. (editors). Academic Press, London, pp.173-180.

Giniatullin, R., **Khiroug**, L., Talantova, M., Nistri, A. (1996) Fading and rebound of currents induced by ATP on rat PC12 cells. *Br. J. Pharmacol.*, **119**, 1045-1053.

Khiroug, L., Giniatullin, R., Talantova, M., Nistri, A. (1997) Role of intracellular calcium in fast and slow desensitization of purinoceptors in PC12 cells. *Br. J. Pharmacol.*, **120**, 1552-1560.

Khiroug, L., Giniatullin, R., Talantova, M., Nistri, A. (1997) The neuropeptide Substance P enhances desensitization of ATP receptors of PC12 cells. - *Brit. J. Pharmacol*, in press.

Khiroug, L., Giniatullin, R., Talantova, M., Nistri, A. (1997) Confocal imaging of intracellular calcium during desensitization of nicotinic acetylcholine receptors of rat chromaffin cells. *J. Physiol.*- submitted.

ABSTRACTS

Kheeroug, L.S., Laikov, T.V., Giniatullin, R.A. The effect of asynchrony of ACh release on the amplitude of endplate currents // VI Simposium "Physiology of Mediators. Peritherical Synapse".- Kazan, 1991.-P. 118

Kheeroug, L.S., Giniatullin, R.A. Modeling of secretion process from motor nerve endings: the role of early and late release // International Simposium "Intracellular Channels, Organells and Cell Function". - Trieste, 1993.- P. 51.

Khiroug, L. Temporal-spatial analysis of Ca oscillations in rat chromaffin cells studied with confocal microscopy. // EMBO Course on Optical Probes for Intracellular Signalling in Living Cells. - Babraham, Cambridge, England, 1994.

Laikov, T.V., **Kheeroug**, L.S., Giniatullin, R.A. Changes in the time-course of mediator secretion during the rythmic activity of neuro-muscular junction // V Simposium "Physiology of Mediators. Peritherical Synapse".- Kazan, 1994.

Afzalov, R.A., Giniatullin, R.A., **Khiroug**, L., Kotov, N.V. Modelling of quantal transmitter release mechanism in motor nerve ending // III Symposium on Neuropharmacology. - San Diego, 1995.

Khiroug, L., Andjus, P.R., Cherubini, E., Nistri, A. Changes in intracellular calcium concentration induced by activation of glutamate receptors in cultured rat hippocampal neurones // Annual Meeting on Neuroscience. - San Diego, 1995.

Giniatullin, R., **Khiroug**, L., Talantova, M., Nistri, A. (1996) Role of calcium ions in neuronal cholinergic and purinergic receptors function. Neurochemistry, 13(3), 221.